Aalto University
School of Engineering

Aake Korkelainen

A Theoretical Risk Period Analysis and Safety Optimisation of Approach Flight Profiles in Commercial Single-Engine Turbine Operations

Thesis submitted in partial fulfillment of the requirements
for the degree of Master of Science in Technology

Espoo, August 12, 2017
Supervisor: Professor Jukka Tuhkuri
Advisor: Tuukka Takala, M.Sc. (Tech.)

Aalto University
School of Engineering

Aalto University, P.O. BOX 11000
00076 AALTO
www.aalto.fi

Abstract of master's thesis

Author	Aake Korkelainen
Title of thesis	A Theoretical Risk Period Analysis and Safety Optimisation of Approach Flight Profiles in Commercial Single-Engine Turbine Operations
Degree programme	Mechanical Engineering
Major	Aeronautical Engineering **Code** K3004
Thesis supervisor	Professor Jukka Tuhkuri
Thesis advisor	Tuukka Takala, M.Sc. (Tech)
Date 12.8.2017	**Number of pages** 60 + 46 **Language** English

Abstract

The European Aviation Safety Agency has recently approved commercial operations on single-engine turbine aeroplanes at night and in poor weather. Growth in the operations in this sector can be reasonably expected. In addition to regulations applicable to all commercial operators, the single-engine turbine operators must fulfil various single-engine safety related demands. For example, an emergency landing site must be available within gliding distance unless a risk period is utilised. Approach phase is one of the critical phases of the flight due to relatively low flying altitudes. It is also complicated to examine due to variance in actual flight routes in approach.

A theoretical model for studying the risk period is developed in this thesis. The applicability of the method is tested with a case study. The first objectives are to find equations and boundary conditions required in the analysis. Then simulated flight profiles are constructed and the risk periods arising in the approach flight phase are calculated. Moreover, the geographical location of the risk areas is identified. Aim is to first calculate the risk periods assuming still air conditions and then study and compare the effect of headwind. Furthermore, possible risk mitigation methods are discussed and their effect to the risk periods and risk areas are examined.

As an outcome, a spreadsheet computation tool was developed. The case study focused on Pilatus PC-12 aircraft flying approaches at Helsinki Airport. A total of 40 different standard instrument arrivals were studied. The analysis was highly theoretical and the simulated flight profiles do not precisely correspond to actual flight routes at Helsinki Airport. However, the results were credible and distinctive. The results indicate that the total risk period can vary greatly depending on the relation between the arrival direction and the runway in use, as well as on the altitude constraints in the instrument approach procedures. Headwind had a significant effect in the risk period. It decreased the aeroplane's gliding capability and ground speed, thus increasing the risk area and exposure time. In some cases, both with and without the headwind effect, risk mitigation was necessary to fulfil the requirements set for the maximum duration of the risk period. The main mitigation means identified were utilising higher descent angle and speed profiles in the approach and selecting an alternative emergency landing site in addition to the runway in use. By utilising these means the risk period could be significantly reduced.

Keywords SET-IMC, single-engine, engine failure, risk period , flight safety, approach

Aalto-yliopisto
Insinööritieteiden korkeakoulu

Aalto-yliopisto, PL 11000
00076 AALTO
www.aalto.fi

Diplomityön tiivistelmä

Tekijä Aake Korkelainen

Työn nimi Lähestymisprofiilien teoreettinen riskiperiodianalyysi ja turvallisuusperusteinen optimointi kaupallisessa toiminnassa yksimoottorisilla potkuriturbiinikoneilla

Koulutusohjelma Konetekniikka

Pääaine Lentotekniikka **Koodi** K3004

Työn valvoja Professori Jukka Tuhkuri

Työn ohjaaja Diplomi-insinööri Tuukka Takala

Päivämäärä 12.8.2017 **Sivumäärä** 60 + 46 **Kieli** englanti

Tiivistelmä

Euroopan lentoturvallisuusvirasto on äskettäin antanut hyväksyntänsä yksimoottoristen potkuriturbiinikoneiden kaupalliselle operoinnille yöllä ja huonon sään vallitessa. On siis perusteltua odottaa operaatiomäärien kasvavan tällä sektorilla. Niiden määräysten lisäksi, jotka koskevat kaikkia kaupallisia operaattoreita, yksimoottorisia turbiinikoneita käyttävien operaattoreiden on täytettävä useita yksimoottoristen lentokoneiden turvallisuuteen liittyvä vaatimuksia. Esimerkiksi, pakkolaskupaikka on oltava aina saavutettavissa liitomatkan päässä, ellei riskiperiodia hyödynnetä. Lähestyminen on tässä mielessä yksiä kriittisimpiä lennon vaiheita, koska silloin lennetään suhteellisen matalalla. Lähestyminen on myös monimutkainen tutkia, sillä todelliset lentoreitit vaihtelevat paljon.

Tässä diplomityössä kehitetään teoreettinen malli, jolla voidaan tutkia riskiperiodeja. Mallin toimivuutta käytännössä testataan esimerkkitapauksen avulla. Työn ensimmäiset tavoitteet ovat etsiä analyysissä tarvittavat matemaattiset yhtälöt sekä määrittää rajaarvot. Seuraavaksi rakennetaan simuloidut lentoprofiilit ja lasketaan lähestymisvaiheessa syntyvät riskiperiodit. Lisäksi tunnistetaan riskialueiden maantieteelliset sijainnit. Tarkoituksena on ensin laskea riskiperiodit tyynessä säässä sekä sen jälkeen tutkia ja vertailla vastatuulen vaikutusta. Lisäksi pohditaan mahdollisia keinoja riskien pienentämiseksi ja tutkitaan niiden vaikutuksia riskiperiodeihin ja riskialueisiin.

Työn tuloksena kehitettiin taulukkolaskentatyökalu. Esimerkkitapaus keskittyi Pilatus PC-12 -lentokoneeseen ja Helsinki-Vantaan lentoaseman lähestymismenetelmiin. Yhteensä tarkasteltiin 40 vakiotuloreittiä. Tehty analyysi on hyvin teoreettinen ja simuloidut lentoprofiilit eivät vastaa tarkasti todellisia lentoreittejä Helsinki-Vantaalla. Saadut tulokset ovat kuitenkin selkeitä ja uskottavia. Tulokset osoittavat, että riskiperiodin pituus voi vaihdella suuresti riippuen tulosuunnan ja käytössä olevan kiitotien välisestä suhteesta sekä mittarilähestymismenetelmän korkeusrajoituksista. Vastatuulella oli merkittävä vaikutus riskiperiodiin. Se heikensi lentokoneen liitokykyä ja pienensi maanopeutta, samalla kasvattaen altistusaikaa riskialueilla. Joissain tapauksissa sekä ilman vastatuulen vaikutusta että sen kanssa tarvittiin keinoja riskiperiodin pienentämiseksi, jotta täytettiin riskiperiodin maksimipituudelle asetetut vaatimukset. Tärkeimmät löydetyt keinot olivat jyrkemmän liukukulman ja suuremman lentonopeuden käyttäminen sekä vaihtoehtoisen pakkolaskupaikan valinta käytössä olevan kiitotien lisäksi. Niiden avulla riskiperiodia saatiin huomattavasti pienennettyä.

Avainsanat SET-IMC, yksimoottorinen, moottorihäiriö, riskiperiodi, lentoturvallisuus, lähestyminen

Preface

Aviation is my passion and profession. This thesis has been a great personal opportunity to combine acquired knowledge and operational experience from both the aeronautical engineering studies and more practical piloting aspect of aviation. The idea for this study saw daylight when I was employed by a start-up Pilatus operator and was taking part in the planning of the daily operations. I would like to thank my friend Roope Kekäläinen for giving me an opportunity to undergo a PC-12 NG class rating course and to have an insight in the back office work of a certified airline operator. The ambitious aim of this thesis is to further improve single-engine flight safety. The goal is to provide the operators a new tool for managing the engine failure risks related to single-engine operations.

I am grateful to my supervisor professor Jukka Tuhkuri for providing the necessary guidance. I wish to express my gratitude also to my friend, colleague and instructor M.Sc. Tuukka Takala for valuable feedback and for outlining the topic and contents of this thesis with me.

Finally, I wish to thank my family for supporting me throughout my studies. Special thanks to Mira for understanding the meaning of this exertion – you truly encouraged and supported me to complete this thesis.

Espoo, August 12, 2017

Aake Korkelainen

Table of Contents

List of Symbols

E	Glide ratio
E_{max}	Maximum glide ratio
M	Mach number
R	Glide range
V	Indicated airspeed
V_{GS}	Ground speed
V_{md}	Minimum drag airspeed
V_{TAS}	True airspeed
a	Local speed of sound
d	Distance between two coordinates
f	Fraction between two coordinates
g	Gravitational acceleration
h	Altitude
h_{eq}	Equivalent altitude
Δh_{turn}	Altitude lost during a turn
Δh_V	Altitude converted from speed
$\dot{h}$	Vertical speed
r	Earth's mean radius
v_W	Wind velocity
γ	Flight path angle / glide angle
γ_{min}	Minimum glide angle
γ_w	Glide angle with wind
δ	Angular distance
θ	True bearing
λ	Longitude
ρ	Air density
ρ_0	Air density at sea level
φ	Latitude

Abbreviations

AFM	Airplane Flight Manual
AIP	Aeronautical Information Publication
ALARP	As Low As Reasonably Practicable
AMC	Acceptable Means of Compliance
AOC	Air Operator Certificate
ATC	Air Traffic Control
ATS	Air Traffic Services
CAA	Civil Aviation Authority
CAT	Commercial Air Transport
CDA	Continuous Descent Approach
CDR	Comment Response Document
EFHK	Helsinki Airport (ICAO code)
FAF	Final Approach Fix
FAP	Final Approach Point
FDM	Flight Data Monitoring
IAF	Initial Approach Fix
IAP	Instrument Approach Procedure
IAS	Indicated Airspeed
ICAO	International Civil Aviation Organization
IFR	Instrument Flight Rules
ILS	Instrument Landing System
IMC	Instrument Meteorological Conditions
ISA	International Standard Atmosphere
JAA	Joint Aviation Authorities
MTOM	Maximum Takeoff Mass
NG	Next Generation
NM	Nautical Mile
NPA	Notice of Proposed Amendment
RWY	Runway
SARPs	Standards and Recommended Practices
SET	Single-Engine Turbine

SMM	Safety Management Manual
SMS	Safety Management System
SOP	Standard Operating Procedures
STAR	Standard Instrument Arrival
TAS	True Airspeed
THR	Runway Threshold
VFR	Visual Flight Rules
VMC	Visual Meteorological Conditions

1 Introduction

1.1 Background

The International Civil Aviation Organization (ICAO) has approved commercial single-engine turbine (SET) operations at night and in instrument meteorological conditions (IMC) over 10 years ago. Also, some major ICAO member countries such as USA, Canada and Australia have allowed these operations. There has been a lengthy debate in Europe since the early 1990's whether or not the commercial SET operations fulfil the required safety standards but the operations had been forbidden until now.

Finally, also the European aviation authorities have acknowledged the need to update the regulatory status as the turbine engine reliability and flight instruments have further developed. The rulemaking process was completed in the first quarter of 2017. This predicts a strong growth in operations on single-engine turbine aeroplanes. Even before the recent regulatory update, some European countries had granted permission for SET operations in IMC under exemptions from common European regulations. Therefore a handful of operators already exist in Europe as well.

1.2 Need

Despite the fact that modern turboprop engines are very reliable, a minor possibility for an engine failure is always present. With single-engine aircraft this means that an emergency landing needs to be performed. The regulations state that the operator must have an emergency landing site available for all phases of the flight unless a particular risk period is used. In this context, takeoff and approach are the most critical phases of flight due to relatively low flying altitudes. Of these two, the approach is often more complex to analyse.

A standard instrument arrival route, an air traffic control vectored arrival or a combination of these will be flown around the airport and during this it is inevitable that there will be periods of time when, in the event of an engine failure, the gliding aircraft could not reach the destination airport. The pre-flight planning does not need to examine the arrival and other segments of approach phase in detail but some estimation of the duration of the risk period must be provided. This indicates a need for this thesis – a similar and as detailed study on the subject has not been previously conducted. One rough estimate for a possible approach phase risk period duration, used in a SET-IMC operations risk assessment, was about four and a half minutes (Bradley, 2007).

Flight safety is the number one priority to most of the operators. Safety has indeed developed greatly during the history of commercial aviation. Achieving a zero accident rate is practically impossible and the means to further improve the current safety rate can sometimes be very costly. However, if the total risk can be reduced, implementing these means is highly recommended, especially if they can be adopted without significantly increasing the total cost. The minimum safety level is regulated with a great number of different rules by the aviation authorities. New regulations concerning SET-IMC operations in Europe have just recently entered into force and the operators need to fulfil these. Even if the local authorities would accept some other, less sophisticated estimation

of the approach risk period and the minimum requirements could thus be fulfilled, common sense says a more detailed study would increase the safety level.

1.3 Purpose and Method

The purpose of this thesis is to develop a simple method for SET-IMC operators to examine possible risk areas in approach and in particular during the arrival segment. Focusing on a particular case example this thesis examines the theoretical length of the arising risk period and by what means and how much the risk area could be reduced. Possible means to mitigate the risk are, for example, using steeper descent profile and maintaining higher speeds as well as improved coordination with the air traffic control in the arrival phase. One of the first objectives is to find the required equations and to develop calculation method suitable for the analysis.

The case study is used to test the applicability of the developed method by identifying the risk periods and risk areas for Pilatus PC-12 NG at Helsinki Airport. All standard instrument arrivals for different runways are examined. For this, a descent profile must be simulated. By varying the variables in the simulation, the effect of different operating procedures on the risk period can be studied.

1.4 Limitations

The case study is limited to a specific aircraft model and airport combination. Thus, the results might not be directly applicable to other combinations. However, the method can be easily modified to other airports and aeroplanes. If there is a significant amount of obstacles or high terrain around the studied airport the method would need to be modified further.

The method developed here is highly theoretical and would best suit the need of pre-flight planning and meeting the demands of a route risk analysis. It must be kept in mind that the flight profiles in this study are simulated. A complete standard arrival route is rarely flown in its entirety at Helsinki Airport. Often at some point vectors – headings and speed limitations – are provided by the air traffic control (ATC). These are practically impossible to predict in advance as, among other variables, other traffic and weather conditions affect significantly on the decisions made by the controller. On the other hand, the operator could make a cooperative request to ATC on how they wish to fly their approaches, if deemed necessary. Actual flight data should be utilised to obtain more realistic results for a specific aircraft. At the time of the writing, there were no such data available for the author.

In addition, the study focuses solely on minimising the risk period and thus maximising safety in the engine failure situation, but does not take costs and economics into account. These two are somewhat contradicting aspects. Applying steeper descent profiles and higher speeds will most probably lead to increased fuel consumption. However, the modern turboprops are relatively fuel efficient and increasing safety at the cost of slight increase in fuel burn might be justified. The safety optimisation is further limited to only minimising the risk period. Incremental risks possibly yielding, for example, from the use of higher speeds or steeper descent profiles are not considered in this study.

1.5 Structure

To understand the scope of this thesis some key concepts are first shortly described in the second chapter. Third chapter opens up the broad regulatory field behind commercial single-engine operations. The idea is to find the most relevant parts in the context of this thesis. Also, relevant safety issues are addressed and some aircraft types introduced. In the fourth chapter, the theory and the formulas needed for the analysis are presented. A flight path simulation, as realistic as possible, is constructed with the help of experienced Pilatus pilots.

The final part of this thesis is a case study where the developed method is tested with standard instrument arrival routes at Helsinki Airport simulated to be flown with the Pilatus PC-12. Different descent profiles are tested to find out where the possible geographical risk areas are located and how much the risk period could be affected. Finally, the results are presented and the applicability of the method discussed and summarised.

2 Terms and Definitions

2.1 Commercial Operations

For simplification, two types of civil aeroplane operations can be identified – general aviation and commercial air transport (CAT). As general aviation refers to operations conducted privately, commercial air transport, on the contrary, is defined by the International Civil Aviation Organization (ICAO) to include scheduled and non-scheduled international air transport operations for remuneration or hire (ICAO, 2010).

Some of the aviation regulations are the same for both commercial and general aviation. However, many of the regulations are specified separately for both forms of operations. Naturally, when in commercial operations companies are taking money to transport passengers and cargo, the regulations are stricter than in private general aviation. This is due to, for example, high level of safety required and to keep competition between companies as fair as possible. The regulations concerning commercial single-engine turbine operations are described in more detail in the chapter 3.

2.2 Instrument Meteorological Conditions

There are specific weather minima defined in the aviation regulations for visibility, cloud ceiling and flying distance from a cloud. When the weather conditions are above these minima, Visual Meteorological Conditions (VMC) prevail. When the minima are not fulfilled, the prevailing conditions are said to be Instrument Meteorological Conditions (IMC). Consequently, IMC and VMC are mutually exclusive. (EASA, 2012b)

In layman's terms, flying in IMC means flying in poor weather and in cloud. When the IMC prevails, pilots must fly with sole reference to the aircraft's instruments to navigate and to avoid obstacles. In VMC, pilots can determine the aircraft attitude primarily by the horizon and other outside visual cues. Also navigation is done by visual reference to the ground and obstacles.

It is important to understand the meaning of IMC in the context of this thesis. If an engine failure occurs in VMC for a single-engine aeroplane, it is relatively easy for a pilot to make a decision about the forced landing site by looking outside and selecting the most suitable piece of terrain and then continue the approach and landing with visual cues. In IMC, this is usually not possible. The pilot must determine the aircraft's position relative to suitable emergency landing site by some other means – the instruments.

Generally, to fly in IMC, the flight must be conducted according to Instrument Flight Rules (IFR). It is important not to confuse IMC with IFR – it is normal to fly under IFR when the prevailing meteorological conditions fulfil the criteria for VMC. In fact, most of the commercial operators in Europe operate with only IFR despite the weather conditions. This is due, for example, to have single operating procedures for all weather conditions and to allow continuing of the flight in case of unpredicted weather deterioration. Furthermore, the IFR have more safety barriers included in the regulations than in its counterpart Visual Flight Rules (VFR).

2.3 Approach Flight Phase

A single flight can be roughly divided in the following phases: taxi-out, takeoff, climb, cruise, descent, approach, landing and taxi-in. Taxonomies for different flight phases vary slightly depending on a source, but this general division is sufficient in the context of this thesis.

Approach is a phase at the end of the flight before landing. During approach, aircraft is navigated to final track, slowed down and configured for landing including, for example, lowering a landing gear and extending landing flaps and slats. When flying with Instrument Flight Rules (IFR), approaches are flown according to Instrument Approach Procedures (IAP). An IAP may contain five separate segments: the arrival, initial, intermediate, final and missed approach segments. In addition, an area for circling the aerodrome under visual conditions is also considered. The different approach segments begin and end at designated fixes. However, under some circumstances certain of the segments may begin at specified points where no fixes are available. The approach segments and relative fixes are illustrated in the Figure 1 below. (ICAO, 2006)

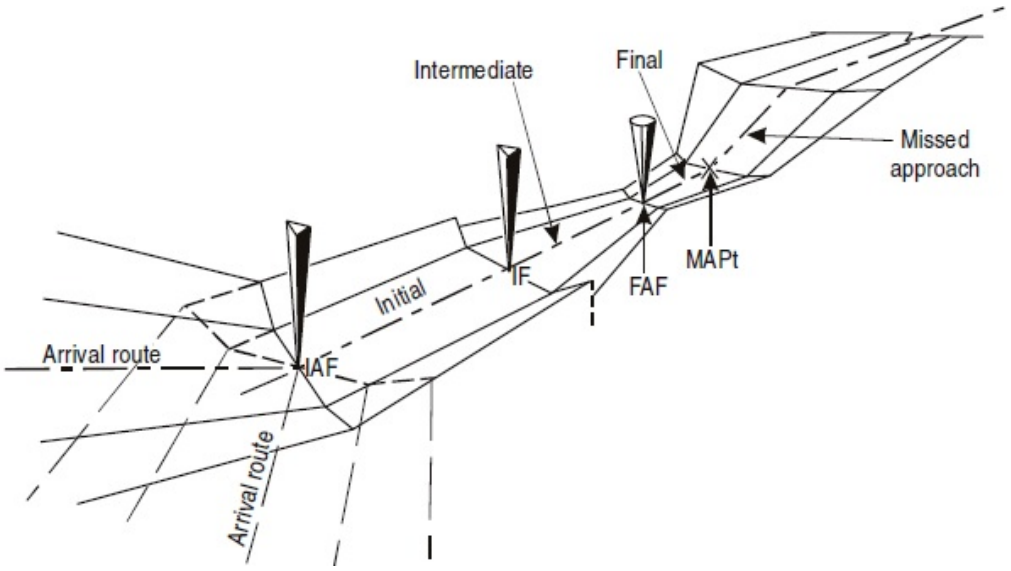

Figure 1. Segments of an instrument approach. (ICAO, 2006)

An optimum and minimum descent angle in the final approach segment is 3.0 degrees. The angle may vary slightly between approaches to different runways. Nonetheless, it guarantees obstacle clearance requirements according to procedure design criteria. (ICAO, 2006) Designed final approach angle is published in instrument approach charts and cannot be modified by pilots. Thus, in the final segment the aircraft altitude at each position is predetermined. Generally, the final descent angle is smaller than the best and lowest glide angle current SET aeroplanes can achieve without engine power. Consequently, in the final approach segment, the approaching aircraft is often beyond gliding distance from the runway in use. The only means of possibly decreasing this risk area and increasing gliding distance is using higher approach speeds and delaying the configuration of the aeroplane for the landing. Extension of flaps and landing gear will increase drag and decrease the gliding capability of the aeroplane.

However, in the segments preceding the final approach, the pilots may affect the decent profile more, as the descent angle is not usually fixed. Especially in the often relatively long arrival segment, it may be possible to use higher descent angle than the nominal three degrees and to maintain high speeds. Arrival routes permit transition from the en-route phase, normally from an Air Traffic Services (ATS) route, to the approach phase. The arrival route normally ends at the Initial Approach Fix (IAF) (ICAO, 2006). As an example, Helsinki Airport (ICAO code: EFHK) runway 15 Standard Instrument Arrival (STAR) routes can be seen in the Figure 2. In general, STAR construction can vary significantly between airports. At some locations, for example traffic flow and noise abatement procedures might require flying longer periods of time below or above the optimal altitude. These constraints are published in the instrument charts.

An IAP may be flown in IMC or VMC depending on the weather conditions. Considering an engine failure, IMC poses more challenges to the pilots to carry out an emergency landing safely. At least the final part of final approach segment is almost exclusively conducted in VMC, when the aircraft descents below the cloud base. Exceptions are highly automated and sophisticated high category precision approaches, but current SET aircraft on the market are not qualified for these.

This thesis focuses solely on the approach flight phase. The safety during approach is studied as it is probably the riskiest phase for a single-engine aircraft, considering the possibility of an engine failure. This is due to flying relatively long periods of time in low altitudes from where the forced landing to destination aerodrome is not always possible. The arrival segment routes vary greatly depending, for example, on which runway is in use and from which direction the flight arrives. Taking all variables into account, the approach is also possibly the most complex flight phase to examine. The operators are, however, required to provide an estimate on the risks involved in each phase.

Also the initial climb after takeoff includes low altitude flying. In general, the aeroplane will momentarily be on such an altitude from where a landing back to the departure aerodrome cannot be executed (neither landing ahead on the remaining runway nor turn back). But as the climb gradient with working engine is often greater than the glide gradient without engine power, the aeroplane will sooner or later gain enough altitude to always carry out an emergency landing back to the departure runway. Usually, some 1000 feet of altitude is required to make a 180-degree turn back. Therefore, the initial climb phase is generally much more straightforward and easier to examine than the approach. This applies unless there are significant climb restrictions in the instrument departure procedures.

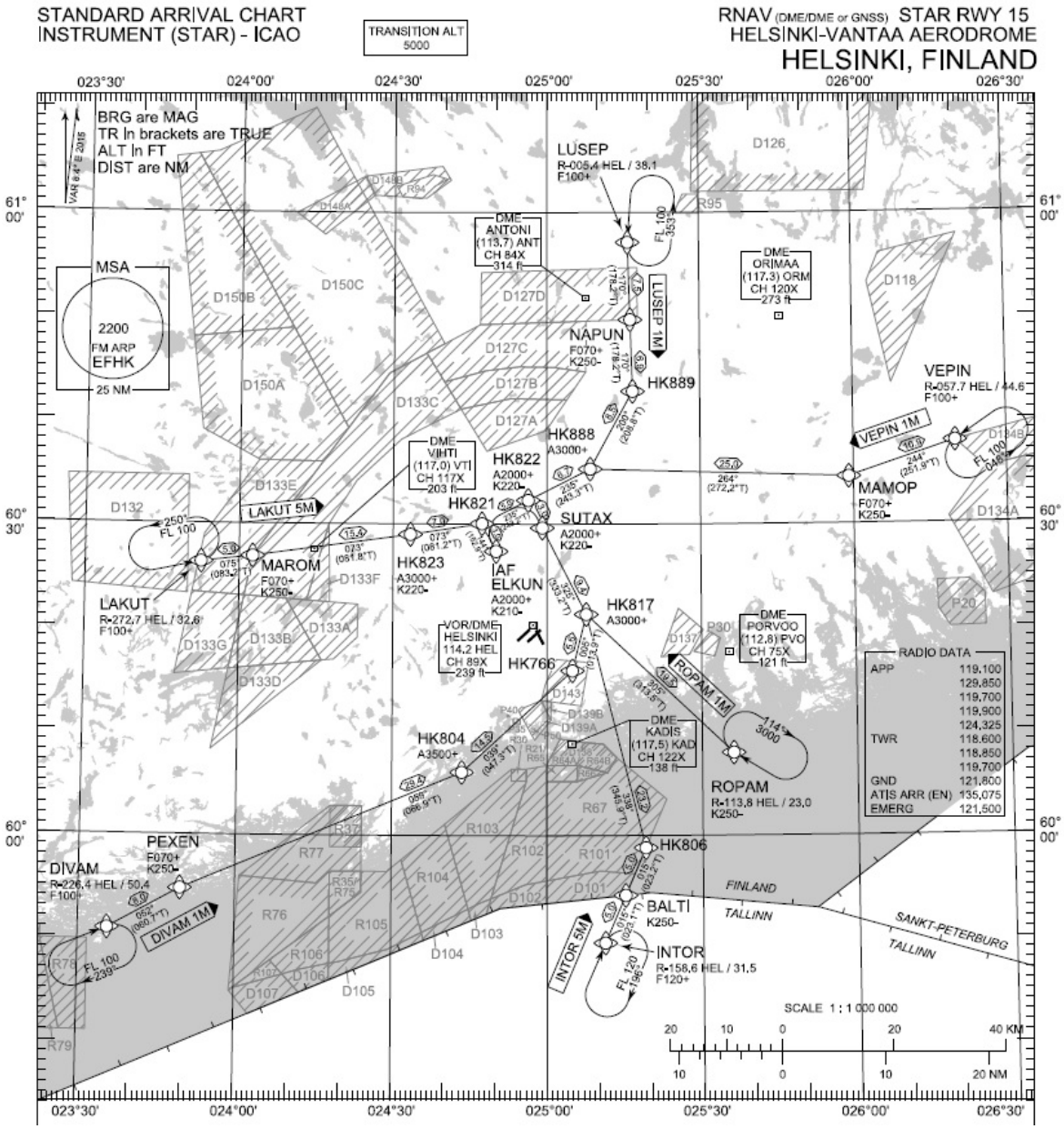

Figure 2. Helsinki Airport runway 15 standard arrival routes. (Finavia, 2017)

2.4 Flight Safety

Safety of the flight operations is or at least should be of top priority for each operator. The concept and aim of flight safety is rather obvious: to decrease the number of incidents and accidents. Being simple as a high level definition does not mean that it would be easy to manage. Achieving 100 per cent safety level is practically an impossible goal. Often, but not always, increasing safety level means analogously increasing costs of the safety management. After some point the costs start to rise exponentially compared to the achieved improvement in safety level. For this reason, risk management models such as ALARP (As Low As Reasonably Practicable) where risks are lowered to a reasonable level without exceeding unacceptable increases in investments, are commonly used (Lee, 2006). One definition of aviation safety is given in ICAO's Safety Management Manual (SMM):

"While the elimination of aircraft accidents and/or serious incidents remains the ultimate goal, it is recognized that the aviation system cannot be completely free of hazards and associated risks. Human activities or human-built systems cannot be guaranteed to be absolutely free from operational errors and their consequences. Therefore, safety is a dynamic characteristic of the aviation system, whereby safety risks must be continuously mitigated. It is important to note that the acceptability of safety performance is often influenced by domestic and international norms and culture. As long as safety risks are kept under an appropriate level of control, a system as open and dynamic as aviation can still be managed to maintain the appropriate balance between production and protection." (ICAO, 2013b)

As the highest-level aviation regulator, ICAO has published their safety related rules and recommendations for the member states. Even a new annex (Annex 19 Safety Management) was released in 2013 to consolidate the existing SMM. The new annex collects common safety management elements from the existing annexes to make them easier to find. The purpose of the annex 19 is to support the continued evolution of a proactive strategy to improve safety performance (ICAO, 2013a). Together with SMM, it provides the framework for a comprehensive Safety Management System (SMS), a systematic approach to managing safety for different aviation organisations. A following definition is given for an SMS:

"An SMS is a system to assure the safe operation of aircraft through effective management of safety risk. This system is designed to continuously improve safety by identifying hazards, collecting and analysing data and continuously assessing safety risks. The SMS seeks to proactively contain or mitigate risks before they result in aviation accidents and incidents. It is a system that is commensurate with the organization's regulatory obligations and safety goals." (ICAO, 2013b)

The European aviation rule maker, European Aviation Safety Agency (EASA), has adopted ICAO's SMS concept in its regulations. Elements of SMS are divided in various regulatory texts for different organisation forms (airworthiness, flight crew training, operators and air traffic management). For example, the regulations concerning operators are included in the Commission Regulation (EU) No 965/2012 (Air Operations) and the related agency rules. (EASA, 2017c)

These safety addressing regulations set the frames for operators to help them achieve the minimum acceptable level of safety. Yet, when the operators themselves put more effort in safety, the highest safety levels are achieved. With the help of harmonisation of regulations and organised safety management work, the aviation industry has been continuously able to decrease the number of incidents and accidents throughout the history of aviation. As an example, the development of fatal accidents for commercial jets can be seen from the Figure 3 below (Airbus, 2014).

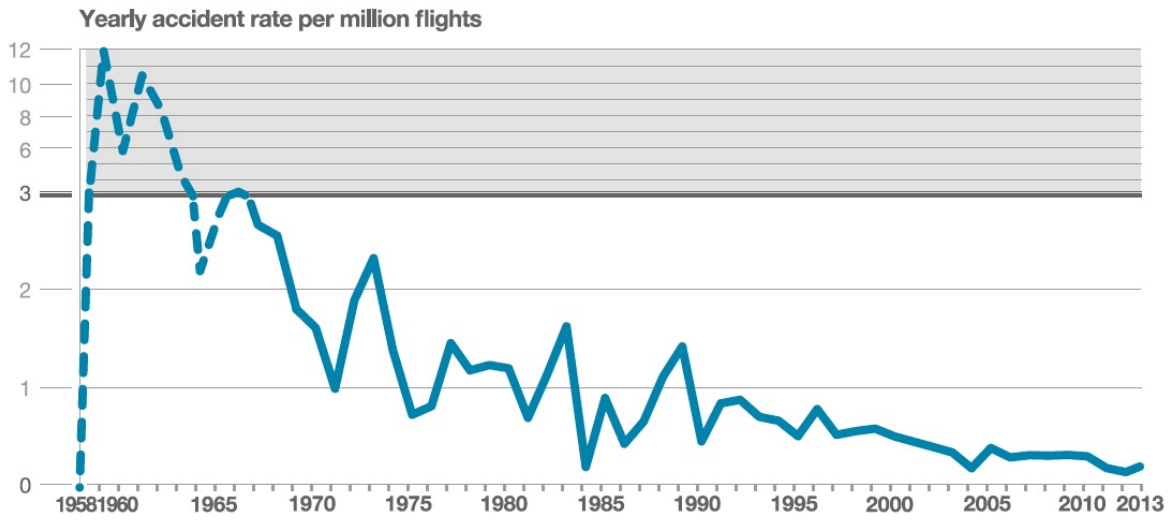

Figure 3. Fatal accident rates for commercial air transport jets. (Airbus, 2014)

In the spirit of current safety culture development, this thesis aims to give single-engine turbine Air Operator Certificate (AOC) holders one relatively simple tool for their SMS to identify hazards related to possible loss of thrust and manage the risks involved.

3 Commercial Single-Engine Turbine Operations

3.1 Introduction

The nature of commercial flight operations in general depends on the aircraft used. There are some regulatory differences concerning, for instance, required equipment, flight planning and data monitoring that depend on factors such as the maximum takeoff mass (MTOM), certified passenger capacity, and number and type of engines. Some issues are not regulated by the authorities but might require insight from the operator to conduct safe operations. This chapter introduces the main regulations and other specialties related to commercial single-engine turbine operations.

3.2 Regulations

As in any aviation, the regulations concerning operations are multileveled and constantly changing. The International Civil Aviation Organization (ICAO) forms the global base for aviation regulations by setting standards and recommended practices (SARPs). In Europe, European Aviation Safety Agency (EASA), a community agency established in 2002 under the European Union, is the highest level of aviation authorities. Yet, the national civil aviation authorities (CAA) still have some power of decision. Typically, EASA adopts most of the ICAO SARPs as they are, but this is not always the case.

In general, commercial single-engine operations have long been approved in relatively good Visual Meteorological Conditions (VMC) in daylight, but not in IMC or at night. To conduct feasible commercial operations, especially in weather sensitive Europe, utilization of IMC must be available. Otherwise, unpredictable weather conditions would inevitably cause too many flight cancellations.

3.2.1 ICAO

ICAO has accepted commercial operations of single-engine turbine-powered aeroplanes at night and/or in IMC since 2005 when it published additional requirements for the operations. These requirements can be found in Annex 6: Operation of Aircraft, and the related appendix and guidance material. Relevant in the context of this thesis is the requirement that the state of the operator shall ensure the overall level of safety is on sufficient level provided by, for instance, the reliability of the turbine engine, the operator's operating practices, flight dispatch procedures and crew training programmes. (ICAO, 2010)

All aforementioned issues are related to the possible loss of engine power and the proactive actions the operator should do to minimise consequent injuries, as well as damages to the aircraft and third parties. Safety aspects, such as the engine reliability and pre-flight planning are discussed in more detail in the next subchapters. The general idea is, however, that a safe forced landing in the event of an engine failure or major malfunction can be carried out. Some exceptions are given to aeroplanes with very high engine reliability, additional systems and operational equipment, procedures and training requirements (ICAO, 2010).

ICAO has also set some additional guidance on the given requirements. Operators are required to include all necessary information relevant to operations in their operations

manuals. This covers procedures and training required for such operations, including pre-planning and risk analysis for engine failure cases. Related to operator certification and validation, ICAO member states aviation authorities should ensure the adequacy of the operator's procedures for normal, abnormal and emergency operations, including actions following engine, systems or equipment failures. The operators should address specific training procedures to cover engine failure and malfunction situations in different flight phases. They should also examine departure and arrival procedures and possible route limitations for operations on single-engine turbine-powered aeroplanes. One example of route limitation is operations over water. According to ICAO's recommendations, the distance that the aeroplane may be operated from a land mass suitable for a safe forced landing should be determined. This comes from distance an aeroplane is capable of gliding from the cruise altitude without engine power, assuming still air conditions. Member states may add some restrictions considering the type of operation and likely prevailing conditions, such as the sea conditions. If member states decide to allow extensions the total time beyond the gliding distance should not exceed 15 minutes at the aeroplane's normal cruise speed. (ICAO, 2010)

3.2.2 EASA

EASA had not brought the ICAO SARPs related to single-engine turbine commercial operations at night and in IMC into effect until recently. EASA refers to associated regulations as CAT SET-IMC. The establishment of European SET-IMC regulations was completed on 1 March 2017 when the regulations entered into force, during the writing of this thesis. This means the European regulatory framework was misaligned with ICAO standards for well over a decade. It was also out of sync with some other major third ICAO member states, such as the United States of America, Canada and Australia who had already allowed SET-IMC operations (EBAA, 2016).

Already in 1991 the EASA predecessor Joint Aviation Authorities (JAA) started to consider the possibility to allow cargo and passenger carrying at night or in IMC with SET aircraft but were unable to present proposals acceptable to all member states (EBAA, 2016). There was a long controversy on the required safety standards. During the recent years, European countries woke up to realise that modern turbine engines and aircraft instruments have become very reliable making SET operation safer than it used to be. Some studies suggest that such operations might be even safer than similar operations with older twin-engine aeroplanes (JAA, 2004). In addition, SET operations will open up economic possibilities for new low-density routes, not forgetting the environmental benefits coming from lower fuel consumption of modern single-engine turboprops (EBAA, 2016).

In 2013 EASA announced a new rulemaking task RMT.0232 & RMT.0233 which aimed to develop rules to allow commercial SET-IMC operations. The process went through a formal rulemaking steps: Notice of Proposed Amendment (NPA) was published in 2014 and the related Comment Response Document (CDR) late 2015 with 157 comments from interested parties, including EU competent authorities, aircraft manufacturers, air operators, and different associations (EASA 2015b). Based on the comments and responses, also an Opinion No 06/2015 was developed and published in order to assist the European Commission in its preparation of proposals for amended regulations (EASA, 2015a). Above mentioned rulemaking documents are based on NPA (NPA OPS 29 Rev 2) published in 2004 by JAA but not accepted by all EU member states at the time, an

independent study on the risks of SET-IMC operations and possible mitigating factors by QinetiQ (Bradley, 2007) and the ICAO Annex 6. According to the opinion No 06/2015, the publication of the final decision, with some changes to the proposed amendments, was initially planned to the third quarter of 2016 but was eventually delayed by a few months.

The regulations concerning all commercial air transport (CAT) operations can be found from Commission Regulation (EU) No 965/2012 Annex IV (Part-CAT), Annex III (Part-ORO - Organisation Requirements for Air Operations) and Annex V (Part-SPA - Operations requiring Specific Approvals). This initial regulation has since been amended several times. The amending regulation that brought CAT SET-IMC into force was Commission Regulation (EU) 2017/363. It introduced a new Subpart L for Annex V (EASA, 2017b). Some of the SET-IMC regulations relevant in the context of this thesis are introduced below.

The EASA regulations state that single-engine aeroplanes shall not be operated at night or in IMC unless the operator is given a specific approval by a competent authority. (CAT.POL.A.300). Also EASA requires operations on routes where a safe forced landing can be executed, unless the operator makes use of a particular risk period (CAT.OP.MPA.136 and CAT.POL.A.320). If the competent authority has not otherwise specified, the aeroplane should be capable of reaching a point 1000 feet above the preselected landing area (AMC1 CAT.POL.A.320). Additionally, when verifying the ability to reach a suitable place for a forced landing, the aeroplane's best glide gradient must be increased by a gradient of 0.5 % to add safety margin in flight planning (CAT.POL.A.320). These requirements are given for the en-route phase. (EASA, 2017a)

The competent CAAs are required to assess the operator's safety performance. The operator's capability to appropriately manage any unexpected event which could endanger the safety of their operations should be continuously monitored. (AMC3 ARO.OPS.200) This thesis aims to improve any operator's safety performance by preparing for the power loss at a critical phase of the flight.

The general requirements for the aeroplane equipment, engine reliability, crew training, flight planning and contingency procedures are somewhat in accordance with ICAO Annex 6. However, EASA has given more detailed guidelines for these in the related Acceptable Means of Compliance (AMC) texts. The AMC standards for the flight planning defining the use of the risk period are important. AMC1 SPA.SET-IMC.105(d)(2) gives the following means to comply with the related rule:

(a) "The operator should establish flight planning procedures to ensure that the routes and cruising altitudes are selected so as to have a landing site within gliding range.

(b) Notwithstanding (a) above, whenever a landing site is not within gliding range, one or more risk periods may be used for the following operations:
    (1) over water;
    (2) over hostile environment; or
    (3) over congested areas.

    Except for the take-off and landing phase, the operator should ensure that when a risk period is planned, there is a possibility to glide to a non-congested area.

> The total duration of the risk period per flight should not exceed 15 min unless the operator has established, based on a risk assessment carried out for the route concerned, that the cumulative risk of fatal accident due to an engine failure for this flight remains at an acceptable level (see GM2 SPA.SET-IMC.105(d)(2)).”

Thus, the total duration of the risk period can be a maximum of 15 minutes unless a separate risk assessment for a specific route is conducted. In the landing (and approach) phase it is not required to reach a non-congested area. However, common sense says it would be desired to the extent possible. Furthermore, for the arrival phase AMC2 SPA.SET-IMC.105(d)(2) gives a recommendation the operators should only use, to the extent possible, arrival procedures that guarantee flight path which would allow the aeroplane to land on a pre-determined landing site, in case of a loss of thrust. Also, AMC1 SPA.SET-IMC.105(d)(4) states that when the risk period is used for the landing phase, the contingency procedures after an engine failure should include information for the pilots on the path to be followed. (EASA, 2017a) For these purposes, the operators would need to examine the arrival routes and identify possible risk areas.

GM2 SPA.SET-IMC.105(d)(2) gives an example of a safety risk assessment for a specific route. With the help of this assessment the operator might be able to extend the duration of the risk period. The methodology is to divide the route in different segments, arrival being one of them. The risk profile is an estimate of the probability of an unsuccessful forced landing if the engine fails during one of the identified segments. The most important variable, when assessing the risk for a segment, is the total energy (potential and kinetic) of the aeroplane and the position relative to an emergency landing site. Other variables are, for example, weather conditions, aerodrome lighting, aircraft equipment and the operator’s standard procedures for an emergency landing. When the probability of an unsuccessful landing in a segment, assumed engine failure rate and segment exposure time are known, the segment risk factor can be calculated. (EASA, 2017a) With thorough preparation, the probability of an unsuccessful emergency landing can be decreased. Furthermore, by using high speeds the critical segment’s exposure times can be somewhat reduced.

3.2.3 National Regulations in Europe

During the past years the regulatory foundation of civil aviation in Europe has gone through a constant change. Regulations have been harmonised by EASA. National civil aviation authorities (CAA) in Europe have a duty to supervise regulations set by EASA are complied with in that country. In addition, some regulations are left by EASA for national authorities to decide. Usually then national authorities are obligated to inform EASA about the decisions made. Moreover, there are still some forms of civil aviation where the regulatory harmonisation is yet uncompleted and are not regulated by common European rules. In many areas the process is advancing but until then, national CAA’s are responsible of the rulemaking and compliance.

Some EASA countries, like Finland and France, had approved commercial SET-IMC operations even before the common acceptance, based on a derogation given in the Article 6 of the original Commission Regulation No 965/2012. It stated that member countries are allowed to grant an exemption to CAT.POL.A.300(a) but shall notify the Commission before the change is implemented (EASA, 2012a). There was an uneven playing field issue

as some operators were allowed to operate SET aircraft in IMC but others located in different countries were not. The recent changes to European aviation regulations corrected these grievances. Now these granted exemptions are valid until 2 September 2017 (EASA, 2017a). After this date the exiting operators must have an approval in accordance with the new CAT SET-IMC regulations if they wish to continue their operations.

3.3 Safety Aspects

3.3.1 Engine Reliability

It is desired that the power plant reliability is on a very high level so as to minimise the risk of a forced landing following a loss of thrust. The aircraft turbine engine reliability has indeed developed significantly over the years. However, there is always a possibility for a failure of the engine or related systems. The aviation regulators have defined a minimum target levels for the acceptable loss of power rate. The engine types in question should have accumulated sufficient experience in service for the data to be reliable. Also, some requirements have been set considering engine related systems that would either help preventing a failure or increase redundancy in case of a failure.

ICAO defines power loss as any loss of power independent of whether the cause is a faulty engine or engine component design or installation, including engine control systems and the fuel ancillary. For a turbine engine to be approved for commercial IMC operations, it is required to have shown a power loss rate of less than 1 per 100 000 engine hours. To help achieve this, the engine must be equipped with a trend monitoring system, an automatically activated ignition system, magnetic particle detection for the engine and gearboxes, and for the case of failure of the fuel control unit there must be an emergency engine power control device. The engine trend monitoring is the operator's responsibility and should include an oil consumption monitoring and engine condition monitoring. According to ICAO's guidance, the data used in reliability analysis should be derived from commercial operations and supplemented with data from similar private operations. The minimum service experience is deemed to be 20 000 hours on particular aeroplane-engine combination. Alternatively, data from sufficiently similar engine variants can be utilised or the minimum hours decreased with some additional testing. When making the reliability assessment, statistical estimates derived from world fleet database may be used. (ICAO, 2010)

The fundament of the new EASA's regulations for commercial operations is to allow operations on aeroplanes meeting specified power plant reliability and equipment requirements (EASA, 2015a). The CAT SET-IMC regulations use the same 1 per 100 000 flight hours maximum power loss rate as ICAO. To demonstrate the required level of reliability, the in-service experience of the airframe-engine combination in question should be at least 100 000 hours – significantly exceeding the ICAO's recommendation. EASA too approves supplementary means, such as testing and analysis, to demonstrate that the reliability criteria are met if the required experience has not been accumulated. When the operations are established, the operators are required to report power loss occurrences to the authorities who should then make an assessment of the operator's capability to achieve and maintain an acceptable level of propulsion system reliability. (EASA, 2017a)

The requirements related to engine reliability were overall very similar already in JAA proposals (NPA OPS 29 Rev 2) in 2004. The propulsion system in-flight shutdown or loss

of power rate of less than 10 per 10^6 hours was derived and with many other fundamental requirements it has then been adopted to the EASA regulatory base. A thorough study was performed on the associated risks and compared also to operations on comparable light twin-engine aeroplanes. The conducted meta-analysis showed that the loss of power rate for single-engine turboprops in commercial and appropriate government operations in western countries between 1991 and 2002 was 1.38 per 10^6 hours. Thus the existing airframe-engine combinations included in the JAA's study (Cessna 208, Pilatus PC-12 and Socata TBM-700) seem to fulfil the ICAO/EASA target. (JAA, 2004) If the target of 10 per 10^6 hours is used in risk analysis it can be considered conservative. This is desirable taking into account a low statistical confidence of the meta-analysis yielding from relatively narrow database representing the commercial operations on single-engine turboprops. Many of the figures are based on estimates and may have errors of tens of per cents. Furthermore, the JAA study leaves out private operations that make a significant part of SET operations.

Another estimate on the Pilatus PC-12 turboprop engine PT6A reliability is commonly accepted shut down rate of around 2.7 per 10^6 hours (Simpson, 2016). This is still well below the regulatory target rate. However, one more reliability survey of UK registered twin-engine turbine aircraft below 5700 kg and powered by the PT6 engines indicated a failure rate of 43 per 10^6 hours, for the period from 2000 to 2004 (Bradley, 2007). This is about four times greater than the target set for the SET-IMC operations. Although the study period was relatively short and included also general aviation, a clear explanation for the discrepancy compared to other studies on the same topic was not found.

3.3.2 Emergency Landing Sites

The success of a forced landing depends on the aircraft's total energy at the point of an engine failure and position with relation to a sufficient landing area. The area should be free of obstacles with the surface allowing a safe landing run. Moreover, the success is affected by the cues available for the flight crew to navigate to the landing field and to execute the manoeuvres required for a safe power off landing. (Bradley, 2007)

According to ICAO, the operator must "identify aerodromes or safe forced landing areas available for use in the event of engine failure" in the flight planning. All relevant information shall be taken into account when evaluating intended routes. For example, it is important to consider the nature of the terrain to be overflown. The terrain should enable carrying out a safe forced landing. ICAO's definition for a safe forced landing area is that "it can reasonably be expected that it will not lead to serious injury or loss of life, even though the aeroplane may incur extensive damage". An exemption is given for aeroplanes with high engine reliability, trend monitoring systems and equipment – a forced landing area does not need to be available at all points along a route. (ICAO, 2010) Basically this means utilisation of a pre-determined risk period of which maximum duration is specified by the competent aviation authorities. However, the aircraft systems must always "include a certified area navigation system capable of being programmed with the positions of aerodromes and safe forced landing areas, and providing instantly available track and distance information to those locations" (ICAO, 2010).

EASA regulations concerning the emergency landing site availability were already briefly discussed in the subchapter 3.2.2. Here the focus is more on expected landing site characteristics. Accepted landing site is defined in AMC3 SPA.SET-IMC.105(d)(2):

> "A landing site is an aerodrome or an area where a safe forced landing can be performed by day or by night, taking into account the expected weather conditions at the time of the foreseen landing."

The operators are required to develop a system for the assessment of each new route. They must select aerodromes suitable for landing along the route. When evaluating the applicability of the landing site it is recommended to consider at least size and shape of the landing area, longitudinal and lateral slope, obstacles and type of ground surface. The outcome should be that a safe forced landing can be reasonably expected without injuries to people on board the aeroplane or on ground. Suitable landing sites should be readily programmed into the navigation system in such a way that distance and course to the sites are immediately available. For the arrival segment the operator should use, to extent possible, the arrival procedures that enable the aeroplane to land on a safe forced landing area. (EASA, 2017a)

In the approach phase the most natural selection for an emergency landing site is the destination airport. When flying STARs or being vectored around the airport to align the aircraft for the final approach, it is not always possible to be within gliding distance from the landing runway. For these situations the operator can either use the risk period or determine another emergency landing site.

3.3.3 Fatal Accident Rate

The concept of accepted fatal accident rate can be compared to previously mentioned ALARP model. A small probability for the engine failure always exists and sometimes the following emergency landing can be fatal. Therefore, an acceptable level for these accidents must be determined. Fatalities can furthermore result from other root causes than engine failure. But in the context of this thesis, only the fatal accident rate following an engine failure is relevant.

EASA's safety target for an overall fatal accident rate in the SET-IMC operations including all causes is less than 4 per 10^6 flight hours. Based on accident databases, it can be considered the propulsion system failure does not contribute by more than 33 % to the total fatal accident rate. Thus, EASA target is that the probability for a fatal accident following an engine failure remains below 1.3 per 10^{-6} for each flight. This figure forms the basis for operator's safety risk assessment for the flown routes. (EASA, 2017a)

According to a statistical study conducted by JAA in the beginning of the millennium the fatal accident rate in commercial operations due to power loss was 0 per million flight hours. This study had disregarded one fatal power loss accident in 1985 which was caused by taking off with both fuel selectors off. Reasoning was the event occurring before the examined time period (1991 – 2002) and that the same result would have been expected also for a twin-engine aircraft. The overall fatal accident rate in the same study is 4.79 per 10^6 hours. Most of the accidents have happened to Cessna 208 Caravan and none to Pilatus PC-12. (JAA, 2004) Once again, the statistics should be reviewed critically as the sample size for commercial SET-IMC operations is rather low.

A more recent study on power loss accident cases for turboprops have been published in 2013 by Robert E. Breiling Associates. It covers the accidents occurred amidst U.S. and

Canadian registered fleets from the aircraft introduction until 2012. (Robert E. Breiling Associates, 2013) Summary of the key figures relevant for this thesis have been extracted to Table 1 below. The studies indicate that the respective EASA safety targets can be fulfilled and allowing commercial SET-IMC operations is justified.

A critical factor affecting the fatal accident rate is the probability of a successful forced landing. According to a study 88 per cent of emergency landings, both day and night, for single-engine turboprops are non-fatal (JAA, 2004). Indeed, if the engine failure occurs on relatively high altitude on cruise phase giving the pilots enough time to find a suitable landing area and prepare for the landing the chances are rather good. If the failure occurs on low altitude and/or above unsuitable terrain (for example built-up or mountainous areas) the probability for a successful emergency landing decreases. Also the prevailing weather conditions, especially visibility and cloud base are contributing factors.

Table 1. SET aeroplane accident data for U.S. and Canadian registered fleets. (Robert E. Breiling Associates, 2013)

	Cessna 208	**TBM-700/ TBM-850**	**PC-12**	**PA-46-500TP**
Fleet size (by year end 2012)	878	422	794	363
Hours flown	8 445 005	734 072	2 958 834	575 456
Accidents due power loss / mechanical malfunction / failure	20	2	4	2
Power loss accident rate per 10^6 flight hours	2.4	2.7	1.4	3.5
Power loss fatal accident rate per 10^6 flight hours	0.12	0	0	0
All fatal accidents per 10^6 flight hours	6.5	16.3	3	19.1

As previously mentioned, during approach phase the aeroplane is flying on a lower altitude and often the number of suitable landing sites are furthermore decreased by man-made buildings and infrastructure around the destination airport. Moreover, flying over densely populated areas includes higher risk for third parties. Fortunately, STARs tend to be coincident with minimum noise routes, avoiding densely built-up areas. On arrival segment, whether on a STAR or ATC vectors, pre-determined emergency landing spots programmed into the aircraft navigation system could improve the probability for a successful landing, thus reducing the fatal accident rate following an engine failure.

3.4 Aircrafts for SET Operations

The number of single-engine turbine (SET) aircraft models suitable for commercial air transportation is currently quite limited. Some of the most common models on the market are Pilatus PC-12, Socata TBM, Cessna 208 Caravan and Piper PA-46-500TP Malibu

Meridian. For example, at the time of the writing there is one operator in Finland, Hendell Aviation, operating with Pilatus PC-12 (Hendell Aviation, 2017). In addition, French operator Voldirect uses PC-12 and TBM 850 (Voldirect, 2017) and Swedish Nordflyg Air Logistics transports cargo with Cessna 208B Caravan (Nordflyg Air Logistics, 2017). Outside Europe there are several operators using varying SET aircraft fleets.

Some manufacturers are aiming for the growing SET market and developing new models to compete with the existing ones. For example, Textron Aviation has recently revealed plans to develop a single-engine turboprop for eight passengers (Bergqvist, 2016). In the perspective of the case study in this thesis, the focus will be on Pilatus PC-12/47E as already one operator in Finland operates with this make and model introduced in more detail below.

3.4.1 Pilatus PC-12/47E

The Pilatus PC-12/47E (Figure 4) is the most recent commercial variant of a Swiss made single-engine turboprop aircraft Pilatus PC-12. It is also known as PC-12 NG (Next Generation). The aircraft is powered with 1200 hp Pratt & Whitney Canada PT6A-67P turboprop engine. It is certified for 9 passengers plus two pilots and the maximum takeoff mass (MTOM) is 4740 kg.

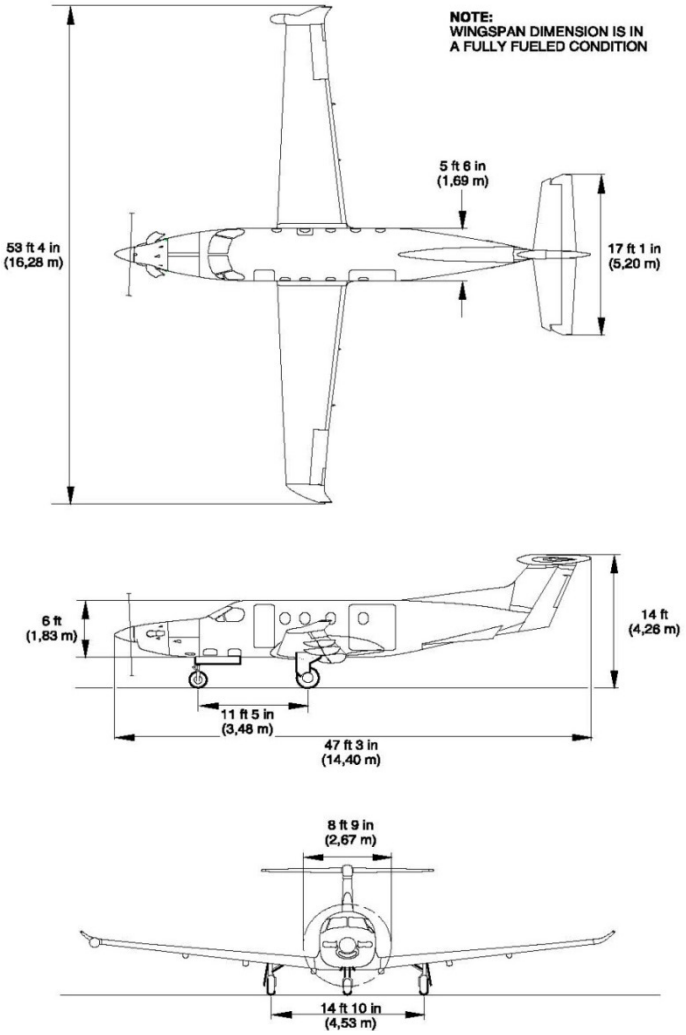

Figure 4. Pilatus PC-12/47E three view and dimensions. (Pilatus Aircraft, 2016)

The PC-12/47E has a pressurised cabin and it can climb to a maximum operating altitude of 30 000 ft and cruise with maximum operating speed of 240 kt indicated airspeed (IAS) or Mach 0.48. The maximum reachable cruise speed in true airspeed (TAS) is 285 kt (= 528 km/h) and the maximum calculated range is 1845 nautical miles (NM) (= 3417 km). A theoretical glide ratio E_{max} with feathered propeller blades is close to 16:1 (exact value 15.798:1), meaning the PC-12 can glide approximately 78 NM from the maximum operating altitude of 30 000 ft down to sea level in still air. The glide time in this case can be over 30 minutes. The glide ratio is an important factor when planning commercial SET-IMC flights and studying possible risk period.

As opposed to older PC-12 variants, the 47E is equipped with sophisticated Honeywell Primus Apex integrated avionics system. It comprises a full glass cockpit – there are no traditional analog instruments but only electronic displays for presenting flight instruments and navigation information to pilots. The Pilatus PC-12 NG can be furthermore equipped with an optional Primus Apex Smartview synthetic vision system. It provides the flight crew an excellent aid for navigation and avoiding obstacles, for example, in the case of an engine failure in IMC. The Smartview is not approved to be used as sole reference for navigation. But as the displayed synthetic 3D scenery of the outside world is similar to what the pilots would see through the windshield during daylight in good weather conditions, it decreases the pilot workload significantly in emergency situations. An example of the PC-12 primary flight display view with the synthetic vision system is given in the Figure 5 below. (Pilatus Aircraft, 2016)

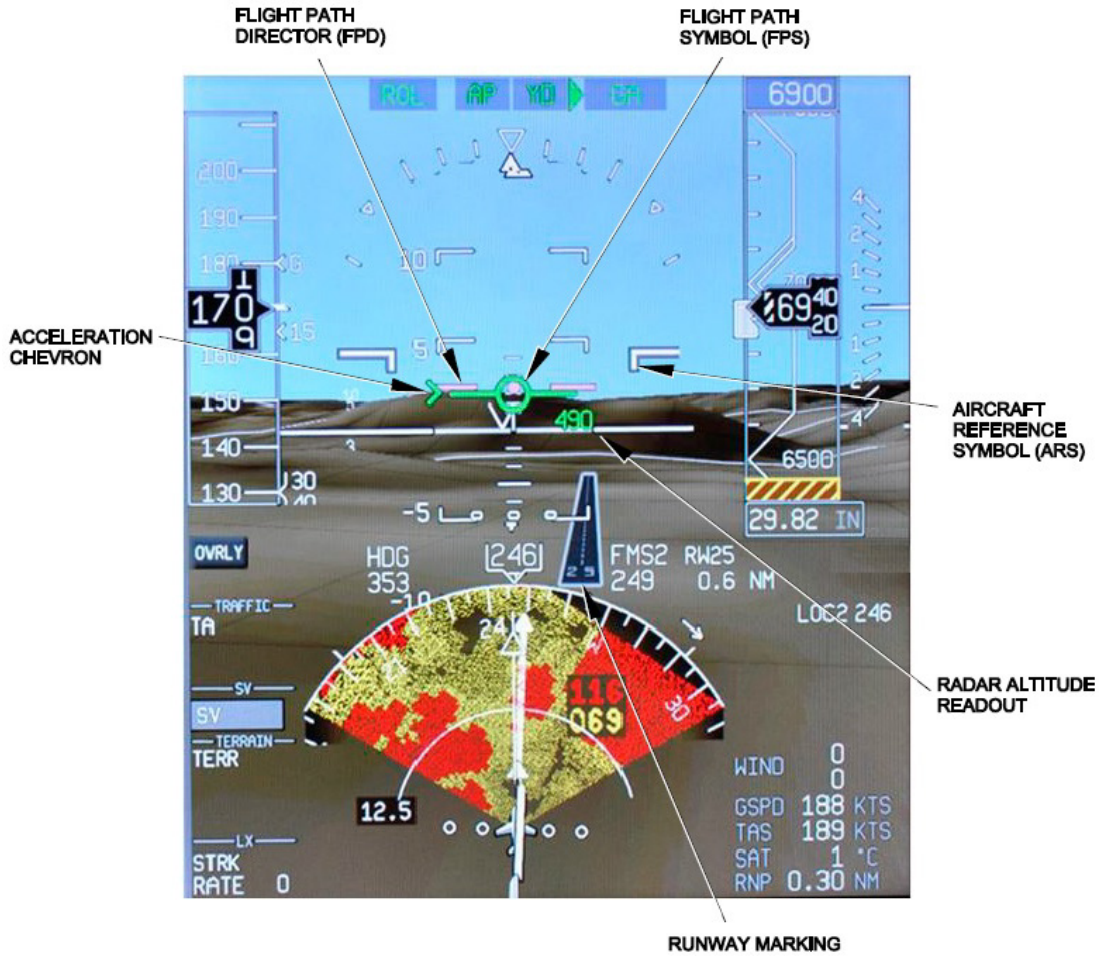

Figure 5. Smartwiev synthetic vision system on the Pilatus PC-12. (Pilatus Aircraft, 2016)

4 Theory for the Analysis

4.1 Gliding Flight Mechanics

When the engine fails completely in a single-engine aircraft it practically becomes a glider. Reaching the maximum gliding capability requires feathering the propeller that is turning the propeller blades parallel to the airflow. Otherwise the windmilling propeller would cause excessive drag increasing the glide angle. This study assumes the propeller feathering system is operative. A partial power loss is also possible. In that case, the engine is capable of producing some thrust, possible consequent still being an emergency landing but with smaller gliding angle. A total and immediate power loss is assumed in this thesis, meaning that thrust is set to zero instantly when the engine failure occurs.

A stationary gliding flight with a relatively shallow glide angle or flight path angle γ is assumed. Thus it can be estimated that $\cos\gamma \approx 1$ and $\sin\gamma \approx 0$ (with γ in radians). Furthermore, the glide angle in steady wind can be extracted from the following equation: (Hoffren and Rahikainen, 1992)

$$\gamma = -\frac{1}{E} \tag{1}$$

where E is the glide ratio of the aircraft. The Equation 1 yields a negative value for flight path angle γ (downwards) but for this thesis the glide angle is defined to be always positive and the minus sign is discarded. Furthermore, the glide ratio can be calculated with the equation below:

$$E = \frac{R}{\Delta h} \tag{2}$$

where R is the glide range and Δh the change in altitude. The relation between the altitude, glide range, glide ratio and glide angle can also be seen geometrically from the Figure 6. The glide ratio E and glide angle γ are independent of the aircraft weight and air density. (Hoffren and Rahikainen, 1992)

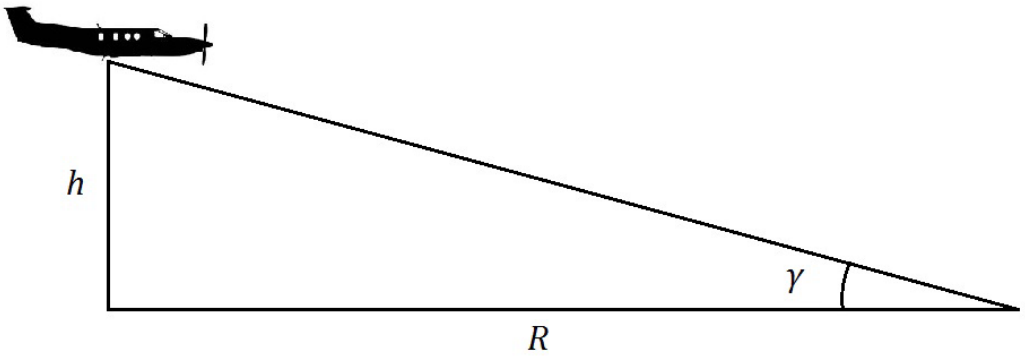

Figure 6. The gliding flight.

As mentioned in the previous chapter, the Pilatus PC-12 can glide approximately 78 NM from the altitude of 30 000 ft. Thus, the best glide ratio E_{max} for this aircraft is 15.798 and

calculated with the Equation 1, the minimum theoretical glide angle γ_{min} is 3.67°. It is not, however, meaningful to use the best theoretical values for the analysis as many factors, such as piloting accuracy and degrading of the aerodynamic efficiency, de facto decrease the gliding capability. The EASA required flight planning safety margin increment of 0.5 % for the best glide gradient is applied and the value rounded up. Thus the calculations in the analysis are made with γ_{min} of 3.95°. Moreover, the effect of wind is discussed separately in the next subchapter 4.1.1.

In steady state gliding flight the indicated airspeed V is practically constant. To reach the maximum glide distance in still air, the glide must be flown with minimum drag airspeed V_{md} (Hoffren and Rahikainen, 1992). The minimum drag or best glide speed depends on the aeroplane current weight. The given values for Pilatus PC-12 vary between 93 kt and 119 kt (IAS) for weights at range 2900 – 4740 kg (Pilatus Aircraft, 2016). The speed that an operator will use in case of engine failure might also depend on the operator's standard operating procedures (SOP). In the approach phase, it is not reasonable to use the V_{md} given for the maximum mass as the aircraft never weights this much after burning fuel in the previous flight phases. For simplicity, a fixed value of V_{md}= 116 kt, corresponding to aeroplane mass of 4500 kg is used in this study.

If the aircraft has excess speed compared to V_{md} when the engine fails, the kinetic energy can partially be transformed into potential energy. This transformation cannot, of course, be done without energy losses. Lacking a better knowledge and taking human factors (reaction time and piloting skills) into account, an estimate that 50 % of the excess speed can be converted to altitude is applied in this research. The conversion is calculated with the revised total energy equation below.

$$\Delta h_V = 0.5 \cdot \frac{(V - V_{md})^2}{2g} \tag{3}$$

where Δh_V is the change in the aeroplane's altitude, V the indicated speed at the moment when the engine fails and g the constant gravitational acceleration of 9,81 m/s^2. It is assumed that the speed is transformed into height instantly at the engine failure, increasing the equivalent altitude h_{eq} at the beginning of the glide.

One glide performance related factor that must be taken into account is the turns needed to align the aeroplane to the landing runway heading. Altitude is lost during these turns. A standard "rate one turn" often used in instrument flying is accomplished at a heading change of 3° per second resulting a full 360-degree turn in two minutes. At altitudes below 10 000 feet, the Pilatus PC-12 weighing 4500 kg loses 5000 feet in approximately 6 to 7 minutes in glide, depending on the air temperature (Pilatus Aircraft, 2016). This means that the vertical speed would be around 800 feet per minute. Thus the Pilatus PC-12 loses approximately 1600 feet during a 360-degree rate one turn during the glide. For a lighter PC-12 the rate would be less. According to practical experience, the PC-12 can make a 360-turn even within 1000 feet lost altitude if a steeper bank (30°) than what is required for a rate one turn is applied (Keltanen, 2017). To be conservative, the calculated value of 1600 ft/min is used in this study.

A current heading between each STAR waypoint can be seen in the instrument charts in the Appendix 1. This heading is first compared to the heading required to reach an

emergency landing key point (the concept of the key point is explained later in this chapter). Then, a final turn from the key point heading to the runway heading is calculated. Adding together these two heading changes gives the total amount of required turns. The altitude lost during the turns Δh_{turn} can be calculated and the result is subtracted from the equivalent altitude h_{eq} at each point. The equivalent altitude is consequently:

$$h_{eq} = h + \Delta h_V - \Delta h_{turn} \tag{4}$$

4.1.1 Effect of Wind

The wind is practically never completely calm. Wind conditions vary greatly and are difficult to take into account accurately. Thus it is often general regulatory practice to assume still air conditions. For example, ICAO Annex 6 guidance for SET-IMC operations over water states: "The distance that the aeroplane may be operated from a land mass suitable for a safe forced landing should be determined. This equates to the glide distance from the cruise altitude to the safe forced landing area following engine failure, assuming still air conditions" (ICAO, 2010).

However, EASA's regulatory material stipulates that when operators are assessing a new route they should evaluate specific weather conditions that might affect the capability of the aeroplane to reach the selected forced landing area (AMC1 SPA.SET-IMC.105(d)(2)). The likely ambient conditions (cloud ceiling, visibility, wind and light) should be taken into account in the safety risk assessment for each flight segment (GM2 SPA.SET-IMC.105(d)(2)) (EASA, 2017a). Furthermore, it is worth noting that the selection of the runway in use is usually done so that the landings are performed into headwind. The headwind has a negative effect on the glide performance as it increases the actual minimum glide angle. Therefore it is reasonable to also study the effect of wind to the risk period. As an example, the effect of a constant 20 kt headwind for the PC-12 gliding flight is next examined.

The Equations 1 and 2 can also be written in a form:

$$\gamma = \frac{\dot{h}}{\dot{R}} = \frac{\dot{h}}{V_{GS}} \tag{5}$$

where $\dot{h}$ is vertical speed and V_{GS} ground speed. Applying the Equation 5 above, the Pilatus PC-12 vertical speed can also be analysed numerically. In zero wind and at low altitude, the ground speed is practically the same as indicated best glide speed V_{md} = 116 kt = 59.68 m/s. Inserting the known γ_{min} = 3.95° in radians, we get:

$$\dot{h} = 0.06894 \text{ rad} \cdot 59.68 \ \frac{\text{m}}{\text{s}} \approx 4.114 \frac{\text{m}}{\text{s}} \approx 810 \frac{\text{ft}}{\text{min}} \tag{6}$$

which confirms the value extracted from the aeroplane flight manual. Next the Equation 5 is applied again keeping the vertical speed same but with 20 kt smaller ground speed, giving the glide angle with wind effect γ_w.

$$\gamma_w = \frac{4.114 \frac{\text{m}}{\text{s}}}{49.39 \frac{\text{m}}{\text{s}}} \approx 0.083296 \text{ rad} \approx 4.77° \quad (7)$$

It can be seen that, in this case, the 20 kt constant headwind increases the minimum glide angle with about 0.82 degrees. Again, this value is rounded up and the glide angle γ_w of 4.8 degrees is used in this study when examining how a headwind affects the risk periods and areas in approach. The effect of wind to power off glide angle is illustrated in the Figure 7 below.

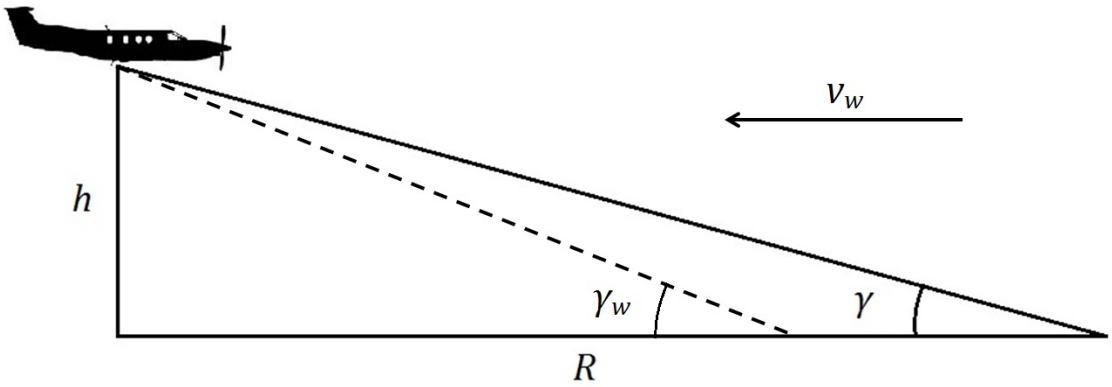

Figure 7. The effect of wind to glide angle and distance.

The equation for estimating the wind effect at low altitudes in general can also be expressed as:

$$\gamma_w = \frac{\gamma V_{md}}{V_{md} + v_w} \quad (8)$$

where v_w is the wind speed (headwind/tailwind component), headwind being a negative value.

The indicated best glide speed is independent of altitude. Yet, the true airspeed (TAS) and ground speed increase when the air density decreases with altitude. This results also in a higher vertical speed during the glide. Utilising the Equations 5 – 7, it can be easily seen that with higher ground speed and vertical speed the negative effect to the minimum glide angle is smaller. Thus, using the same sea level value of γ_w for all altitudes gives conservative results. Furthermore, the negative effect of headwind could actually be compensated by slightly increasing the gliding speed, but here the same constant value for the glide speed is assumed for all cases.

4.2 Coordinate Calculation

4.2.1 Distance between Coordinates

Coordinates needed for this analysis – runway thresholds and standard instrument arrival route points – can be extracted from the Finnish Aeronautical Information Publication

(AIP) (Finavia, 2017). A spherical law of cosines is used for calculating the distances between different coordinates (Williams, 2017):

$$d = \arccos(\sin\varphi_1 \cdot \sin\varphi_2 + \cos\varphi_1 \cdot \cos\varphi_2 \cdot \cos(\lambda_2 - \lambda_1)) \cdot r \tag{9}$$

where d is the distance, φ is latitude and λ is longitude of the two coordinates (in radians) and r is Earth's mean radius of 6371 kilometres. The formula 9 gives accurate enough distances for the purpose of this thesis. Some of the STAR coordinates given with an accuracy of fractions of an arc second are rounded to the closest full arc second. Resulting error magnitude is only a few metres at maximum and thus acceptable.

4.2.2 Intermediate Points between Coordinates

The published STAR waypoints are not themself sufficient for the analysis. Intermediate points (φ_i, λ_i) at fractions between each two waypoint must be determined. For this purpose, the following Equations 10 – 16 can be utilised:

$$a = \frac{\sin((1-f)\cdot\delta)}{\sin\delta} \tag{10}$$

$$b = \frac{\sin(f\cdot\delta)}{\sin\delta} \tag{11}$$

$$x = a \cdot \cos\varphi_1 \cdot \cos\lambda_1 + b \cdot \cos\varphi_2 \cdot \cos\lambda_2 \tag{12}$$

$$y = a \cdot \cos\varphi_1 \cdot \sin\lambda_1 + b \cdot \cos\varphi_2 \cdot \sin\lambda_2 \tag{13}$$

$$z = a \cdot \sin\varphi_1 + b \cdot \sin\varphi_2 \tag{14}$$

$$\varphi_i = \operatorname{atan2}\left(z, \sqrt{x^2 + y^2}\right) \tag{15}$$

$$\lambda_i = \operatorname{atan2}(y, x) \tag{16}$$

where f is a fraction along the great circle route (f = 0 is point 1, f = 1 is point 2) and δ is the angular distance d/r between the two points in radians. (Williams, 2017) A suitable interval for the intermediate points is determined later on in the subchapter 4.4.2 for horizontal approach profile simulation.

4.2.3 Destination with Given Distance and Bearing from Start

To calculate the location of the emergency landing key point as a bearing and distance from the runway threshold the following equations are used:

$$\varphi_2 = \arcsin(\sin\varphi_1 \cdot \cos\delta + \cos\varphi_1 \cdot \sin\delta \cdot \cos\theta) \tag{17}$$

$$\lambda_2 = \lambda_1 + \operatorname{atan2}(\sin\theta \cdot \sin\delta \cdot \cos\varphi_1, \cos\delta - \sin\varphi_1 \cdot \sin\varphi_2) \tag{18}$$

where θ is the true bearing from the start point. (Williams, 2017)

4.2.4 Course between Coordinates

True course θ from start point to destination can be calculated with equation (Williams, 2017):

$$\theta = \text{atan2}(\sin(\lambda_2 - \lambda_1) \cdot \cos\varphi_2 , \cos\varphi_1 \cdot \sin\varphi_2 - \sin\varphi_1 \cdot \cos\varphi_2 \cdot \cos(\lambda_2 - \lambda_1)) \quad (19)$$

When moving along a great circle path between two coordinates, the actual bearing changes gradually. The equation above gives the initial course and is used to determine the heading from any point on the STAR route to the emergency landing key point. The distances in this study are so short that the heading can be considered constant.

4.3 Conversions between IAS, TAS, Ground Speed and Mach

The most important speed for the pilot is the indicated airspeed IAS. It is used for planning and executing normal operations (below crossover altitude) to comply with the published STAR speed restrictions and restrictions given by the ATC, and to adjust the glide in case of an engine failure. IAS for the best glide is constant in steady state gliding flight. Due to atmospheric characteristics – variations in pressure, density and air temperature at different altitudes – the true airspeed V_{TAS} differs from the IAS. To calculate the total time for the risk period in the approach, ground speed must be known. It can be easily calculated from TAS by subtracting or adding the effect of a wind component:

$$V_{GS} = V_{TAS} + v_w \quad (20)$$

In the Pilatus PC-12 NG's Primus Apex avionics the IAS shown for the pilot is corrected for position error (Pilatus Aircraft, 2016). Other possible minor instrument errors as well as the air compressibility error is disregarded – for the Pilatus PC-12's speed and altitude regime the compressibility error is not significant bearing in mind the nature of this study. The difference is of some 2 per cent at maximum between the equivalent airspeed and calibrated airspeed at high altitudes and close to maximum speeds (Hoffren and Rahikainen, 1992). Thus the relation between IAS and TAS can be expressed as:

$$V_{TAS} = V\sqrt{\frac{\rho_0}{\rho}} \quad (21)$$

where ρ_0 is the air density at sea level and ρ the air density at the examined altitude (Hoffren and Rahikainen, 1992). The International Standard Atmosphere (ISA) is assumed in this study. Some of its most important characteristics are:

- the air is a dry, perfect gas
- the temperature at sea level is 15°C
- the pressure at sea level is 1013.2 hPa
- the temperature gradient is −1.98°C per 1000 feet from sea level up to the altitude at which the temperature is −56.5°C (approximately 36 100 ft). (Pilatus Aircraft, 2016)

Values for some relevant ISA variables are listed in the Table 2 at 1000 feet intervals. Moving upwards in the atmosphere the density decreases but the lapse rate is not quite linear. The density ratio needed in Equation 21 is interpolated from the table values at 10 feet intervals.

The Mach number is a comparison between TAS and the local speed of sound a (Airbus, 2002):

$$M = \frac{V_{TAS}}{a} \tag{22}$$

The speed of sound in air (assuming ideal gas) depends on the air temperature. Thus, if IAS (or TAS) is maintained constant with increasing altitude, the Mach number increases as air cools. At some point the Mach number becomes more limiting and must be in turn maintained constant. This point is called crossover altitude. The crossover altitude depends on the desired IAS and Mach number values. The relation between IAS, TAS and Mach number below the tropopause is illustrated in the Figure 8 below.

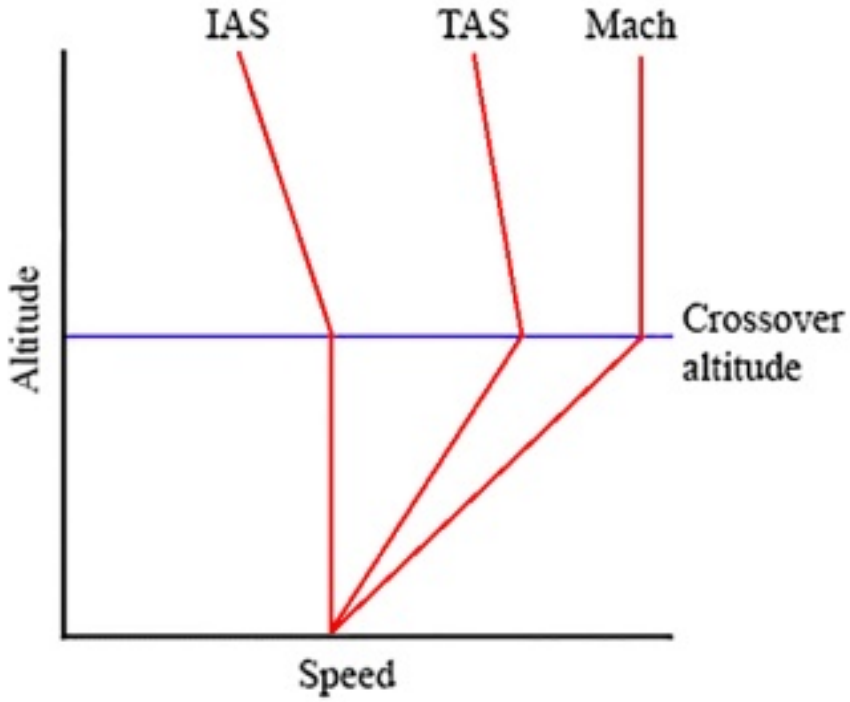

Figure 8. The relative behaviour of IAS, TAS and Mach number as a function of altitude.

The speed of sound in air can be approximated with an equation:

$$a = 20.05\sqrt{273.15 + T} \tag{23}$$

where T is the air temperature in Celsius – the result being in metres per second (Airbus, 2002). Hence, combining the Equations 22 and 23 we get:

$$V_{TAS} = M \cdot 20.05\sqrt{273.15 + T} \tag{24}$$

Table 2. The International Standard Atmosphere. (Airbus, 2002)

Altitude [ft]	**Temp. [°C]**	**Pressure [hPa]**	**Pressure ratio $\frac{p}{p_0}$**	**Density ratio $\frac{\rho}{\rho_0}$**	**Speed of sound [m/s]**	**Altitude [m]**
40 000	- 56.5	188	0.1851	0.2462	295.1	12 192
39 000	- 56.5	197	0.1942	0.2583	295.1	11 887
38 000	- 56.5	206	0.2038	0.2710	295.1	11 582
37 000	- 56.5	217	0.2138	0.2844	295.1	11 278
36 000	- 56.3	227	0.2243	0.2981	295.3	10 973
35 000	- 54.3	238	0.2353	0.3099	296.6	10 668
34 000	- 52.4	250	0.2467	0.3220	298.0	10 363
33 000	- 50.4	262	0.2586	0.3345	299.3	10 058
32 000	- 48.4	274	0.2709	0.3473	300.6	9 754
31 000	- 46.4	287	0.2837	0.3605	301.9	9 449
30 000	- 44.4	301	0.2970	0.3741	303.2	9 144
29 000	- 42.5	315	0.3107	0.3881	304.6	8 839
28 000	- 40.5	329	0.3250	0.4025	305.9	8 534
27 000	- 38.5	344	0.3398	0.4173	307.2	8 230
26 000	- 36.5	360	0.3552	0.4325	308.5	7 925
25 000	- 34.5	376	0.3711	0.4481	309.7	7 620
24 000	- 32.5	393	0.3876	0.4642	311.0	7 315
23 000	- 30.6	410	0.4046	0.4806	312.3	7 010
22 000	- 28.6	428	0.4223	0.4976	313.6	6 706
21 000	- 26.6	446	0.4406	0.5150	314.8	6 401
20 000	- 24.6	466	0.4595	0.5328	316.1	6 096
19 000	- 22.6	485	0.4791	0.5511	317.4	5 791
18 000	- 20.7	506	0.4994	0.5699	318.6	5 406
17 000	- 18.7	527	0.5203	0.5892	319.9	5 182
16 000	- 16.7	549	0.5420	0.6090	321.1	4 877
15 000	- 14.7	572	0.5643	0.6292	322.3	4 572
14 000	- 12.7	595	0.5875	0.6500	323.6	4 267
13 000	- 10.8	619	0.6113	0.6713	324.8	3 962
12 000	- 8.8	644	0.6360	0.6932	326.0	3 658
11 000	- 6.8	670	0.6614	0.7156	327.2	3 353
10 000	- 4.8	697	0.6877	0.7385	328.4	3 048
9 000	- 2.8	724	0.7148	0.7620	329.7	2 743
8 000	- 0.8	753	0.7428	0.7860	330.9	2 438
7 000	+ 1.1	782	0.7716	0.8106	332.1	2 134
6 000	+ 3.1	812	0.8014	0.8359	333.3	1 829
5 000	+ 5.1	843	0.8320	0.8617	334.5	1 524
4 000	+ 7.1	875	0.8637	0.8881	335.6	1 219
3 000	+ 9.1	908	0.8962	0.9151	336.8	914
2 000	+ 11.0	942	0.9298	0.9428	338.0	610
1 000	+ 13.0	977	0.9644	0.9711	339.2	305
0	+ 15.0	1013	1.0000	1.0000	340.3	0
- 1 000	+ 17.0	1050	1.0366	1.0295	341.5	- 305

4.4 Approach Profile Simulation

The profile simulation in this study consists of two fundamentally different scenarios: the approach profiles that will be flown when the operations are normal and the emergency profile in case of an engine failure. The possibility for an engine failure must be considered when planning the normal flight profile as the total energy of the aircraft defines whether the risk period must be utilised or not. Many other factors, such as the aircraft performance capabilities and STAR constraints set the boundary conditions for possible approach profiles. The normal flight profile is first discussed in this subchapter.

With the lack of actual Flight Data Monitoring (FDM) data from the PC-12, the flight profile must be simulated. The benefit of exploiting theoretical, simulated profile and published STAR routes is that it leads to results with less variance than actualised profiles. The actual flight route is different for each flight and thus it would be difficult to study, for example, the effect of steeper vertical profile to the risk area. In addition, the aeroplane navigation system usually calculates the top of descent point and vertical profile according to the input STAR route.

For flight planning purposes, studying the published routes sets an excellent starting point for determining the duration of the theoretical risk period and finding possible alternative emergency landing sites. For any deviations from the STAR routes, pilots can make operative inflight calculations when considering the capability to reach the airport or other landing sites. The simulated profile is divided in horizontal, vertical and speed profiles. Each of them is separately described below.

4.4.1 Speed Profile

When constructing the speed profile, important factors to be accounted for are the aircraft speed limitations set in the Airplane Flight Manual (AFM). The Pilatus PC-12 maximum certified operating speeds are 240 kt indicated airspeed (IAS) or Mach 0.48. Above the defined crossover altitude of 15 200 feet the maximum operating Mach number becomes more limiting. The AFM descent performance section assumes the airspeed used is Mach 0.48 or 236 knots IAS, whichever is lower. (Pilatus Aircraft, 2016) In this study, the desired speed during the descent defines the crossover altitude. Above the crossover altitude the Mach number 0.46 is used as maximum to provide margin to the maximum operating Mach number. The corresponding TAS and IAS values are calculated with Equations 24 and 21. The TAS is needed to calculate the time between each coordinate and further the exposure time in risk areas.

Two different speed profiles (A and B) are examined to study the effect of speed to the risk period. Speed profile B is the same as profile A but with fixed 10 knot addition to all indicated air speeds. This means approximately 5 to 10 % increments to the IAS.

The speed after the crossover altitude is maintained constant until deceleration for final approach is deemed necessary. The published speed constraints in the STAR routes are respected and checked for the simulation. For the speed profile A, the initial descent speed is 220 kt (or a lower value if limited by the Mach number 0.46) but at least 10 kt below any possible STAR speed limitation. The speed at base leg is 200 kt and 190 kt at the beginning of the final. By the final approach point (FAP) or final approach fix (FAF) the speed is reduced to 170 kt to allow landing gear extension. The maximum landing gear

operation speed for the PC-12 is 180 knots IAS (Pilatus Aircraft, 2016). There forward the speed is reduced gradually to final approach speed as landing configuration for flaps and landing gear are extended. Speed reduction is done so that 150 knots is reached by 4 NM final and the final speed 90 knots approximately 30 seconds and 0.7 NM before the runway threshold. The relatively high speed profile is intentional so as to reduce the exposure time in risk areas. However, it should be realistic to fly and to allow required deceleration capability considering the PC-12 performance characteristics (Keltanen, 2017). The speeds are practicable also from the ATC point of view (Karila, 2017). Again, to validate the applicability of the simulated profile, test flights and FDM data would be needed.

Any changes in speeds are simulated to happen gradually, approximately at a rate of 1 knot per second. More accurately, the speed change rate is actually 1 knot per simulated data point. The data point interval is defined so that the time between each point is close to one second (within a couple tenths of a second) until the FAP or FAF. This is done to make the data processing simpler. After FAP/FAF the aircraft speed is reduced so that one data point interval corresponds to approximately 1.5 – 3.5 seconds.

4.4.2 Horizontal Profile

As mentioned, the horizontal profile is assumed to be flown according to published STAR routes. Waypoints included in the STAR can be seen in the instrument charts in the Appendix 1 and their respective coordinates in the Appendix 2. To examine the full route to be flown and to get simulated data between the published waypoints, a sufficient amount of intermediate coordinates must be calculated with Equations 10 – 16. The true airspeed range for the Pilatus PC-12 during the arrival segment is approximately 180 – 300 knots. This means the aircraft travels about 3 to 5 NM per minute over the ground. As a reference, 4 NM/min (1/15 NM/s) is selected to get data points at approximately one second intervals. Thus, 14 intermediate points are calculated for every nautical mile.

Headings between waypoints can again be seen in the instrument charts. Magnetic directions are used and minor differences in magnetic variation between two geographical points are disregarded. Changes in the aeroplane heading are simulated as approximately standard rate turns (3 degrees per second or to be more precise, per simulated data point).

4.4.3 Vertical Profile

According to a modern practise the vertical profile is planned as continuous descent approach (CDA) without any level flight segment. The descent gradient after the FAP or FAF is defined in the instrument approach charts and the final approach segment is simulated accordingly. The optimum final approach descent design gradient is 5.2% (or 3.0°) (ICAO, 2006).

In the segments preceding the final approach segment the descent angle may be affected by the flight crew. In this thesis, the effect of different descent gradients to the risk period is examined. Altitude at each simulated data point is calculated applying a fixed descent angle and distance to the published FAP/FAF via the approach route and then added to the intermediate approach altitude. In addition, any published STAR altitude restrictions are complied with. The examined descent angles are 3°, 4° and 5°. If applicable, a limiting en-route cruise altitude is 28 000 feet. The vertical profile simulation is visualised in the Figure 9.

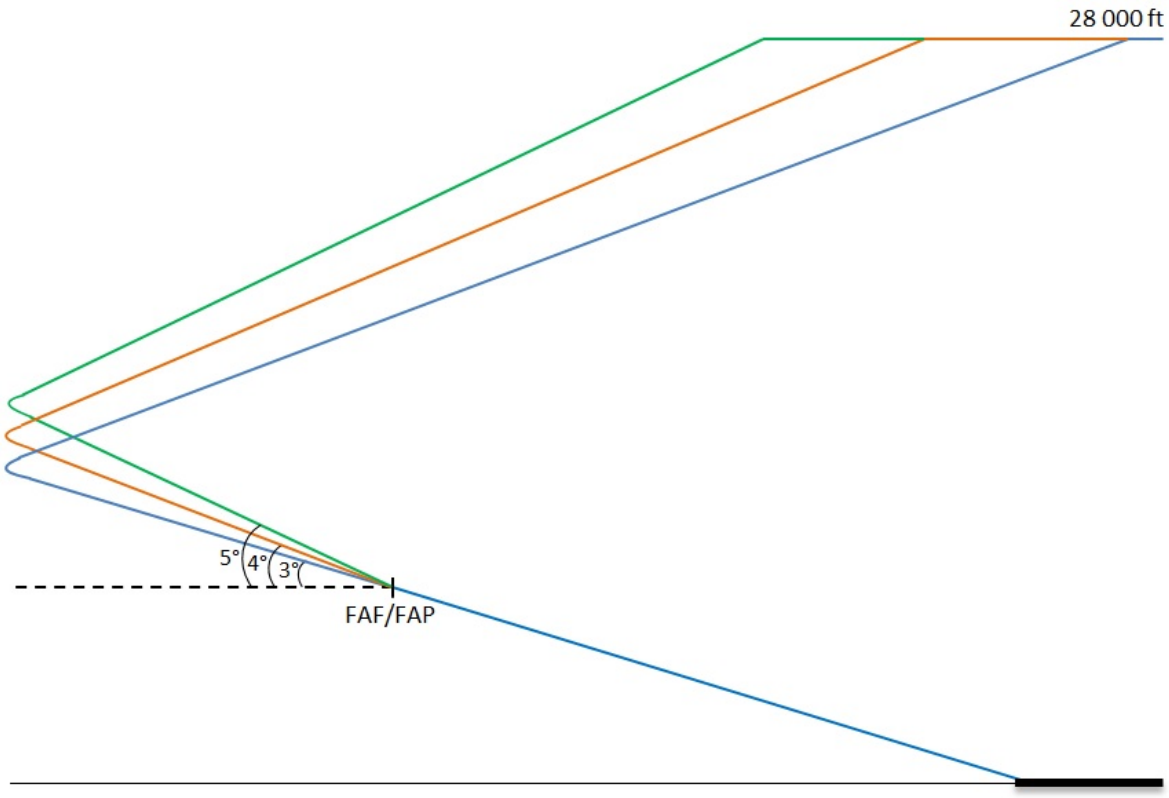

Figure 9. Vertical profiles.

The default descent angle in the Pilatus PC-12 NG Primus Apex avionics is 3 degrees. This can be easily modified by the pilot for each waypoint leg. After the modification the system calculates new vertical path guidance. The maximum allowable angle is 8 degrees and the lowest allowable angle is 1 degree. (Honeywell, 2014)

4.5 Glide Profile

When the engine fails and thrust is lost, the aeroplane becomes a glider. The glide profile is discussed next. Two different glide profiles are studied: in still air with clean configuration glide angle γ_{min} of 3.95 degrees and in 20 kt headwind with glide angle γ_w of 4.8 degrees. The headwind is considered constant regardless of the aircraft heading and altitude. The scenario is a bit unrealistic but enables the study of wind effect in theory. In reality, the number of different wind conditions at different altitudes is infinite.

An immediate and complete loss of thrust is assumed. When the engine failure occurs, the aeroplane heading is initially turned towards an emergency landing key point located on a short final. The new heading can be calculated with the Equation 19. The calculation gives true course which is converted into magnetic heading by subtracting a local variation in the area (an average from all given runway threshold variations is used in this study). A second turn needed is the final alignment from the initial key point heading to the runway heading. As stated before, the Pilatus PC-12 loses altitude approximately 1600 feet during a full 360-degree turn. This estimate is applied when calculating the lost altitude during the manoeuvring. Furthermore, 50 per cent of any excess kinetic energy the aeroplane may have compared to the best glide speed at the moment of the engine failure is converted to altitude. An equivalent altitude, taking into account the required manoeuvring and excess speed, is calculated with the Equation 4.

It is not realistic or reasonable to assume that the emergency glide could be made directly to the runway threshold with the best clean configuration glide angle from any point in the STAR route. The aeroplane must be aligned to the runway heading and configured for landing. After lowering the landing gear and extending the flaps, the best glide angle is significantly steeper due to increased drag. It would be more reasonable to examine the gliding capability to some predetermined point on the final. For this reason, a special key point is defined. The key point is located on short final from where the landing can be completed. The glide angle for approach or landing configuration is not usually given in the AFM and must be estimated. This is the case also with the Pilatus PC-12. The key point procedure in this study is specified in the subchapter 4.5.1 below.

The key point is the glide reference from any point on the STAR and intermediate approach before the FAF/FAP. After the FAF/FAP the aeroplane is already aligned for the final approach and the reference point then for the examination is located 50 feet above the runway threshold. A distance from any coordinate to the key point (or threshold) can be calculated with the Equation 9. When the distance, altitude and the glide angle are known it is easy to calculate whether the aeroplane can glide to the desired point.

4.5.1 Emergency Landing Key Point

Various key point methods are developed worldwide for single-engine aircraft engine failure cases. The idea of a key point is to align the aircraft safely for landing without engine power. Some key point methods utilise multiple points (high key – low key) and might require even 2000 feet height above the landing site for manoeuvring. A single key point located on 0.5 NM final and at the altitude of 500 feet above the runway threshold (THR) elevation is used in this study (see Figure 10). This yields in approximately 9.3 degree angle for the final glide. The idea of this single key point method is to minimise the risk period when flying at low altitudes around the destination aerodrome. Coordinates for the key point for each runway are calculated with the Equations 17 and 18.

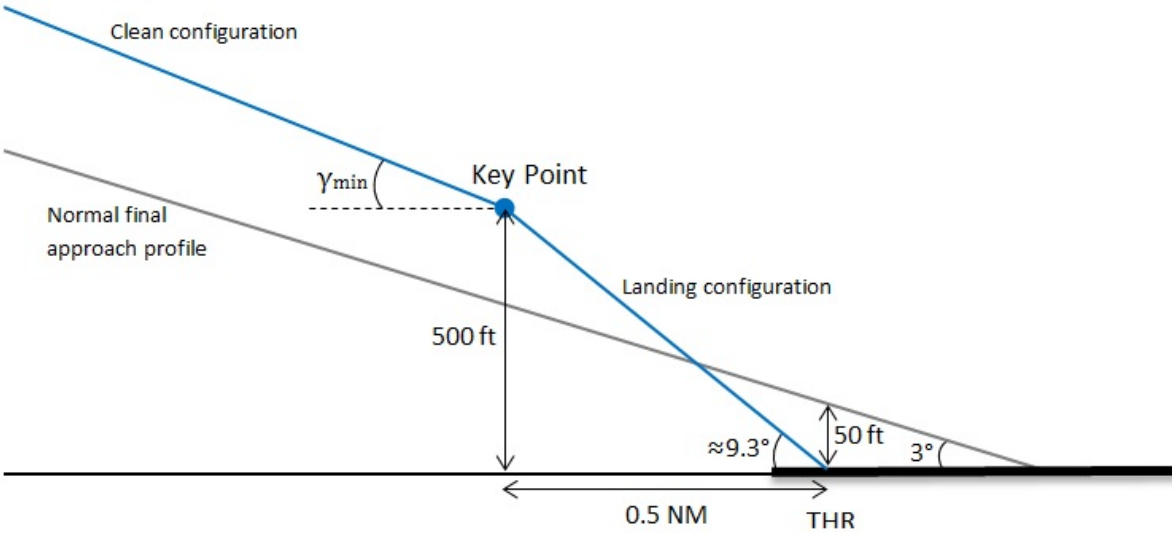

Figure 10. The key point profile in this study.

The defined key point should allow safe emergency landing in most cases, considering the sophisticated navigational capabilities of the PC-12 (Keltanen, 2017). The aeroplane is flown to the key point in clean configuration and with the defined best glide speed. The landing configuration is selected and final alignment is done after the key point. The actual

gliding capability of the PC-12 in other than clean configuration is unknown. A similar estimation of a typical SET aeroplane's gliding capability in landing configuration (10 degrees) was made by the QinetiQ working group in their SET-IMC operations risk assessment (Bradley, 2007).

Cloud base of approximately 500 feet above the ground level should be enough for the pilot to make a visual contact with the touchdown point and yet have enough time to make final alignment and configure the aircraft for landing. If the prevailing cloud base is lower or the visibility on ground is poor, the help of navigation instruments is needed. The key point should be programmed into the navigation system together with the threshold coordinates. With the help of these two points the autopilot function could be utilised to reduce the pilot workload. However, if the aircraft is equipped with a sophisticated synthetic vision system (optionally available for the Pilatus PC-12 NG) it could be exploited to navigate the aeroplane directly to the threshold also in weather conditions well below the VMC minima. Furthermore, if the runway is equipped with ILS the correct frequency should be tuned to provide additional situational information.

5 Case Study: Pilatus PC-12/47E at Helsinki Airport

5.1 Introduction

The reason for selecting Helsinki Airport (EFHK) for the case study is not only because it is the most familiar airport for the author but also because Finnish CAA has been a forerunner and supporter of commercial SET-IMC operations. The first approved Pilatus PC-12 operator in Europe, Hendell Aviation, is located in Finland and its main base is on Helsinki Airport. They got their Air Operator Certificate (AOC) already in 2013 (Hendell Aviation, 2017). Since then, also another PC-12 operator, Go! Aviation, were granted an AOC in 2016 by the Finnish CAA but the company faced unbearable financial difficulties and the operations were run down in 2017. Moreover, there is no high terrain or extensive amount of other obstacles around the Helsinki Airport, which would unnecessarily increase the complexity of the study.

The Pilatus PC-12 has been a particularly popular aircraft for commercial SET operations in North America. Also in Europe, the PC-12 is the most active aeroplane for non-commercial business aviation flights. (Koe, 2016) The aircraft is very suitable for commercial operations due to its performance capabilities, versatility, modern avionics and economical features. These are without a doubt also the reasons why the previously mentioned AOC holders have ended up with Pilatus PC-12. And it can be reasonably expected to become the choice for many of the future SET operators in Europe.

As a natural consequence, the Pilatus PC-12 was selected as the reference aeroplane in this study. The technical specifications of the PC-12 are introduced in more detail in the subchapter 3.4.1 and in the chapter 4. With this aeroplane-airport combination, this thesis would have the potential to provide valuable information for operators.

5.2 EFHK Approaches and Runways

5.2.1 Introduction

There are three runways at Helsinki Airport. All runways have instrument landing procedures for both opposite runway ends. Therefore, there are a total of six landing directions. Descent gradient at final segment is 5.2% (3.0°) for all EFHK approaches except for runway 33 approaches it is 6.1% (3.5°). (Finavia, 2017) The runway characteristics are presented in the Table 3. For the approach profile simulation in this study, the published instrument landing system (ILS) procedures are applied when available. According to the ILS procedure, a minimum speed of 150 kt IAS is required to be maintained until 4 NM from the touch down zone (Finavia, 2017). This has been taken into account in the simulated speed profile. At EFHK the only runway without ILS is the runway 33. For this runway, an approach based on area navigation (RNAV) system is utilised in the simulation.

The preferential runway (RWY) for landing at EFHK is in the following order: RWY 15, RWY 22L, RWY 04L, RWY 04R, RWY 22R and RWY 33. The selection of runway in use is based on temporary restrictions concerning runway availability and safety aspects, such as wind direction and runway condition. (Finavia, 2017)

All runways have at least six STAR routes that begin from waypoints called DIVAM, INTOR, LAKUT, LUSEP, ROPAM and VEPIN. The STARs are named accordingly, for example DIVAM 1M for runway 15 from point DIVAM. For parallel runways 04L/04R and 22L/22R dependent or independent parallel approaches are possible, especially during the airport peak hours. To keep the minimum required radar separation, there must be at least 1000 feet vertical (or 3 NM lateral) separation between the two aircraft approaching parallel runways final course. The northern runway 04L/22R is the lower side. Therefore, the aircraft approaching this runway need to fly prolonged periods of time at lower than optimum altitudes. This is has been taken into account also in the STAR design with maximum altitude constraints. For the parallel approaches, there are three additional STARs for 04L and one for 22R. The total number of STARs at Helsinki Airport is 40. (Finavia, 2017).

Table 3. Helsinki Airport runway physical characteristics. (Finavia, 2017)

Runway	Magnetic bearing [°]	Magnetic variation [°E]	Dimensions [m]	Runway THR position [Lat / Long]	Elev. [ft]	Final appr. angle [°]
04L	039	8.47	3060 x 60	601846.61N / 0245413.93E	133.6	3
22R	219	8.50		601952.11N / 0245638.01E	179.2	3
04R	039	8.04	3500 x 60	601840.65N / 0245610.94E	151.6	3
22L	219	8.54		601950.49N / 0245844.73E	148.6	3
15	145	8.51	2901 x 60	601948.99N / 0245752.19E	162.9	3
33	325	8.06		601825.44N / 0245917.83E	147.1	3.5

The magnetic variations are calculated differences between published magnetic and geographical runway bearings. The average magnetic variation of all runway thresholds is approximately 8.35°E. This value is needed when converting true courses between two coordinates into magnetic headings.

In the vicinity of Helsinki Airport, there are no significant high obstacles or terrain that would have to be considered during an emergency glide. Thus the emergency landing procedure can be planned directly towards the key point or runway threshold.

5.2.2 Risk Mitigation Means

There are three main measures identified in this study to mitigate the risk yielding from flying at low altitudes during the approach phase. First, a steeper than nominal descent angle can be utilised in the arrival segment. Sometimes altitude constraints are published and must be taken into account. Helsinki Airport is suitable for this study due to low number of altitude restrictions that would require being at or below a defined altitude. Only a few STARs have these constraints to meet the requirements of parallel approaches. Therefore, both the effect of unrestricted higher profile and the influence of altitude constraints can be examined. From the ATC perspective, there are no other restrictions related to, for example, separation to other aircraft that would prevent the use of steep descent. Lateral separation is applied for the approaching traffic (Karila, 2017).

Second, increased speeds can be used during the approach. This will decrease the exposure time over the risk areas and possibly reduce the risk area, when excess speed is converted to altitude. Some speed constraints are given for the approaches at EFHK and they must be respected unless the restrictions are specifically cancelled by the ATC. On the other hand, considering the PC-12 approach phase speed range, the published maximum speed limitations might not become limiting in most cases. Moreover, the ATC can normally accept, for example, a speed of 210 kt during the base leg and 200 kt until 10 NM final during the parallel approaches if required (Karila, 2017).

Third, alternative emergency landing sites can be preselected to avoid using the risk period. This can be done when the geographical risk areas are identified. One objective of this thesis is to locate these risk areas around the Helsinki Airport. Due to flat terrain and relatively sparsely populated areas there should be a great number of suitable emergency landing sites in the vicinity of EFHK.

6 Results

In this study, 40 standard instrument arrivals were examined for three runways from both landing directions at Helsinki Airport. The simulated data set for each STAR consisted of 400 – 1400 data points making the total number of data points in the study approximately 35 000. Each data point was linked with more than 20 parameters. The parameter values altered when the descent and speed profiles were varied and headwind component added.

As a result, an Excel spreadsheet calculation tool was constructed. An example of the view from the software is given in the Figure 11. For clarity, all of the spreadsheet parameters are not presented in the figure. Own spreadsheet tab was constructed for each STAR, consisting the related actual waypoints, intermediate points, headings in between these points and altitude and speed constraints.

The spreadsheet requires input values for the speed profile and descent angle. It then returns the total time spent in the approach phase and the total risk period. If the equivalent altitude at any point is less than the required altitude, the time interval is counted as risk period. Other variables that could be easily altered in the spreadsheet for further study include:

- the desired best glide speed
- best glide angle
- altitude lost during a 360-turn
- headwind component
- maximum limited en-route altitude
- maximum Mach number
- percentage amount of excess speed converter to altitude; and
- the emergency landing key point location (height above and distance from the runway threshold).

For these parameters, fixed values presented in the previous chapters were used in this thesis.

Full results for the total time in approach, risk periods and the effect of altering descent and speed profiles (both in still air and in headwind) can be found in the Tables A3.1. – A3.8. in the Appendix 3. Furthermore, for better visualisation of the results, the geographical risk areas are illustrated over a map in the Appendix 4 Figures A4.1 – A4.42. Red colour indicates an area from where the aeroplane could not reach the runway in use whereas the green dots represent safe areas. The most important results are next presented and analysed in this chapter.

Microsoft Excel - EFHK STAR RWY15

	A	B	C	F	G	L	M	O	P	Q	R	S	T	V	W	Y	Z	AA	AB	AD	AE	AG	AH	AJ	AL	AM	AN	AO	AP
1	Name	Constraints		Lat	Long	Distance to THR via STAR	Altitude	Heading	Heading to key point	Required initial turn	Key point HDG diff. to RWY HDG	Altitude lost during turns	IAS (Desired)	IAS (Mach limited)	IAS	TAS (from desired IAS)	TAS (Mach limited)	TAS	GS	Mach	Vertical Speed	Speed to Altitude	Equivalent Altitude	Distance to key point (or to THR after FAP/FAF)	Required Altitude	Equivalent Altitude - Req. Altitude	Color	Time in segment	Risk period
2		LVL [ft]	Speed [kt]	[°]	[°]	[NM]	[ft]	[°]	[°]	[°]	[°]	[ft]	[kt]	[kt]	[kt]	[kt]	[kt]	[kt]	[kt]		[ft/min]	[ft]	[ft]	[NM]	[ft]	[ft]		[s]	[s]
1007	SUTAX	2000	220	60.4939	24.9847	19.4614	6416.4	325	177	148	32	800.00	210	210	210	231.13	231.13	231.1	231.1	0.357	-1226	195.52	5811.873	9.414052	4612.57	1199.305	green	1.0305	
1008		2000	220	60.4949	24.9837	19.3949	6395.2	325	176	149	31	800.00	210	210	210	231.06	231.06	231.1	231.1	0.357	-1225	195.52	5790.697	9.470547	4636.27	1154.426	green	1.03611	
1009		2000	220	60.4959	24.9827	19.3284	6374	325	176	149	31	800.00	210	210	210	230.99	230.99	231	231	0.357	-1225	195.52	5769.521	9.527171	4660.03	1109.494	green	1.03642	
1010		2000	220	60.4969	24.9817	19.2619	6352.8	325	176	149	31	800.00	210	210	210	230.92	230.92	230.9	230.9	0.357	-1224	195.52	5748.345	9.583923	4683.84	1064.508	green	1.03674	
1011		2000	220	60.4978	24.9807	19.1954	6331.7	325	176	149	31	800.00	210	210	210	230.85	230.85	230.8	230.8	0.357	-1224	195.52	5727.169	9.640799	4707.7	1019.47	green	1.03706	
1012		2000	220	60.4988	24.9796	19.1289	6310.5	325	176	149	31	800.00	210	210	210	230.78	230.78	230.8	230.8	0.357	-1224	195.52	5705.994	9.697797	4731.61	974.3804	green	1.03738	
1013		2000	220	60.4998	24.9786	19.0624	6289.3	325	175	150	30	800.00	210	210	210	230.67	230.67	230.7	230.7	0.356	-1223	195.52	5684.818	9.754916	4755.58	929.2404	green	1.03785	
1014		2000	220	60.5008	24.9776	18.9959	6268.1	325	175	150	30	800.00	210	210	210	230.6	230.6	230.6	230.6	0.356	-1223	195.52	5663.642	9.812153	4779.59	884.0509	green	1.03817	
1015		2000	220	60.5018	24.9766	18.9294	6246.9	325	175	150	30	800.00	210	210	210	230.53	230.53	230.5	230.5	0.356	-1222	195.52	5642.466	9.869506	4803.65	838.8127	green	1.03848	
1016		2000	220	60.5028	24.9756	18.8629	6225.8	325	175	150	30	800.00	210	210	210	230.46	230.46	230.5	230.5	0.356	-1222	195.52	5621.291	9.926973	4827.76	793.5265	green	1.0388	
1017		2000	220	60.5038	24.9745	18.7964	6204.6	325	175	150	30	800.00	210	210	210	230.39	230.39	230.4	230.4	0.356	-1222	195.52	5600.115	9.984552	4851.92	748.1933	green	1.03912	
1018		2000	220	60.5048	24.9735	18.7299	6183.4	325	174	151	29	800.00	210	210	210	230.32	230.32	230.3	230.3	0.356	-1221	195.52	5578.939	10.04224	4876.13	702.8139	green	1.03943	
1019		2000	220	60.5057	24.9725	18.6634	6162.2	325	174	151	29	800.00	210	210	210	230.25	230.25	230.2	230.2	0.356	-1221	195.52	5557.763	10.10004	4900.37	657.389	green	1.03975	
1020		2000	220	60.5067	24.9715	18.5969	6141.1	325	174	151	29	800.00	210	210	210	230.18	230.18	230.2	230.2	0.356	-1220	195.52	5536.587	10.15794	4924.67	611.9194	green	1.04007	
1021		2000	220	60.5077	24.9705	18.5304	6119.9	325	174	151	29	800.00	210	210	210	230.07	230.07	230.1	230.1	0.355	-1220	195.52	5515.412	10.21595	4949.01	566.4059	green	1.04054	
1022		2000	220	60.5087	24.9695	18.4639	6098.7	325	174	151	29	800.00	210	210	210	230	230	230	230	0.355	-1220	195.52	5494.236	10.27406	4973.39	520.8493	green	1.04086	
1023		2000	220	60.5097	24.9684	18.3974	6077.5	325	174	151	29	800.00	210	210	210	229.93	229.93	229.9	229.9	0.355	-1219	195.52	5473.06	10.33228	4997.81	475.2502	green	1.04117	
1024		2000	220	60.5107	24.9674	18.3309	6056.4	325	173	152	28	800.00	210	210	210	229.86	229.86	229.9	229.9	0.355	-1219	195.52	5451.884	10.39059	5022.27	429.6093	green	1.04149	
1025		2000	220	60.5117	24.9664	18.2644	6035.2	325	173	152	28	800.00	210	210	210	229.79	229.79	229.8	229.8	0.355	-1218	195.52	5430.709	10.449	5046.78	383.9275	green	1.0418	
1026		2000	220	60.5127	24.9654	18.1979	6014	325	173	152	28	800.00	210	210	210	229.72	229.72	229.7	229.7	0.355	-1218	195.52	5409.533	10.50751	5071.33	338.2052	green	1.04212	
1027		2000	220	60.5136	24.9644	18.1314	5992.8	325	173	152	28	800.00	210	210	210	229.65	229.65	229.7	229.7	0.355	-1218	195.52	5388.357	10.56611	5095.91	292.4434	green	1.04244	
1028		2000	220	60.5146	24.9633	18.0649	5971.7	325	173	152	28	800.00	210	210	210	229.58	229.58	229.6	229.6	0.354	-1217	195.52	5367.181	10.6248	5120.54	246.6424	green	1.04276	
1029		2000	220	60.5156	24.9623	17.9984	5950.5	325	173	152	28	800.00	210	210	210	229.51	229.51	229.5	229.5	0.354	-1217	195.52	5346.005	10.68359	5145.2	200.8031	green	1.04308	
1030		2000	220	60.5166	24.9613	17.9319	5929.3	325	172	153	27	800.00	210	210	210	229.41	229.41	229.4	229.4	0.354	-1216	195.52	5324.83	10.74246	5169.9	154.9261	green	1.04356	
1031		2000	220	60.5176	24.9603	17.8654	5908.1	325	172	153	27	800.00	210	210	210	229.34	229.34	229.3	229.3	0.354	-1216	195.52	5303.654	10.80143	5194.64	109.0119	green	1.04388	
1032		2000	220	60.5186	24.9593	17.7989	5887	325	172	153	27	800.00	210	210	210	229.27	229.27	229.3	229.3	0.354	-1216	195.52	5282.478	10.86048	5219.42	63.06122	green	1.04421	
1033		2000	220	60.5196	24.9583	17.7324	5865.8	325	172	153	27	800.00	210	210	210	229.2	229.2	229.2	229.2	0.354	-1215	195.52	5261.302	10.91962	5244.23	17.07459	green	1.04453	
1034		2000	220	60.5206	24.9572	17.6659	5844.6	325	172	153	27	800.00	210	210	210	229.12	229.12	229.1	229.1	0.353	-1215	195.52	5240.126	10.97884	5269.07	-28.9474	red	1.04485	1.0448
1035		2000	220	60.5215	24.9562	17.5994	5823.4	325	172	153	27	800.00	210	210	210	229.05	229.05	229.1	229.1	0.353	-1215	195.52	5218.951	11.03814	5293.95	-75.0042	red	1.04517	1.0452
1036		2000	220	60.5225	24.9552	17.5329	5802.3	325	171	154	26	800.00	210	210	210	228.98	228.98	229	229	0.353	-1214	195.52	5197.775	11.09753	5318.87	-121.095	red	1.04549	1.0455
1037		2000	220	60.5235	24.9542	17.4664	5781.1	325	171	154	26	800.00	210	210	210	228.91	228.91	228.9	228.9	0.353	-1214	195.52	5176.599	11.15699	5343.82	-167.22	red	1.04581	1.0458
1038		2000	220	60.5245	24.9532	17.3999	5759.9	322	171	151	26	786.67	210	210	210	228.81	228.81	228.8	228.8	0.353	-1213	195.52	5168.757	11.21654	5368.8	-200.044	red	1.04629	1.0463
1039		2000	220	60.5255	24.9521	17.3334	5738.7	319	171	148	26	773.33	210	210	210	228.74	228.74	228.7	228.7	0.353	-1213	195.52	5160.914	11.27616	5393.82	-232.901	red	1.04661	1.0466
1040		2000	220	60.5265	24.9511	17.2669	5717.6	316	171	145	26	760.00	210	210	210	228.67	228.67	228.7	228.7	0.353	-1212	195.52	5153.072	11.33586	5418.86	-265.791	red	1.04693	1.0469
1041		2000	220	60.5275	24.9501	17.2004	5696.4	313	171	142	26	746.67	210	210	210	228.6	228.6	228.6	228.6	0.353	-1212	195.52	5145.229	11.39563	5443.94	-298.711	red	1.04725	1.0473
1042		2000	220	60.5285	24.9491	17.1339	5675.2	310	170	140	25	733.33	210	210	210	228.53	228.53	228.5	228.5	0.352	-1212	195.52	5137.387	11.45548	5469.05	-331.663	red	1.04757	1.0476
1043		2000	220	60.5294	24.9481	17.0674	5654	307	170	137	25	720.00	209	209	209	227.37	227.37	227.4	227.4	0.351	-1206	191.38	5125.407	11.5154	5494.19	-368.784	red	1.05291	1.0529
1044		2000	220	60.5304	24.947	17.0009	5632.9	304	170	134	25	706.67	208	208	208	226.21	226.21	226.2	226.2	0.349	-1199	187.29	5113.471	11.5754	5519.36	-405.89	red	1.05829	1.0583
1045		2000	220	60.5314	24.946	16.9344	5611.7	301	170	131	25	693.33	207	207	207	225.06	225.06	225.1	225.1	0.347	-1193	183.24	5101.579	11.63546	5544.56	-442.982	red	1.06373	1.0637

DIVAM 1M | INTOR 5M | LAKUT 5M | LUSEP 1M | ROPAM 1M | VEPIN 1M | Values for calculations | EFHK Waypoints and Fixes | Intermediate point calculator | Altitude

Figure 11. A consolidated example of the Excel spreadsheet risk period calculation tool.

6.1 Still Air

6.1.1 Risk Period and Risk Mitigation

First, the results in still air are reviewed. The total time in approach for the STARs at Helsinki Airport, simulated to be flown with the Pilatus PC-12 varied between approximately 7.5 and 23 minutes for all descent and altitude profiles. The average duration was around 15 minutes. By using 10 kt higher indicated airspeed throughout the approach (speed profile B), 30 to 50 seconds could be saved depending on the length of the approach. Also, flying higher descent profile led to increased TAS and thus less time (5 to 25 seconds) in the approach. The combined effect was 1 minute 10 seconds at maximum.

However, the more interesting results are related to the risk period. The average risk period for the nominal 3 degree glide and speed profile A was 9 minutes 4 seconds. The result is substantially high, considering the maximum usable risk period is 15 minutes for the whole flight. The maximum theoretical risk period was as much as 16 minutes 53 seconds (PEXEN 4B for runway 04L). The minimum value was slightly over 6 minutes.

The variation in how much the steeper descent decreases the risk period was remarkable – for example 4 degree descent reduced the risk period on runway 22R LUSEP 3V arrival only a few seconds (−0.9 %) but over 6 and a half minutes (−56.0 %) on runway 15 LUSEP 1M arrival. This example already revealed the relevance of the altitude constraints in the arrival. Both final approach segments have the same 3 degree profile and begin from 2000 feet. Both arrivals are close to 45 NM in length but runway 22R has longer final and the altitude restricted to at 2000 feet already on the base leg due to possible parallel approaches.

On average, the 4 degree descent before FAF/FAP decreased the risk period 16.8 % and 5 degree angle 30.9 % in still air. The 5 degree descent could reduce the risk period up to over 65 % in some cases. This might be more than 8 minutes in time. On the other hand, for some altitude restricted approaches even the 5 degrees were not enough to significantly affect the risk period. These are however special cases at EFHK and usually the reduction is at least 15 % compared to 3 degree nominal descent. The average risk period for a 4 degree speed A profile was 7 minutes 34 seconds and for 5 degree profile 6 minutes 9 seconds. These sound more acceptable than the over 9 minutes for 3 degree profile. The shortest risk periods were only 3.5 minutes for the runway 33. The risk periods for runway 33 are generally somewhat smaller than for the other runways. This is due to slightly higher final approach angle 3.5°.

Applying the speed profile B provided an incremental risk period reduction of approximately 5 % or on average 30 seconds for all descent angles. The total effect of applying higher speed comes from two reasons – it will naturally decrease the time spent in the risk area but it also makes the risk area somewhat smaller as more excess kinetic energy can be transformed into altitude.

The total risk periods for all STARs and different flight profiles can be seen in Table 4. Values exceeding 15 minutes are shown in red. The changes in risk periods compared to the 3 degree descent with speed profile A are furthermore presented in the Table 5.

Table 4. Approach risk period in still air.

		Risk period (still air) [min:s]					
Runway	**STAR**	**3 degree profile**		**4 degree profile**		**5 degree profile**	
		Speed profile A	**Speed profile B**	**Speed profile A**	**Speed profile B**	**Speed profile A**	**Speed profile B**
04L	DIVAM 1B	13:27	12:45	13:10	12:34	05:01	04:37
	INTOR 4B	06:51	06:23	05:38	05:15	05:02	04:40
	LAKUT 5B	06:48	06:20	05:37	05:13	05:02	04:40
	LUSEP 1B	06:32	06:07	05:37	05:13	05:02	04:40
	ROPAM 1B	06:42	06:17	05:38	05:15	05:02	04:40
	VEPIN 1B	06:42	06:17	05:38	05:15	05:02	04:40
	MAROM 4B	10:42	09:57	09:20	08:47	09:06	08:34
	NAPUN 1B	09:38	09:04	09:20	08:47	09:06	08:34
	PEXEN 4B	16:53	16:02	16:37	15:50	12:32	11:50
04R	DIVAM 1R	13:46	13:03	13:31	12:54	06:45	06:15
	INTOR 4R	07:34	07:06	06:50	06:23	06:12	05:47
	LAKUT 5R	07:54	07:24	06:49	06:22	06:11	05:47
	LUSEP 1R	07:42	07:14	06:49	06:22	06:11	05:47
	ROPAM 1R	07:34	07:06	06:50	06:23	06:12	05:47
	VEPIN 1R	07:34	07:06	06:50	06:23	06:12	05:47
15	DIVAM 1M	06:12	05:48	05:13	04:51	04:37	04:17
	INTOR 5M	06:12	05:48	05:13	04:51	04:37	04:17
	LAKUT 5M	11:14	10:38	05:34	05:10	04:40	04:18
	LUSEP 1M	11:50	10:51	05:13	04:51	04:37	04:17
	ROPAM 1M	06:12	05:48	05:13	04:51	04:37	04:17
	VEPIN 1M	08:19	07:32	05:13	04:51	04:37	04:17
22L	DIVAM 2A	07:15	06:48	06:27	06:01	05:51	05:27
	INTOR 3A	07:15	06:48	06:27	06:01	05:51	05:27
	LAKUT 3A	07:23	06:55	06:27	06:01	05:51	05:28
	LUSEP 2A	12:36	11:56	06:27	06:01	05:48	05:24
	ROPAM 2A	07:24	06:56	06:27	06:01	05:51	05:27
	VEPIN 2A	13:08	12:26	10:33	09:47	06:14	05:45
22R	DIVAM 2V	08:14	07:45	07:47	07:19	07:26	06:58
	INTOR 3V	08:44	08:12	07:56	07:27	07:27	06:59
	LAKUT 3V	10:24	09:47	09:29	08:55	09:02	08:30
	LUSEP 3V	13:03	12:22	12:57	12:16	12:50	12:09
	PEXEN 3V	10:24	09:47	09:29	08:55	09:02	08:30
	ROPAM 2V	10:28	09:45	08:11	07:41	07:29	07:01
	VEPIN 2V	13:37	12:54	13:22	12:42	10:12	09:35
33	DIVAM 1W	09:07	08:41	05:20	04:59	03:30	03:09
	INTOR 4W	09:43	09:11	07:55	07:23	03:30	03:09
	LAKUT 5W	06:31	06:06	05:20	04:59	03:30	03:09
	LUSEP 1W	06:31	06:06	05:20	04:59	03:30	03:09
	ROPAM 1W	08:15	07:47	05:20	04:59	03:30	03:09
	VEPIN 1W	06:33	06:08	05:20	04:59	03:30	03:09
Min.		06:12	05:48	05:13	04:51	03:30	03:09
Max.		16:53	16:02	16:37	15:50	12:50	12:09
Average		**09:04**	**08:31**	**07:34**	**07:06**	**06:09**	**05:44**

Table 5. Risk period change with different profiles compared to 3 degree speed A profile in still air.

		Risk period change (still air) [%]					
Runway	**STAR**	**3 degree profile**		**4 degree profile**		**5 degree profile**	
		Speed profile A	**Speed profile B**	**Speed profile A**	**Speed profile B**	**Speed profile A**	**Speed profile B**
04L	DIVAM 1B	-	−5.2 %	−2.2 %	−6.6 %	−62.7 %	−65.6 %
	INTOR 4B	-	−6.7 %	−17.8 %	−23.4 %	−26.5 %	−31.8 %
	LAKUT 5B	-	−6.9 %	−17.4 %	−23.1 %	−25.9 %	−31.2 %
	LUSEP 1B	-	−6.3 %	−14.1 %	−20.1 %	−23.0 %	−28.5 %
	ROPAM 1B	-	−6.3 %	−15.9 %	−21.7 %	−24.8 %	−30.2 %
	VEPIN 1B	-	−6.3 %	−15.9 %	−21.7 %	−24.8 %	−30.2 %
	MAROM 4B	-	−7.0 %	−12.8 %	−17.9 %	−14.9 %	−19.9 %
	NAPUN 1B	-	−5.8 %	−3.1 %	−8.7 %	−5.4 %	−11.0 %
	PEXEN 4B	-	−5.1 %	−1.6 %	−6.3 %	−25.7 %	−30.0 %
04R	DIVAM 1R	-	−5.2 %	−1.8 %	−6.3 %	−50.9 %	−54.6 %
	INTOR 4R	-	−6.2 %	−9.8 %	−15.8 %	−18.0 %	−23.6 %
	LAKUT 5R	-	−6.3 %	−13.7 %	−19.4 %	−21.6 %	−26.7 %
	LUSEP 1R	-	−6.2 %	−11.5 %	−17.4 %	−19.6 %	−24.9 %
	ROPAM 1R	-	−6.2 %	−9.8 %	−15.8 %	−18.0 %	−23.6 %
	VEPIN 1R	-	−6.2 %	−9.8 %	−15.8 %	−18.0 %	−23.6 %
15	DIVAM 1M	-	−6.4 %	−15.8 %	−21.8 %	−25.5 %	−30.7 %
	INTOR 5M	-	−6.4 %	−15.8 %	−21.8 %	−25.5 %	−30.7 %
	LAKUT 5M	-	−5.3 %	−50.4 %	−53.9 %	−58.4 %	−61.6 %
	LUSEP 1M	-	−8.3 %	−56.0 %	−59.1 %	−61.0 %	−63.8 %
	ROPAM 1M	-	−6.4 %	−15.8 %	−21.8 %	−25.5 %	−30.7 %
	VEPIN 1M	-	−9.6 %	−37.4 %	−41.8 %	−44.6 %	−48.5 %
22L	DIVAM 2A	-	−6.3 %	−11.0 %	−17.0 %	−19.2 %	−24.8 %
	INTOR 3A	-	−6.3 %	−11.0 %	−17.0 %	−19.2 %	−24.8 %
	LAKUT 3A	-	−6.2 %	−12.5 %	−18.4 %	−20.7 %	−25.9 %
	LUSEP 2A	-	−5.3 %	−48.8 %	−52.2 %	−54.0 %	−57.2 %
	ROPAM 2A	-	−6.4 %	−12.8 %	−18.8 %	−20.9 %	−26.4 %
	VEPIN 2A	-	−5.3 %	−19.7 %	−25.5 %	−52.5 %	−56.2 %
22R	DIVAM 2V	-	−6.0 %	−5.6 %	−11.3 %	−9.9 %	−15.4 %
	INTOR 3V	-	−6.0 %	−9.2 %	−14.7 %	−14.8 %	−20.0 %
	LAKUT 3V	-	−5.9 %	−8.8 %	−14.2 %	−13.1 %	−18.2 %
	LUSEP 3V	-	−5.3 %	−0.9 %	−6.1 %	−1.7 %	−6.9 %
	PEXEN 3V	-	−5.9 %	−8.8 %	−14.2 %	−13.1 %	−18.2 %
	ROPAM 2V	-	−6.9 %	−21.8 %	−26.6 %	−28.6 %	−33.0 %
	VEPIN 2V	-	−5.2 %	−1.8 %	−6.8 %	−25.1 %	−29.6 %
33	DIVAM 1W	-	−4.7 %	−41.5 %	−45.4 %	−61.7 %	−65.4 %
	INTOR 4W	-	−5.5 %	−18.5 %	−24.1 %	−64.1 %	−67.6 %
	LAKUT 5W	-	−6.5 %	−18.1 %	−23.6 %	−46.4 %	−51.7 %
	LUSEP 1W	-	−6.5 %	−18.1 %	−23.6 %	−46.4 %	−51.7 %
	ROPAM 1W	-	−5.7 %	−35.3 %	−39.6 %	−57.6 %	−61.8 %
	VEPIN 1W	-	−6.5 %	−18.6 %	−24.0 %	−46.7 %	−51.9 %
Min.		-	−9.6 %	−56.0 %	−59.1 %	−64.1 %	−67.6 %
Max.		-	−4.7 %	−0.9 %	−6.1 %	−1.7 %	−6.9 %
Average		-	**−6.2 %**	**−16.8 %**	**−22.1 %**	**−30.9 %**	**−35.7 %**

6.1.2 Risk Areas

It is difficult to get a clear picture of the geographical location of the risk areas from the spreadsheet calculation results. Utilising a free web based GPSVisualizer, a map overlaid HTML document can be created and the risk areas examined in more detail and more interactively. The waypoint name, coordinates, altitude and risk period colour columns were extracted into a separate Excel file. This file was input in the GPSVisualiser which returned a graphic map of the risk areas. The map type can be altered but by selecting, for example, a Google aerial/satellite image as the background the risk areas can be identified and possible alternative emergency landing sites scanned initially.

As the runway 15 is the preferred landing runway at the Helsinki Airport, the visualised results for this runway are presented in more detail in this chapter. The results for the other runways can be seen in the Appendix 4.

In addition to STAR altitude constraints, another significant arrival design and structure related factor that can be seen to have effect in the risk period is the relation between the initial point in the STAR and the runway in use. For straight in approaches, when the track miles are considerably less and the route closes more directly towards the runway, risk period was greater compared to arrival routes that circle around the airport. The difference narrowed when higher descent angles were used. This can be seen in the risk area illustrations in the Figures 12 – 17 and in the Appendix 4. In most cases, the risk area behaviour was straightforward – once the aeroplane entered the risk area, the rest of the approach was beyond the glide distance. Occasionally, as in 3 degree VEPIN 1M arrival for the runway 15 (Figure 12), the flight exited the risk area and then entered again later in the approach.

The Table A3.4 in the Appendix 3 reveals that on average the risk period in percentage of total time in approach was roughly 60 % for 3 degree profile, 50 % for 4 degrees and 40 % for 5 degrees. Yet, the dispersion for the values was substantial and for many of the shallower profile or altitude restricted straight in approaches it was 100 %. The finding can be confirmed also from the risk area visualisations.

The final approach after the FAF/FAP was entirely risk period in this study as the final approach angle was always smaller than the best glide angle. The study indicated that it is not possible to fly the approach with such speeds that the excess kinetic energy would be sufficient to enable the glide down to runway threshold without engine thrust. Then again, maintaining high speeds during the final approach will decrease the risk period exposure time. Moreover, it might be a requirement to fly high speed approaches at major airports, such as EFHK, to allow fluent traffic flow among faster aircraft. Therefore, the final approach high speed profile in this study is justified.

Applying 10 knots higher speed (speed profile B) in the approach had only a marginal effect to the geographical risk area (Figures 12 – 17). For this reason, the visualisations for both speed profiles and for all runways are not necessary. Only the speed profile A is visualised in the Appendix 4.

Figure 12. Runway 15 risk areas, 3 degree descent profile, speed profile A, still air.

Figure 13. Runway 15 risk areas, 3 degree descent profile, speed profile B, still air.

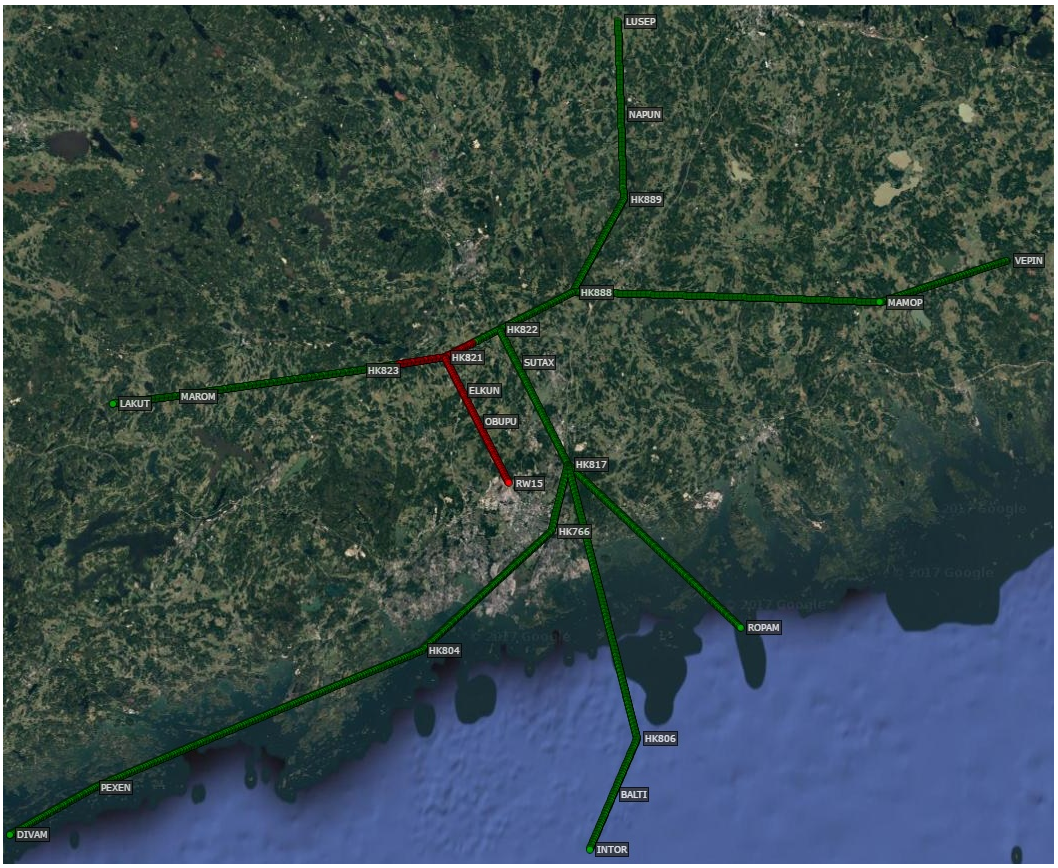

Figure 14. Runway 15 risk areas, 4 degree descent profile, speed profile A, still air.

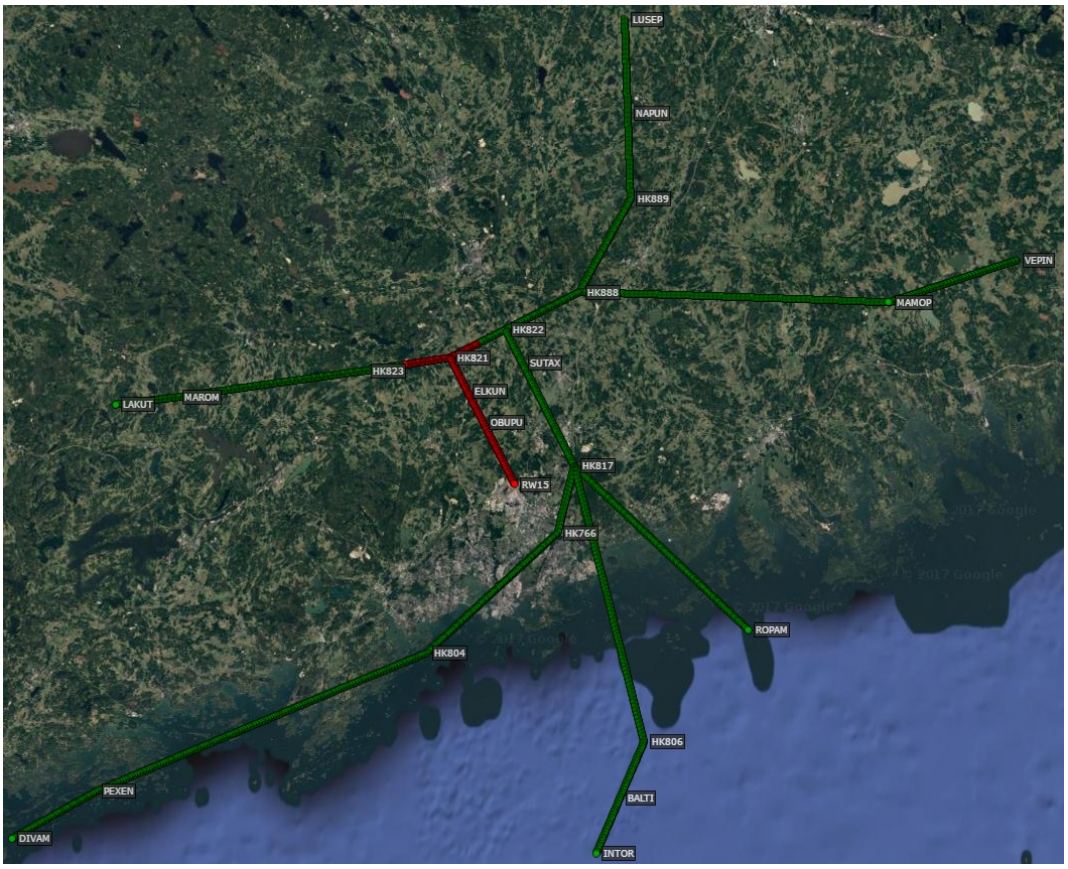

Figure 15. Runway 15 risk areas, 4 degree descent profile, speed profile B, still air.

Figure 16. Runway 15 risk areas, 5 degree descent profile, speed profile A, still air.

Figure 17. Runway 15 risk areas, 5 degree descent profile, speed profile B, still air.

The benefit of GPSVisualizer output file being a HTML file is that the map could be zoomed and the flight path examined quite accurately. An example of a close-up image of runway 15 left base leg (4 degree profile) is given in the Figure 18. It can be seen that nearby there are many potential fields that could fulfil the requirements of an emergency landing area.

Figure 18. A zoomed in aerial image of RWY 15 left base leg.

Another excellent feature of the visualisation tool is the possibility to create a Google Earth compatible KML/KMZ file. The result can be then viewed in 3D. This is a great tool for visualising and comparing different glide angles simultaneously (Figure 19).

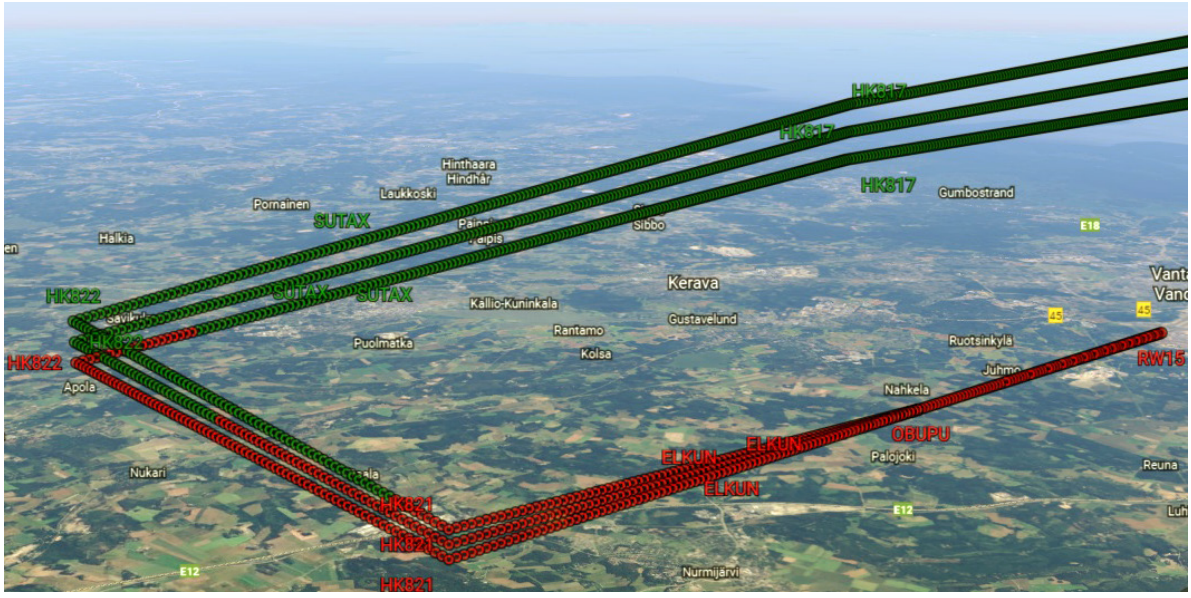

Figure 19. INTOR 5M arrival RWY 15 risk area 3D visualization (3°, 4° and 5° profiles).

6.2 Headwind

6.2.1 Risk Period and Risk Mitigation

One aim of this thesis was to examine the effect of headwind to the risk period and risk area. A constant 20 knot headwind was selected for the study and the results are now discussed and compared to the still air results. The headwind leads to lower ground speed and thus increased total time in the approach phase and risk area exposure time. As mentioned before, it is unrealistic that the headwind component would stay constant regardless of the aircraft altitude and heading. Consequently, the results for the headwind analysis include a greater margin of error than for the still air analysis.

The total approach time varied between 8.5 and 25.5 minutes with the average being approximately 16.5 minutes. Hence, the slower ground speed had an effect of one and a half minute to the total time in approach. The speed profile B decreased the total time slightly more than in the still air case as the percentage addition to ground speed was higher: 35 to 65 seconds. Increased TAS in steeper descent profile reduced approach time by 10 – 30 seconds. The maximum combined effect of higher speed and steeper profile was 1 minute 25 seconds.

The average risk period for 3 degree glide and speed profile A with the headwind was 12 minutes 12 seconds. This was almost 35 % more than in still air. The difference is remarkable and again it must be noted that the total duration of the risk period should not exceed 15 minutes per flight without a risk assessment for the route. In many STARs the risk period was over 15 minutes especially with the 3 degree descent.

With steeper descent profile the risk period can be reduced significantly also in headwind conditions. The results are close to still air conditions in percentages: 4 degree descent decreased the risk period by 16.4 % on average (16.8 % in still air) and the 5 degree descent 26.4 % (30.9 % in still air). The saved time was respectively 2 minutes 21 seconds (4 degrees) and 3 minutes 30 seconds (5 degrees). For some STARs, the higher descent angle reduced the risk period well over 10 minutes and 60 per cents. The average risk period for 4 degree speed A profile was 9 minutes 51 seconds and for 5 degree profile 8 minutes 42 seconds. These averages were yet 30 – 40 % more than without wind. It is also worth noting that even the shortest risk period with speed profile A was 6 minutes 5 seconds compared to 3 minutes 30 seconds in still air.

In headwind, the effect of using higher speed during the descent was slightly emphasised. The speed profile B decreased the risk period by some 40 seconds. In percentages, the reduction was practically the same as in no wind conditions.

The total risk periods for all STARs and different flight profiles in headwind are presented in the Table 6. Values exceeding 15 minutes are again shown in red. The changes in risk periods compared to the 3 degree descent with speed profile A are given in the Table 7.

Table 6. Approach risk period in 20 knot headwind.

		Risk period (20 kt headwind) [min:s]					
Runway	**STAR**	**3 degree profile**		**4 degree profile**		**5 degree profile**	
		Speed profile A	**Speed profile B**	**Speed profile A**	**Speed profile B**	**Speed profile A**	**Speed profile B**
04L	DIVAM 1B	15:00	14:07	14:39	13:53	14:29	13:47
	INTOR 4B	14:41	13:49	07:39	07:04	06:37	06:05
	LAKUT 5B	13:49	13:00	07:33	06:59	06:36	06:04
	LUSEP 1B	07:53	07:19	07:23	06:51	06:36	06:04
	ROPAM 1B	08:04	07:29	07:33	07:00	06:37	06:05
	VEPIN 1B	08:55	08:20	07:33	07:00	06:37	06:05
	MAROM 4B	17:49	16:48	10:50	10:08	10:36	09:54
	NAPUN 1B	13:11	12:26	10:52	10:09	10:36	09:54
	PEXEN 4B	18:48	17:43	18:29	17:29	18:18	17:23
04R	DIVAM 1R	15:22	14:28	15:04	14:17	14:55	14:12
	INTOR 4R	09:06	08:29	08:37	08:00	08:11	07:35
	LAKUT 5R	15:05	14:04	08:57	08:18	08:04	07:28
	LUSEP 1R	09:15	08:36	08:44	08:08	08:05	07:28
	ROPAM 1R	09:06	08:29	08:37	08:00	08:11	07:35
	VEPIN 1R	09:06	08:29	08:37	08:00	08:11	07:35
15	DIVAM 1M	07:29	06:57	06:58	06:27	06:05	05:37
	INTOR 5M	07:29	06:57	06:58	06:27	06:05	05:37
	LAKUT 5M	12:35	11:49	12:19	11:35	06:32	06:01
	LUSEP 1M	14:16	13:25	10:47	09:57	06:05	05:37
	ROPAM 1M	07:29	06:57	06:58	06:27	06:05	05:37
	VEPIN 1M	17:11	16:19	07:15	06:40	06:05	05:37
22L	DIVAM 2A	08:44	08:07	08:14	07:38	07:45	07:08
	INTOR 3A	08:44	08:07	08:14	07:38	07:45	07:08
	LAKUT 3A	09:04	08:26	08:21	07:45	07:38	07:04
	LUSEP 2A	14:07	13:15	13:50	13:02	07:38	07:04
	ROPAM 2A	10:03	09:17	08:23	07:47	07:37	07:03
	VEPIN 2A	14:40	13:47	14:22	13:35	12:24	11:41
22R	DIVAM 2V	11:00	10:20	09:14	08:36	08:50	08:13
	INTOR 3V	12:13	11:19	09:40	08:59	08:59	08:22
	LAKUT 3V	18:35	17:31	11:27	10:42	10:44	10:01
	LUSEP 3V	14:38	13:46	14:30	13:38	14:22	13:30
	PEXEN 3V	17:14	16:22	11:27	10:42	10:44	10:01
	ROPAM 2V	13:04	12:16	10:41	09:56	09:17	08:38
	VEPIN 2V	15:13	14:19	14:55	14:04	14:42	13:56
33	DIVAM 1W	18:16	17:24	07:19	06:46	06:13	05:44
	INTOR 4W	10:57	10:16	10:47	10:06	08:56	08:16
	LAKUT 5W	07:51	07:17	07:17	06:45	06:13	05:44
	LUSEP 1W	07:51	07:17	07:17	06:45	06:13	05:44
	ROPAM 1W	09:21	08:44	08:21	07:25	06:13	05:44
	VEPIN 1W	14:45	13:47	07:18	06:46	06:13	05:44
Min.		07:29	06:57	06:58	06:27	06:05	05:37
Max.		18:48	17:43	18:29	17:29	18:18	17:23
Average		**12:12**	**11:26**	**09:51**	**09:11**	**08:42**	**08:06**

Table 7. Risk period change with different profiles compared to 3 degree speed A profile in 20 knot headwind.

		Risk period change (20 kt headwind) [%]					
Runway	**STAR**	**3 degree profile**		**4 degree profile**		**5 degree profile**	
		Speed profile A	**Speed profile B**	**Speed profile A**	**Speed profile B**	**Speed profile A**	**Speed profile B**
04L	DIVAM 1B	-	−5.9 %	−2.3 %	−7.4 %	−3.5 %	−8.0 %
	INTOR 4B	-	−5.9 %	−47.9 %	−51.8 %	−55.0 %	−58.5 %
	LAKUT 5B	-	−6.0 %	−45.3 %	−49.4 %	−52.2 %	−56.1 %
	LUSEP 1B	-	−7.2 %	−6.5 %	−13.1 %	−16.4 %	−23.1 %
	ROPAM 1B	-	−7.1 %	−6.3 %	−13.2 %	−18.0 %	−24.5 %
	VEPIN 1B	-	−6.5 %	−15.2 %	−21.4 %	−25.8 %	−31.7 %
	MAROM 4B	-	−5.8 %	−39.2 %	−43.1 %	−40.5 %	−44.5 %
	NAPUN 1B	-	−5.6 %	−17.5 %	−22.9 %	−19.5 %	−24.9 %
	PEXEN 4B	-	−5.7 %	−1.7 %	−7.0 %	−2.7 %	−7.5 %
04R	DIVAM 1R	-	−5.9 %	−1.9 %	−7.1 %	−2.9 %	−7.6 %
	INTOR 4R	-	−6.9 %	−5.3 %	−12.1 %	−10.2 %	−16.7 %
	LAKUT 5R	-	−6.7 %	−40.6 %	−44.9 %	−46.5 %	−50.4 %
	LUSEP 1R	-	−7.0 %	−5.6 %	−12.2 %	−12.6 %	−19.2 %
	ROPAM 1R	-	−6.9 %	−5.3 %	−12.1 %	−10.2 %	−16.7 %
	VEPIN 1R	-	−6.9 %	−5.3 %	−12.1 %	−10.2 %	−16.7 %
15	DIVAM 1M	-	−7.3 %	−6.9 %	−13.8 %	−18.7 %	−25.1 %
	INTOR 5M	-	−7.3 %	−6.9 %	−13.8 %	−18.7 %	−25.1 %
	LAKUT 5M	-	−6.1 %	−2.1 %	−8.0 %	−48.1 %	−52.2 %
	LUSEP 1M	-	−5.9 %	−24.4 %	−30.2 %	−57.3 %	−60.7 %
	ROPAM 1M	-	−7.3 %	−6.9 %	−13.8 %	−18.7 %	−25.1 %
	VEPIN 1M	-	−5.1 %	−57.8 %	−61.3 %	−64.6 %	−67.3 %
22L	DIVAM 2A	-	−7.1 %	−5.8 %	−12.6 %	−11.3 %	−18.4 %
	INTOR 3A	-	−7.1 %	−5.8 %	−12.6 %	−11.3 %	−18.4 %
	LAKUT 3A	-	−7.0 %	−7.9 %	−14.5 %	−15.9 %	−22.1 %
	LUSEP 2A	-	−6.1 %	−2.0 %	−7.6 %	−46.0 %	−50.0 %
	ROPAM 2A	-	−7.6 %	−16.6 %	−22.6 %	−24.2 %	−29.8 %
	VEPIN 2A	-	−6.0 %	−2.0 %	−7.4 %	−15.4 %	−20.3 %
22R	DIVAM 2V	-	−6.0 %	−16.0 %	−21.7 %	−19.7 %	−25.3 %
	INTOR 3V	-	−7.4 %	−20.9 %	−26.4 %	−26.4 %	−31.5 %
	LAKUT 3V	-	−5.7 %	−38.4 %	−42.5 %	−42.2 %	−46.1 %
	LUSEP 3V	-	−6.0 %	−0.9 %	−6.9 %	−1.8 %	−7.7 %
	PEXEN 3V	-	−5.1 %	−33.6 %	−38.0 %	−37.7 %	−41.8 %
	ROPAM 2V	-	−6.1 %	−18.2 %	−23.9 %	−29.0 %	−34.0 %
	VEPIN 2V	-	−5.9 %	−1.9 %	−7.6 %	−3.3 %	−8.4 %
33	DIVAM 1W	-	−4.8 %	−59.9 %	−62.9 %	−66.0 %	−68.6 %
	INTOR 4W	-	−6.4 %	−1.6 %	−7.9 %	−18.5 %	−24.5 %
	LAKUT 5W	-	−7.2 %	−7.1 %	−13.9 %	−20.8 %	−26.9 %
	LUSEP 1W	-	−7.2 %	−7.1 %	−13.9 %	−20.8 %	−26.9 %
	ROPAM 1W	-	−6.6 %	−10.7 %	−20.7 %	−33.5 %	−38.7 %
	VEPIN 1W	-	−6.5 %	−50.5 %	−54.1 %	−57.9 %	−61.1 %
Min.		-	−7.6 %	−59.9 %	−62.9 %	−66.0 %	−68.6 %
Max.		-	−4.8 %	−0.9 %	−6.9 %	−1.8 %	−7.5 %
Average		-	**−6.4 %**	**−16.4 %**	**−22.2 %**	**−26.4 %**	**−31.6 %**

6.2.2 Risk Areas

Risk area results for the runway 15 are shown in the Figures 20 – 25. The other runway visualisations are very similar in principle and are presented in the Appendix 4. The speed profile B does not again make a notable difference to the risk area and therefore the visualisations are given here only for the runway 15.

As could be expected, the risk areas have grown to some extent compared to the still air analysis. Otherwise the same regularities could be found from the risk areas for both wind conditions. Straight in approaches are the most prone to extensive risk area exposure. With 5 degree descents the remaining risk areas start to become more reasonable in size from all arrival directions.

As a result from decreased gliding capability in headwind, a greater proportion of the total approach time is risk period. The Table A3.8 in the Appendix 3 indicates that for the 3° descent the percentage of risk period was approximately 75 %, for 4° descent 60 % and for the 5° descent 55 % on average. Geographically the ratio is not quite as high since speed is lower in the later stages of the approach and at lower altitudes. That is also where the risk areas are usually located. The number of approaches that were completely within risk area, regardless of the applied descent angle, was also increased.

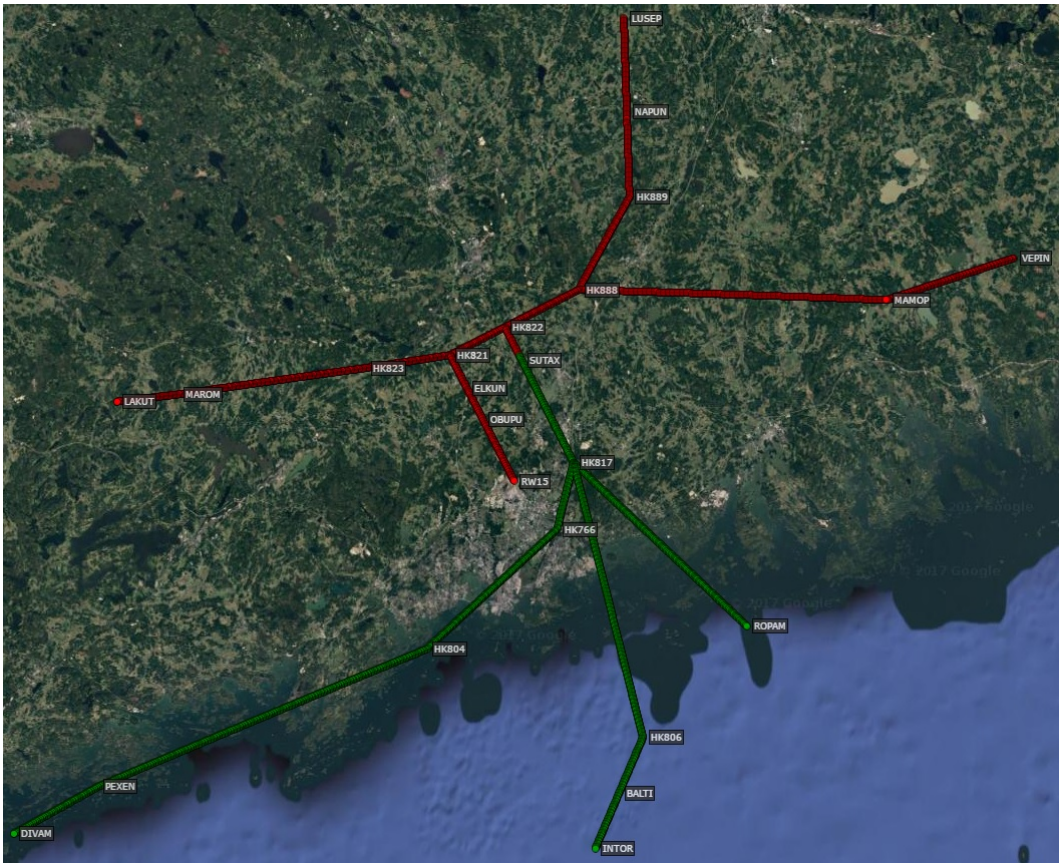

Figure 20. Runway 15 risk areas, 3 degree descent profile, speed profile A, 20 kt headwind.

Figure 21. Runway 15 risk areas, 3 degree descent profile, speed profile B, 20 kt headwind.

Figure 22. Runway 15 risk areas, 4 degree descent profile, speed profile A, 20 kt headwind.

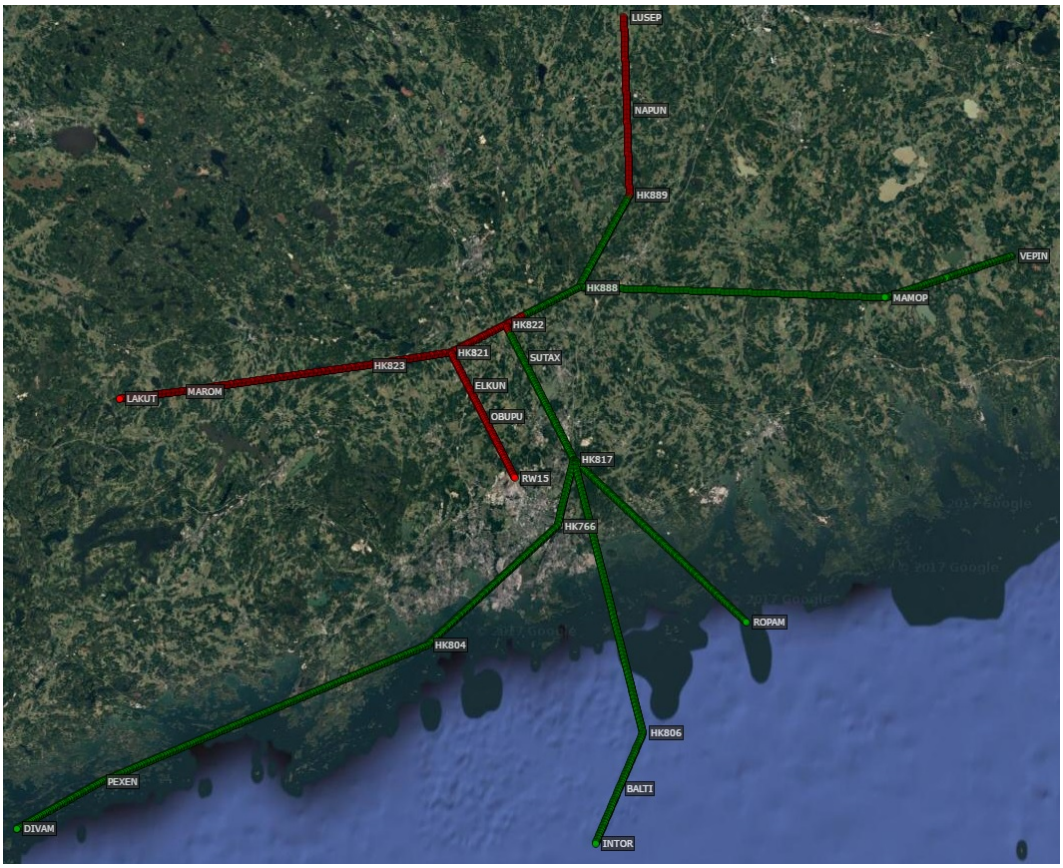

Figure 23. Runway 15 risk areas, 4 degree descent profile, speed profile B, 20 kt headwind.

Figure 24. Runway 15 risk areas, 5 degree descent profile, speed profile A, 20 kt headwind.

Figure 25. Runway 15 risk areas, 5 degree descent profile, speed profile B, 20 kt headwind.

7 Discussion

The method used in this study was a theoretical computational analysis. Due to general nature and unpredictability of commercial aviation, performance and safety related pre-flight calculations made to fulfil the regulations and minimum acceptable safety level, are often theoretical. In that sense, this study is not an exception. This must be kept in mind when making interpretations of the results. The case study is theoretical considering STAR's are rarely flown entirely from the final route waypoint to the IAF at Helsinki Airport. At some point ATC vectors are usually expected. However, the vectored routes often more or less follow the STAR routes. Also shortcuts can be expected. In that case, distance to the runway might stay shorter than in the arrival route and the actual risk period is cut as a consequence.

The results are, nevertheless, reasonable and credible. This analysis provides additional information and a new tool for the SET operators and aviation authorities. In some cases, the arising risk period in the approach was surprisingly high – even over 15 minutes. It must be noted that many conservative estimates and values were applied in this work. The actual risk periods could stay shorter. An approach phase risk period estimate used in QinetiQ working group's SET-IMC risk assessment was approximately 4.5 minutes (Bradley, 2007). Although the flight profile in the study was somewhat different, the applicability of such a short risk period can be questioned for many cases in the light of the results in this thesis.

Risk areas could be identified all around the airport, depending on the runway in use. The risk period can be easily reduced by selecting a predetermined alternative emergency landing site. These landing areas should be explored from all directions suitable distance away from the airport. Taking into account the usual position of the risk areas in this study, a possible location could be close below the final approach course. In addition, there is generally less built-up environment below. For Helsinki Airport, there are plenty of suitable fields in the vicinity and even another airport, Helsinki-Malmi Airport approximately 7 kilometres south-east of the EFHK. Some other uncontrolled aerodromes slightly further away, for instance, in Nummela and in Hyvinkää could be utilised as well. By selecting a sufficient amount of alternative emergency landing sites, the risk period could theoretically be reduced close to zero. However, this might be unnecessarily laborious.

The SET-IMC operators can utilise the method introduced in this thesis at least in three ways. Firstly, if the operators wish to minimise the use of risk period during an arrival segment, they can use the method to identify risk areas and then possibly to select an alternative emergency landing sites for these periods. Secondly, the results of this case analysis clearly indicate that by using higher than nominal 3 degree descent in the arrival the risk period can be significantly reduced. The risk can also be affected by the speed profile. The operators should consider this when planning their SOPs for the SET-IMC operations. Thirdly, if the operators wish to extend the total risk period beyond 15 minutes for some routes, they need to conduct a safety risk assessment. The results of the analysis help to identify the probability of an unsuccessful landing in the approach phase and possible means to mitigate the risk if the cumulative risk is too high.

Operators are encouraged to use the results of this thesis when making their risk analysis for new routes. It is recommended to examine the different arrival routes at least at the operator's base airport, where a majority of the flights will be destined to. The results are suggested to be exploited in development of the contingency procedures and flight crew training. The example illustrations of Helsinki Airport arrival routes can be used to identify the risk areas and to possibly determine alternative emergency landing sites, if the allowed risk period is not desired to be used. The Google maps background already provides an excellent starting point for the search of an alternate landing site.

There are a few related factors this study does not account for. To find the answer to these questions, further study and test flights would be required. First, it is clear that decreasing the risk period improves flight safety considering engine failure cases. But what are the effects of flying steeper descents, higher speeds and vertical speeds for total flight safety, remains unclear. For example, the risk for unstable approach might increase. However, the total effects might be difficult to study and stay under discretion of experts.

Second, the developed method might not be suitable for all environments. It does not take high obstacles and terrain around the airport into account. The obstacles could set restrictions to glide routes and need to be examined separately. Moreover, some airports might have more constrained approach speed and altitude design. Consequently, the utilisation of high descent angles and speeds is more limited. On the other hand, the results showed that restrictions increase risk period. This emphasises the need to identify risk periods and areas. This thesis provides the tools for the analysis.

Third, conditions deviating from the ISA could give differing results. Especially local air temperature and pressure variations could have an impact in the risk period length. As aircraft altimetry is based on pressure levels assuming ISA temperature lapse rate, cold temperatures lead to decreased true altitude, and vice versa for warm temperatures. Therefore, the planned descent angle in normal operations is actually slightly shallower in colder than ISA temperatures. An approximate correction between the indicated and true altitudes is 4 per cent for every 10°C below standard temperature as measured at the aerodrome (ICAO, 2006). For example, in −20°C (35°C below ISA) the actual vertical path angle for 3 degree indicated angle would be approximately 2.63°. Similarly, for 4 degrees the actual angle would be 3.51° and for 5 degrees 4.39°. Hence, the temperature effect for the risk periods and areas can be interpolated from between the results for different angles in this thesis. In actual operations, it would be recommended to use corresponding temperature corrections to the descent angles to maintain the desired true altitudes. Considering warmer than ISA temperatures the results in this analysis are conservative. Another possible atmospheric factor causing differing results is the deviations in pressure. At low altitudes, when flying with the correct local pressure setting below the transition altitude (5000 feet in Finland), the results are correct. However, a standard pressure setting 1013 hPa is used above the transition altitude and this could yield in errors between the indicated and true altitudes. When the actual pressure is below the standard, the true altitude is approximately 30 ft lower per 1 hPa difference (ICAO, 2006). Some flight management systems might be able to automatically take the difference into account in the descent path calculation. If not, then the flight crew should make the necessary calculations to avoid flying below the desired vertical path.

Fourth, in steep high speed descent also the vertical speed increases. In high vertical speeds the pressure change is rapid and could be uncomfortable for the passengers if the aircraft pressurisation system is not efficient enough. This and also other possible downsides of high vertical speed could be facilitated by altering the desired descent angle during the descent. For example in the Pilatus PC-12 NG avionics, a different descent angle can be selected between each waypoint when planning the vertical profile. Then, only the necessary waypoint legs could be planned with higher profile.

Fifth, flying a steeper descent profile could lead to increased fuel consumption. Flight economics has grown in importance and one of the main advantages of SET aircraft is generally low fuel consumption. This asset is desired to be sustained. However, the increment is probably only marginal and could possibly be disregarded.

Finally, a major part of the arising risk period in approach comes from the final approach segment. The speed in this segment is the slowest and thus the exposure time increased. In this study, the final approach was completely included in the risk period. The glide target point in the final approach after FAF/FAP was 50 feet above the runway threshold. However, it might not always be necessary to glide up to the threshold: there are often areas suitable for safe emergency landing, such as runway (if the threshold is displaced), stopway or clearway below the short final. In these cases, the risk period could be reduced from the final segment before the landing. A more detailed study for each runway, taking into account the individual characteristics is needed.

The use of FDM data would provide a more realistic picture of the actual arrival routes at different airports. The problem is that such data is not yet available. Acquiring the data would practically require some of the existing or arising SET-IMC operators to start a systematic FDM program. Even in that case, it would take some time to collect enough data to be used in analysis. At least the Pilatus PC-12 NG could be equipped with an optional light weight data recorder (Pilatus Aircraft, 2016). For the purpose of an elementary FDM program, it would be a sufficient data provider. The collection of the data is relatively easy and a simple tool for the data processing is already available, provided by the Pilatus itself. The same method developed in this thesis could be easily applied also for actual FDM data. When the data is available, it should be utilised for further study to re-examine and possibly validate the results in this thesis.

The issues raised in this chapter would provide excellent topics for follow-up research. It would be interesting to see how the actual flight profiles and risk periods correlate with the theoretical model. Test flights would also provide valuable information on how realistic the simulated vertical and speed profiles are in actual operations considering the performance capabilities of the Pilatus PC-12, and whether further risk mitigation could be possible. Another theme could be studying and comparing the risk periods at different airports and with other SET aircraft. To utilise the method developed in this thesis more efficiently and flexibly, automated and more user-friendly software for the risk period analysis should be developed. There might be a commercial need for such software in the future. Furthermore, current avionic systems do not provide continuous in-flight analysis on the gliding capability, taking into account actual and forecasted winds at different altitudes. The possibility to develop an integrated indication of emergency landing areas within glide distance should be studied. From a pilot's perspective, this would be an excellent feature to reduce the workload in the cockpit.

8 Conclusions

The objectives of this thesis were to first find the equations needed for the risk period analysis and to construct a computation method. The outcome was an Excel spreadsheet calculation tool. Input values for the most important variables could be altered for the computation. Conservative and fixed values were used in this study and the ISA conditions were assumed.

A second target was to construct a simulated flight profile and to calculate theoretical risk periods for a case example. The case was an aeroplane-airport combination of Pilatus PC-12 NG approaching Helsinki Airport. The performance capabilities and limitations of the PC-12 were considered in the flight profile simulation. Also, the altitude and speed constraints and other characteristics of Helsinki Airport approaches were closely followed. A total of 40 standard instrument arrivals were studied. Flying at low altitudes and with relatively slow speed increases the risk period substantially and should be thus avoided to the extent possible.

Aviation regulations for SET-IMC operations were taken into account in this study. Many of the related rules and recommendations indicated a need for this examination. Perhaps the most essential rule when interpreting the risk period results is the limitation of maximum total risk period duration of 15 minutes per flight. The analysis indicated that in some cases the limit could be exceeded in the approach phase alone. The operators should pay attention to the relation between the arrival direction and the runway in use, as well as to the arrival route altitude limitations. Variation between the risk periods for different approaches was considerable. The maximum risk period could be, however, extended if the operator conducts a risk assessment for the route in question.

A third aim was to study how much the arising risk period could be affected with different flight profiles – by altering a descent angle and approach speed. Furthermore, the impact of headwind to the risk period was examined. Steeper descent profile reduced the risk period remarkably both in still air conditions and in headwind. Incremental speed decreases the risk period but mainly due to decreased exposure time to low altitude flying. The risk area also decreases marginally as more excess kinetic energy can be transformed into potential energy. Headwind decreases the gliding capability of an aeroplane and might have substantial influence to the risk period. However, due to unpredictability and variation of wind conditions the wind effect is problematic to reasonably account for in the pre-flight planning. It is clear that the operators can significantly affect the risk period arising from the approach with their SOPs. From the engine failure safety perspective, a three degree descent angle in the arrival segment is not the optimum. Other factors permitting, a higher angle is recommended to be used.

A fourth goal was to identify geographical location of the risk areas in the case study. The results were visualised on a Google maps satellite image. Also the size of the risk area varies significantly depending on the route and possible altitude constraints. In general, the risk area located at least on the final and base legs of the approach. In many of the straight in approaches the complete approach was within risk area. To conclude, the objectives of this thesis were fulfilled and the results provided interesting and detailed information on the risk periods in the approach phase of flight.

References

Airbus, (2002). Getting to Grips with Aircraft Performance. Blagnac, France: Airbus Customer Services. 216 p.

Airbus, (2014). Commercial Aviation Accidents 1958 – 2013. A Statistical Analysis. Blagnac, France: Airbus. 20 p.

Bergqvist, P. (2016). Cessna Turboprop and New Citations Make Progress. Flying, [online]. Available at: http://www.flyingmag.com/cessna-turboprop-and-new-citations-make-progress [Accessed 18 Jul 2016].

Bradley, J. (2007). Risk Assessment for European Public Transport Operations using Single Engine Turbine Aircraft at Night and in IMC. Farnborough, England: QinetiQ Ltd. 54 p.

EASA, (2012a). Commission Regulation (EU) No 965/2012. 148 p.

EASA, (2012b). SERA - Standardised European Rules of the Air. Commission Implementing Regulation (EU) No 923/2012. Brussels, Belgium: EASA. 66 p.

EASA, (2015a). CAT operations at night or in IMC using single-engined turbine aeroplanes. Opinion No 06/2015. 23 p.

EASA, (2015b). CAT operations at night or in IMC using single-engined turbine aeroplanes. Comment-Response Document 2014-18. 112 p.

EASA, (2017a). Air Ops. Annex I to VII. Commission Regulation (EU) No 965/2012 on air operations and related EASA Decisions (AMC & GM and CS-FTL.1). Consolidated version. Revision 9. 1918 p.

EASA, (2017b). Commission Regulation (EU) 2017/363. 9 p.

EASA, (2017c). SMS - Rulemaking Status. [online] EASA website. Available at: https://www.easa.europa.eu/easa-and-you/safety-management/safety-management-system/sms-rulemaking-status. [Accessed 18 Jan 2017].

EBAA, (2016). EASA Committee approves commercial SET-IMC. European Business Aviation Association. Press release. Handbook of Business Aviation [online]. Available at: http://www.handbook.aero/hb_news_story.html?release=34221 [Accessed 19 Jan 2017].

Finavia, (2017). Aeronautical Information Publication (eAIP) Finland. Available at: https://ais.fi/ais/eaip/en/ [Accessed 9 Jan 2017].

Hendell Aviation, (2017). The company website. http://www.hendellaviation.fi/en/ [Accessed 3 Jul 2017].

Hoffren, J. and Rahikainen, M. (1992). Lentokoneen suoritusarvot. Espoo, Finland: Teknillisen korkeakoulun lentotekniikan laitos. 204 p.

Honeywell, (2014). Primus Apex. Integrated Avionics System for the Pilatus PC-12 NG. Pilot's Guide. Revision 5. Phoenix, Arizona, United States: Honeywell International Inc. 1125 p.

ICAO, (2006). Procedures for Air Navigation Services. Aircraft Operations. Volume I. Flight Procedures. Doc 8168. Fifth Edition. Montréal, Quebec, Canada: ICAO. 279 p.

ICAO, (2010). Operation of Aircraft. Part I. International Commercial Air Transport – Aeroplanes. Annex 6 to the Convention on International Civil Aviation. Ninth Edition. Montréal, Quebec, Canada: ICAO. 240 p.

ICAO, (2013a). Safety Management. Annex 19 to the Convention on International Civil Aviation. First Edition. Montréal, Quebec, Canada: ICAO. 44 p.

ICAO, (2013b). Safety Management Manual (SMM). Doc 9859. Third Edition. Montréal, Quebec, Canada: ICAO. 251 p.

JAA, (2004). Single-Engine Commercial Operations at Night and/or in IMC. NPA OPS-29 rev. 2. Hoofddorp, the Netherlands: Joint Aviation Authorities. 92 p.

Karila, J. (2017). Tower and Approach Air Traffic Controller. Helsinki Airport. Interview on 31 Mar 2017.

Keltanen, R. (2017). Pilatus PC-12 Class Rated Military (Finnish Air Force) and Civil Pilot and Flight Instructor. Interview on 15 Jun 2017.

Koe, R. (2016). Single-engines could benefit European bizav. FlyCorporate [online]. Available at: http://www.fly-corporate.com/single-engines-could-befit-euro-bizav/ [Accessed 4 Jul 2017].

Lee, W.-K. (2006). Risk assessment modeling in aviation safety management. Journal of Air Transport Management. Volume 12, Issue 5, September 2006. pp. 267-273.

Nordflyg Air Logistics. (2017). The company website. http://logistics.nordflyg.se/ [Accessed 3 Jul 2017].

Pilatus Aircraft Ltd. (2016). Pilots Operating Handbook and EASA Approved Airplane Flight Manual. Revision 16. Report No. 02277. Stans, Switzerland: Pilatus Aircraft Ltd. 1222 p.

Robert E. Breiling Associates, Inc. (2013). Single Turboprop Powered Aircraft Accident Analysis. U.S. and Canadian Fleet. Aircraft Certification through 2012 for Pilatus Business Aircraft Ltd. Boca Raton, Florida, United States: Robert E. Breiling Associates, Inc. 6 p.

Simpson, R. (2016). Single-engine Turboprops Set to Launch in Europe. FlyCorporate [online]. Available at: http://www.fly-corporate.com/single-engine-turboprops-set-to-launch-in-europe/ [Accessed 19 Jun 2017].

Voldirect. (2017). The company website. http://www.voldirect.aero/en/ [Accessed 3 Jul 2017].

Williams, E. (2017). Aviation Formulary V1.46. [online] Ed Williams' Aviation page. Available at: http://edwilliams.org/avform.htm [Accessed 3 Apr 2017]

List of Appendices

Appendix 1. EFHK Standard Instrument Arrival Routes

Runway 04L

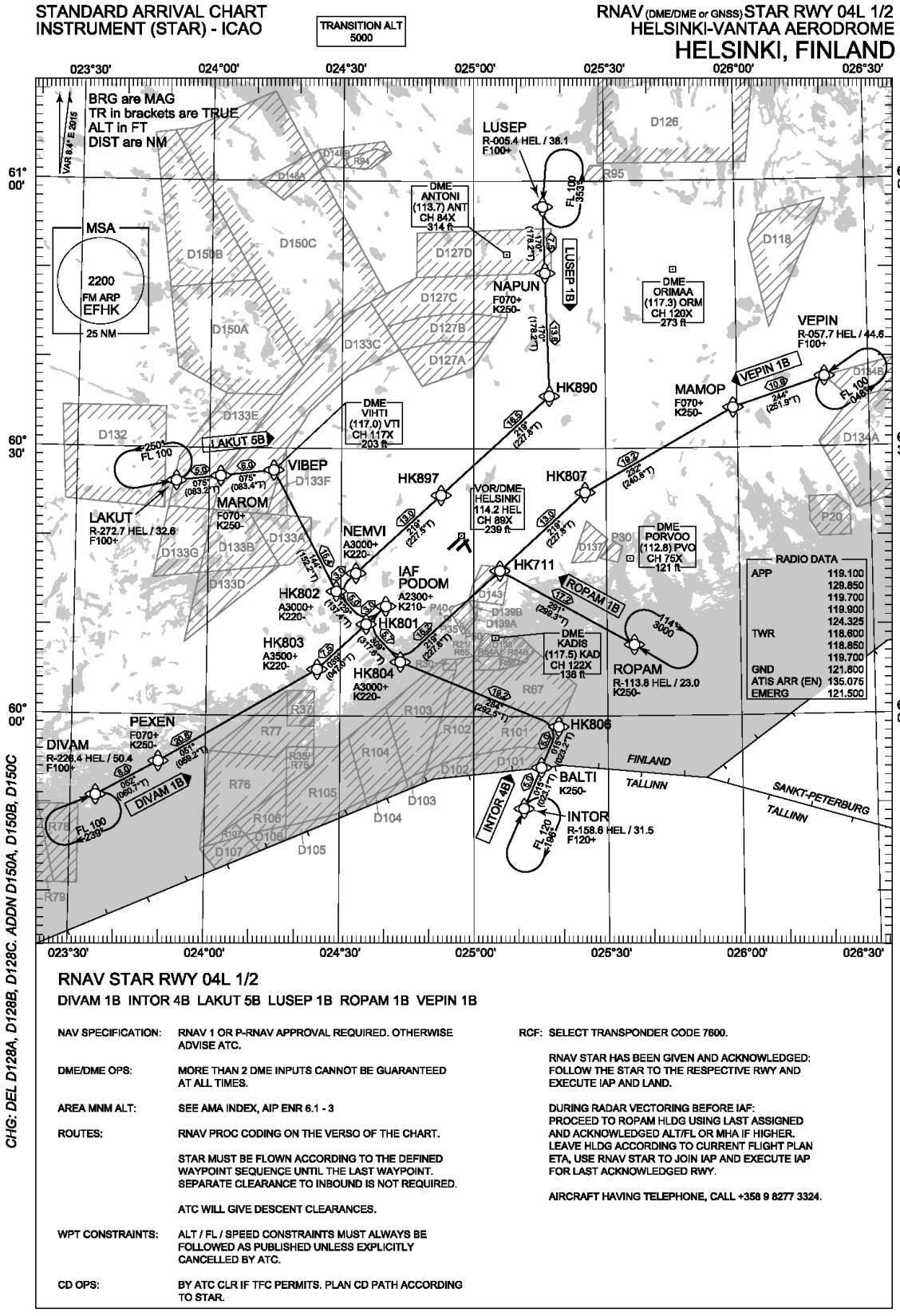

EFHK RNAV STAR RWY 04L 1/2										
RTE NAV SPEC	SEQ NR	P/T	WPT ID	WPT Flyover	MAG	GEO TR	DIST NM	Turn Direction	Constraints LVL	Constraints Speed
DIVAM 1B RNAV 1 or P-RNAV	010	IF	DIVAM	-	-	-	-		F100+	
	020	TF	PEXEN	-	052°	060.7°T	8.0		F070+	K250-
	030	TF	HK803	-	051°	059.2°T	20.6		A3500+	K220-
	040	TF	HK801	-	039°	047.0°T	7.5			
	050	TF	PODOM	-	039°	047.2°T	3.0		A2300+	K210-
INTOR 4B RNAV 1 or P-RNAV	010	IF	INTOR	-	-	-	-		F120+	
	020	TF	BALTI	-	015°	023.1°T	5.0			K250-
	030	TF	HK806	-	015°	023.2°T	5.0	L		
	040	TF	HK804	-	284°	292.5°T	19.2		A3000+	K220-
	050	TF	HK801	-	309°	317.6°T	5.7	R		
	060	TF	PODOM	-	039°	047.2°T	3.0		A2300+	K210-
LAKUT 5B RNAV 1 or P-RNAV	010	IF	LAKUT	-	-	-	-		F100+	
	020	TF	MAROM	-	075°	083.2°T	5.0		F070+	K250-
	030	TF	VIBEP	-	075°	083.4°T	6.0	R		
	040	TF	HK802	-	144°	152.2°T	15.4		A3000+	K220-
	050	TF	HK801	-	129°	137.4°T	5.0	L		
	060	TF	PODOM	-	039°	047.2°T	3.0		A2300+	K210-
LUSEP 1B RNAV 1 or P-RNAV	010	IF	LUSEP	-	-	-	-		F100+	
	020	TF	NAPUN	-	170°	178.2°T	7.5		F070+	K250-
	030	TF	HK890	-	170°	178.2°T	13.8	R		
	040	TF	HK897	-	219°	227.8°T	16.5			
	050	TF	NEMVI	-	219°	227.5°T	13.0		A3000+	K220-
	060	TF	HK802	-	219°	227.2°T	3.0	L	A3000+	K220-
	070	TF	HK801	-	129°	137.4°T	5.0	L		
	080	TF	PODOM	-	039°	047.2°T	3.0		A2300+	K210-
ROPAM 1B RNAV 1 or P-RNAV	010	IF	ROPAM	-	-	-	-			K250-
	020	TF	HK711	-	291°	299.3°T	17.2	L		
	030	TF	HK804	-	219°	227.6°T	15.2	R	A3000+	K220-
	040	TF	HK801	-	309°	317.6°T	5.7	R		
	050	TF	PODOM	-	039°	047.2°T	3.0		A2300+	K210-
VEPIN 1B RNAV 1 or P-RNAV	010	IF	VEPIN	-	-	-	-		F100+	
	020	TF	MAMOP	-	244°	251.9°T	10.9		F070+	K250-
	030	TF	HK807	-	232°	240.8°T	19.2			
	040	TF	HK711	-	219°	227.8°T	13.0			
	050	TF	HK804	-	219°	227.6°T	15.2	R	A3000+	K220-
	060	TF	HK801	-	309°	317.6°T	5.7	R		
	070	TF	PODOM	-	039°	047.2°T	3.0		A2300+	K210-

RNAV Holdings							
ID	INBD TR	INBD MAG	Turn Direction	MAX IAS	MNM HLDG LVL	TIME	DIST NM
DIVAM	067.4°T	059°	Right	230 KT	F100	1 MIN	-
INTOR	023.5°T	016°	Right	230 KT	F120	1 MIN	-
LAKUT	077.9°T	070°	Left	230 KT	F100	1 MIN	-
LUSEP	181.3°T	173°	Left	230 KT	F100	1 MIN	-
ROPAM	302.0°T	294°	Right	230 KT	A3000	1 MIN	-
VEPIN	236.1°T	228°	Left	230 KT	F100	1 MIN	-

WPT COORD
SEE PAGE EFHK AD 2.15 - 1

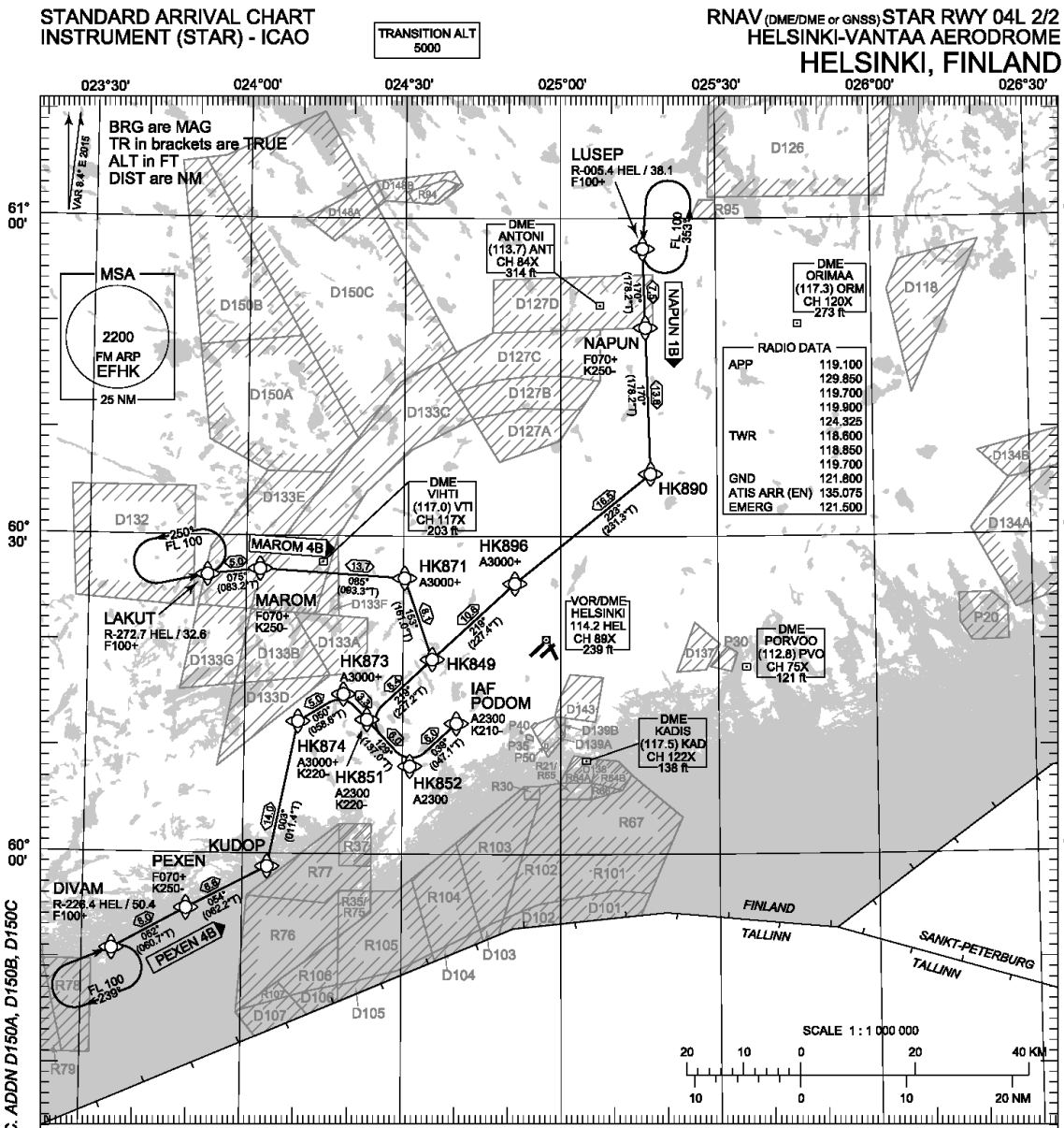

RNAV STAR RWY 04L 2/2

MAROM 4B NAPUN 1B PEXEN 4B

NAV SPECIFICATION:	RNAV 1 OR P-RNAV APPROVAL REQUIRED. OTHERWISE ADVISE ATC.
DME/DME OPS:	MORE THAN 2 DME INPUTS CANNOT BE GUARANTEED AT ALL TIMES.
AREA MNM ALT:	SEE AMA INDEX, AIP ENR 6.1 - 3
ROUTES:	RNAV PROC CODING ON THE VERSO OF THE CHART. STAR MUST BE FLOWN ACCORDING TO THE DEFINED WAYPOINT SEQUENCE UNTIL THE LAST WAYPOINT. SEPARATE CLEARANCE TO INBOUND IS NOT REQUIRED. ATC WILL GIVE DESCENT CLEARANCES.
WPT CONSTRAINTS:	ALT / FL / SPEED CONSTRAINTS MUST ALWAYS BE FOLLOWED AS PUBLISHED UNLESS EXPLICITLY CANCELLED BY ATC.
CD OPS:	BY ATC CLR IF TFC PERMITS. PLAN CD PATH ACCORDING TO STAR.
RCF:	SELECT TRANSPONDER CODE 7600. RNAV STAR HAS BEEN GIVEN AND ACKNOWLEDGED: FOLLOW THE STAR TO THE RESPECTIVE RWY AND EXECUTE IAP AND LAND. DURING RADAR VECTORING BEFORE IAF: PROCEED TO ROPAM HLDG USING LAST ASSIGNED AND ACKNOWLEDGED ALT/FL OR MHA IF HIGHER. LEAVE HLDG ACCORDING TO CURRENT FLIGHT PLAN ETA, USE RNAV STAR TO JOIN IAP AND EXECUTE IAP FOR LAST ACKNOWLEDGED RWY. AIRCRAFT HAVING TELEPHONE, CALL +358 9 8277 3324.

CHG: DEL D128A, D128B, D128C. ADDN D150A, D150B, D150C

EFHK RNAV STAR RWY 04L 2/2										
RTE NAV SPEC	SEQ NR	P/T	WPT ID	WPT Flyover	MAG	GEO TR	DIST NM	Turn Direction	Constraints LVL	Constraints Speed
MAROM 4B RNAV 1 or P-RNAV	010	IF	LAKUT	-	-	-	-		F100+	
	020	TF	MAROM	-	075°	083.2°T	5.0		F070+	K250-
	030	TF	HK871	-	085°	093.3°T	13.7	R	A3000+	
	040	TF	HK849	-	153°	161.0°T	8.1	R		
	050	TF	HK851	-	219°	227.2°T	8.4	L	A2300	K220-
	060	TF	HK852	-	129°	137.0°T	6.0	L	A2300	
	070	TF	PODOM	-	039°	047.1°T	6.0		A2300	K210-
NAPUN 1B RNAV 1 or P-RNAV	010	IF	LUSEP	-	-	-	-		F100+	
	020	TF	NAPUN	-	170°	178.2°T	7.5		F070+	K250-
	030	TF	HK890	-	170°	178.2°T	13.8	R		
	040	TF	HK896	-	223°	231.3°T	16.5		A3000+	
	050	TF	HK849	-	219°	227.4°T	10.6			
	060	TF	HK851	-	219°	227.2°T	8.4	L	A2300	K220-
	070	TF	HK852	-	129°	137.0°T	6.0	L	A2300	
	080	TF	PODOM	-	039°	047.1°T	6.0		A2300	K210-
PEXEN 4B RNAV 1 or P-RNAV	010	IF	DIVAM	-	-	-	-		F100+	
	020	TF	PEXEN	-	052°	060.7°T	8.0		F070+	K250-
	030	TF	KUDOP	-	054°	062.2°T	8.6	L		
	040	TF	HK874	-	003°	011.4°T	14.0	R	A3000+	K220-
	050	TF	HK873	-	050°	058.6°T	5.0	R	A3000+	
	060	TF	HK851	-	129°	137.0°T	3.3		A2300	K220-
	070	TF	HK852	-	129°	137.0°T	6.0	L	A2300	
	080	TF	PODOM	-	039°	047.1°T	6.0		A2300	K210-

RNAV Holdings							
ID	INBD TR	INBD MAG	Turn Direction	MAX IAS	MNM HLDG LVL	TIME	DIST NM
DIVAM	067.4°T	059°	Right	230 KT	F100	1 MIN	-
LAKUT	077.9°T	070°	Left	230 KT	F100	1 MIN	-
LUSEP	181.3°T	173°	Left	230 KT	F100	1 MIN	-

WPT COORD
SEE PAGE EFHK AD 2.15 - 1

Runway 04R

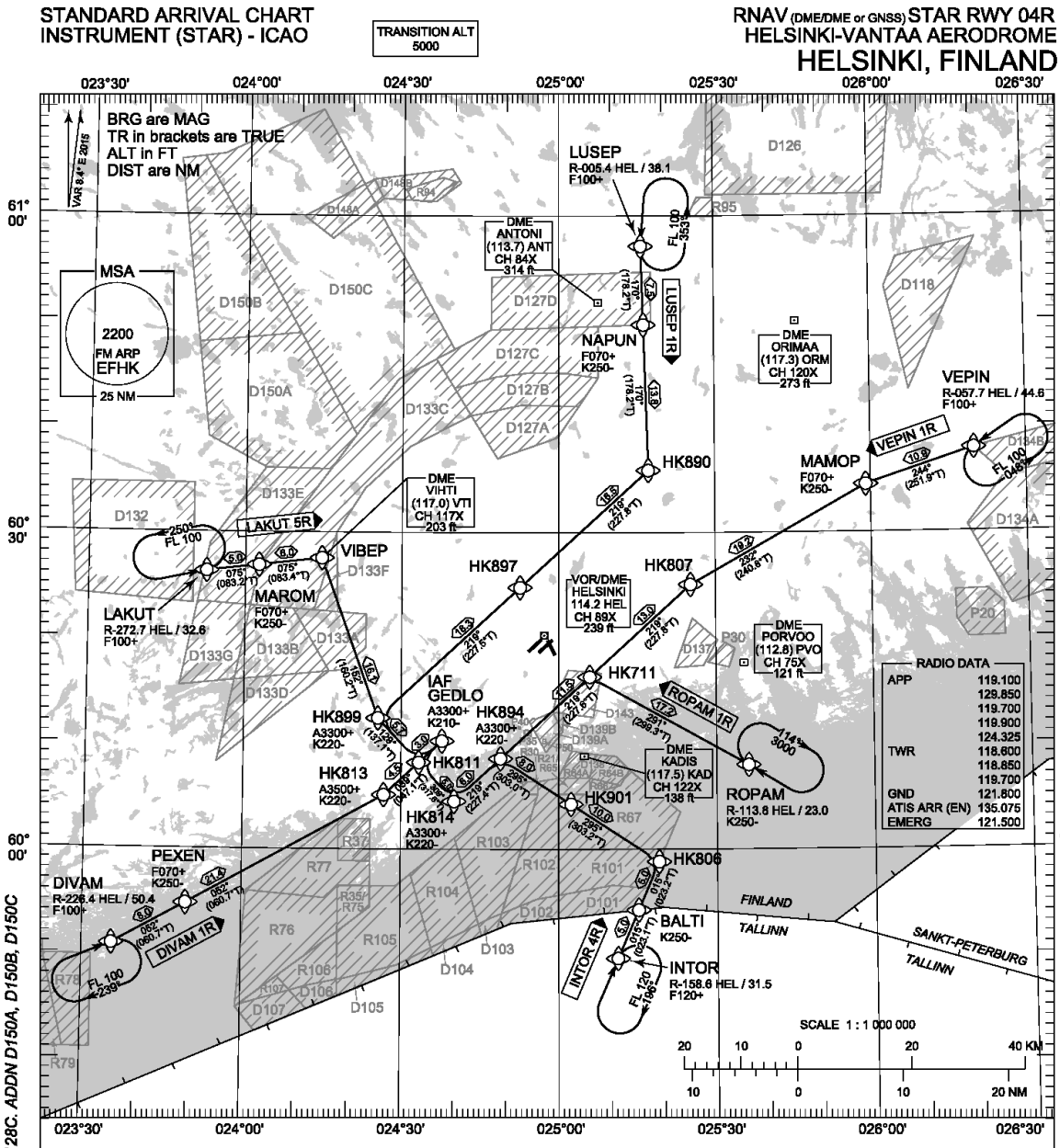

RNAV STAR RWY 04R

DIVAM 1R INTOR 4R LAKUT 5R LUSEP 1R ROPAM 1R VEPIN 1R

NAV SPECIFICATION:	RNAV 1 OR P-RNAV APPROVAL REQUIRED. OTHERWISE ADVISE ATC.
DME/DME OPS:	MORE THAN 2 DME INPUTS CANNOT BE GUARANTEED AT ALL TIMES.
AREA MNM ALT:	SEE AMA INDEX, AIP ENR 6.1 - 3
ROUTES:	RNAV PROC CODING ON THE VERSO OF THE CHART. STAR MUST BE FLOWN ACCORDING TO THE DEFINED WAYPOINT SEQUENCE UNTIL THE LAST WAYPOINT. SEPARATE CLEARANCE TO INBOUND IS NOT REQUIRED. ATC WILL GIVE DESCENT CLEARANCES.
WPT CONSTRAINTS:	ALT / FL / SPEED CONSTRAINTS MUST ALWAYS BE FOLLOWED AS PUBLISHED UNLESS EXPLICITLY CANCELLED BY ATC.
CD OPS:	BY ATC CLR IF TFC PERMITS. PLAN CD PATH ACCORDING TO STAR.
RCF:	SELECT TRANSPONDER CODE 7600. RNAV STAR HAS BEEN GIVEN AND ACKNOWLEDGED: FOLLOW THE STAR TO THE RESPECTIVE RWY AND EXECUTE IAP AND LAND. DURING RADAR VECTORING BEFORE IAF: PROCEED TO ROPAM HLDG USING LAST ASSIGNED AND ACKNOWLEDGED ALT/FL OR MHA IF HIGHER. LEAVE HLDG ACCORDING TO CURRENT FLIGHT PLAN ETA, USE RNAV STAR TO JOIN IAP AND EXECUTE IAP FOR LAST ACKNOWLEDGED RWY. AIRCRAFT HAVING TELEPHONE, CALL +358 9 8277 3324.

CHG: DEL D128A, D128B, D128C. ADDN D150A, D150B, D150C

EFHK RNAV STAR RWY 04R										
RTE NAV SPEC	SEQ NR	P/T	WPT ID	WPT Flyover	MAG	GEO TR	DIST NM	Turn Direction	Constraints LVL	Constraints Speed
DIVAM 1R RNAV 1 or P-RNAV	010	IF	DIVAM	-	-	-	-		F100+	
	020	TF	PEXEN	-	052°	060.7°T	8.0		F070+	K250-
	030	TF	HK813	-	052°	060.7°T	21.4		A3500+	K220-
	040	TF	HK811	-	039°	047.1°T	4.5			
	050	TF	GEDLO	-	039°	047.2°T	3.0		A3300+	K210-
INTOR 4R RNAV 1 or P-RNAV	010	IF	INTOR	-	-	-	-		F120+	
	020	TF	BALTI	-	015°	023.1°T	5.0			K250-
	030	TF	HK806	-	015°	023.2°T	5.0	L		
	040	TF	HK901	-	295°	303.2°T	10.0			
	050	TF	HK894	-	295°	303.0°T	8.0	L	A3300+	K220-
	060	TF	HK814	-	219°	227.4°T	6.0	R	A3300+	K220-
	070	TF	HK811	-	309°	317.6°T	5.0	R		
	080	TF	GEDLO	-	039°	047.2°T	3.0		A3300+	K210-
LAKUT 5R RNAV 1 or P-RNAV	010	IF	LAKUT	-	-	-	-		F100+	
	020	TF	MAROM	-	075°	083.2°T	5.0		F070+	K250-
	030	TF	VIBEP	-	075°	083.4°T	6.0	R		
	040	TF	HK899	-	152°	160.2°T	16.1		A3300+	K220-
	050	TF	HK811	-	129°	137.1°T	5.7	L		
	060	TF	GEDLO	-	039°	047.2°T	3.0		A3300+	K210-
LUSEP 1R RNAV 1 or P-RNAV	010	IF	LUSEP	-	-	-	-		F100+	
	020	TF	NAPUN	-	170°	178.2°T	7.5		F070+	K250-
	030	TF	HK890	-	170°	178.2°T	13.8	R		
	040	TF	HK897	-	219°	227.8°T	16.5			
	050	TF	HK899	-	219°	227.5°T	18.3	L	A3300+	K220-
	060	TF	HK811	-	129°	137.1°T	5.7	L		
	070	TF	GEDLO	-	039°	047.2°T	3.0		A3300+	K210-
ROPAM 1R RNAV 1 or P-RNAV	010	IF	ROPAM	-	-	-	-			K250-
	020	TF	HK711	-	291°	299.3°T	17.2	L		
	030	TF	HK894	-	219°	227.6°T	11.5		A3300+	K220-
	040	TF	HK814	-	219°	227.4°T	6.0	R	A3300+	K220-
	050	TF	HK811	-	309°	317.6°T	5.0	R		
	060	TF	GEDLO	-	039°	047.2°T	3.0		A3300+	K210-
VEPIN 1R RNAV 1 or P-RNAV	010	IF	VEPIN	-	-	-	-		F100+	
	020	TF	MAMOP	-	244°	251.9°T	10.9		F070+	K250-
	030	TF	HK807	-	232°	240.8°T	19.2			
	040	TF	HK711	-	219°	227.8°T	13.0			
	050	TF	HK894	-	219°	227.6°T	11.5		A3300+	K220-
	060	TF	HK814	-	219°	227.4°T	6.0	R	A3300+	K220-
	070	TF	HK811	-	309°	317.6°T	5.0	R		
	080	TF	GEDLO	-	039°	047.2°T	3.0		A3300+	K210-

RNAV Holdings							
ID	INBD TR	INBD MAG	Turn Direction	MAX IAS	MNM HLDG LVL	TIME	DIST NM
DIVAM	067.4°T	059°	Right	230 KT	F100	1 MIN	-
INTOR	023.5°T	016°	Right	230 KT	F120	1 MIN	-
LAKUT	077.9°T	070°	Left	230 KT	F100	1 MIN	-
LUSEP	181.3°T	173°	Left	230 KT	F100	1 MIN	-
ROPAM	302.0°T	294°	Right	230 KT	A3000	1 MIN	-
VEPIN	236.1°T	228°	Left	230 KT	F100	1 MIN	-

WPT COORD
SEE PAGE EFHK AD 2.15 - 1

Runway 15

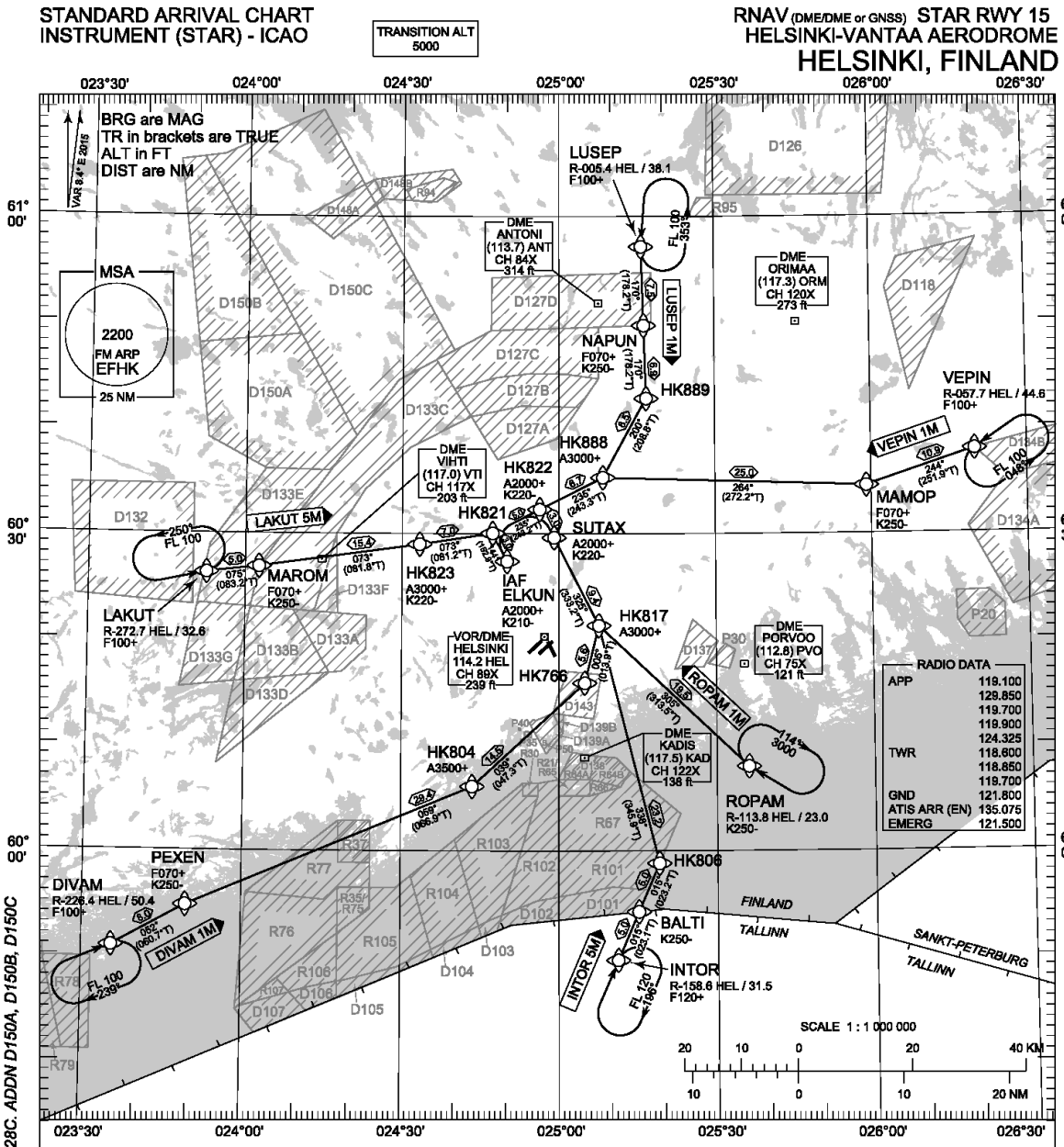

RNAV STAR RWY 15

DIVAM 1M INTOR 5M LAKUT 5M LUSEP 1M ROPAM 1M VEPIN 1M

NAV SPECIFICATION:	RNAV 1 OR P-RNAV APPROVAL REQUIRED. OTHERWISE ADVISE ATC.
DME/DME OPS:	MORE THAN 2 DME INPUTS CANNOT BE GUARANTEED AT ALL TIMES.
AREA MNM ALT:	SEE AMA INDEX, AIP ENR 6.1 - 3
ROUTES:	RNAV PROC CODING ON THE VERSO OF THE CHART. STAR MUST BE FLOWN ACCORDING TO THE DEFINED WAYPOINT SEQUENCE UNTIL THE LAST WAYPOINT. SEPARATE CLEARANCE TO INBOUND IS NOT REQUIRED. ATC WILL GIVE DESCENT CLEARANCES.
WPT CONSTRAINTS:	ALT / FL / SPEED CONSTRAINTS MUST ALWAYS BE FOLLOWED AS PUBLISHED UNLESS EXPLICITLY CANCELLED BY ATC.
CD OPS:	BY ATC CLR IF TFC PERMITS. PLAN CD PATH ACCORDING TO STAR.
RCF:	SELECT TRANSPONDER CODE 7600. RNAV STAR HAS BEEN GIVEN AND ACKNOWLEDGED: FOLLOW THE STAR TO THE RESPECTIVE RWY AND EXECUTE IAP AND LAND. DURING RADAR VECTORING BEFORE IAF: PROCEED TO ROPAM HLDG USING LAST ASSIGNED AND ACKNOWLEDGED ALT/FL OR MHA IF HIGHER. LEAVE HLDG ACCORDING TO CURRENT FLIGHT PLAN ETA, USE RNAV STAR TO JOIN IAP AND EXECUTE IAP FOR LAST ACKNOWLEDGED RWY. AIRCRAFT HAVING TELEPHONE, CALL +358 9 8277 3324.

CHG: DEL D128A, D128B, D128C. ADDN D150A, D150B, D150C

EFHK RNAV STAR RWY 15										
RTE NAV SPEC	SEQ NR	P/T	WPT ID	WPT Flyover	MAG	GEO TR	DIST NM	Turn Direction	Constraints LVL	Constraints Speed
DIVAM 1M RNAV 1 or P-RNAV	010	IF	DIVAM	-	-	-	-		F100+	
	020	TF	PEXEN	-	052°	060.7°T	8.0		F070+	K250-
	030	TF	HK804	-	059°	066.9°T	29.4		A3500+	
	040	TF	HK766	-	039°	047.3°T	14.5	L		
	050	TF	HK817	-	005°	013.9°T	5.6	L	A3000+	
	060	TF	SUTAX	-	325°	333.2°T	9.4		A2000+	K220-
	070	TF	HK822	-	325°	333.1°T	3.0	L	A2000+	K220-
	080	TF	HK821	-	235°	243.2°T	5.0	L		
	090	TF	ELKUN	-	144°	152.9°T	3.0		A2000+	K210-
INTOR 5M RNAV 1 or P-RNAV	010	IF	INTOR	-	-	-	-		F120+	
	020	TF	BALTI	-	015°	023.1°T	5.0			K250-
	030	TF	HK806	-	015°	023.2°T	5.0	L		
	040	TF	HK817	-	338°	345.9°T	23.2		A3000+	
	050	TF	SUTAX	-	325°	333.2°T	9.4		A2000+	K220-
	060	TF	HK822	-	325°	333.1°T	3.0	L	A2000+	K220-
	070	TF	HK821	-	235°	243.2°T	5.0	L		
	080	TF	ELKUN	-	144°	152.9°T	3.0		A2000+	K210-
LAKUT 5M RNAV 1 or P-RNAV	010	IF	LAKUT	-	-	-	-		F100+	
	020	TF	MAROM	-	075°	083.2°T	5.0		F070+	K250-
	030	TF	HK823	-	073°	081.8°T	15.4		A3000+	K220-
	040	TF	HK821	-	073°	081.2°T	7.0	R		
	050	TF	ELKUN	-	144°	152.9°T	3.0		A2000+	K210-
LUSEP 1M RNAV 1 or P-RNAV	010	IF	LUSEP	-	-	-	-		F100+	
	020	TF	NAPUN	-	170°	178.2°T	7.5		F070+	K250-
	030	TF	HK889	-	170°	178.2°T	6.9	R		
	040	TF	HK888	-	200°	208.8°T	8.5	R	A3000+	
	050	TF	HK822	-	235°	243.3°T	6.7		A2000+	K220-
	060	TF	HK821	-	235°	243.2°T	5.0	L		
	070	TF	ELKUN	-	144°	152.9°T	3.0		A2000+	K210-
ROPAM 1M RNAV 1 or P-RNAV	010	IF	ROPAM	-	-	-	-			K250-
	020	TF	HK817	-	305°	313.5°T	19.5		A3000+	
	030	TF	SUTAX	-	325°	333.2°T	9.4		A2000+	K220-
	040	TF	HK822	-	325°	333.1°T	3.0	L	A2000+	K220-
	050	TF	HK821	-	235°	243.2°T	5.0	L		
	060	TF	ELKUN	-	144°	152.9°T	3.0		A2000+	K210-
VEPIN 1M RNAV 1 or P-RNAV	010	IF	VEPIN	-	-	-	-		F100+	
	020	TF	MAMOP	-	244°	251.9°T	10.9		F070+	K250-
	030	TF	HK888	-	264°	272.2°T	25.0	L	A3000+	
	040	TF	HK822	-	235°	243.3°T	6.7		A2000+	K220-
	050	TF	HK821	-	235°	243.2°T	5.0	L		
	060	TF	ELKUN	-	144°	152.9°T	3.0		A2000+	K210-

RNAV Holdings							
ID	INBD TR	INBD MAG	Turn Direction	MAX IAS	MNM HLDG LVL	TIME	DIST NM
DIVAM	067.4°T	059°	Right	230 KT	F100	1 MIN	-
INTOR	023.5°T	016°	Right	230 KT	F120	1 MIN	-
LAKUT	077.9°T	070°	Left	230 KT	F100	1 MIN	-
LUSEP	181.3°T	173°	Left	230 KT	F100	1 MIN	-
ROPAM	302.0°T	294°	Right	230 KT	A3000	1 MIN	-
VEPIN	236.1°T	228°	Left	230 KT	F100	1 MIN	-

WPT COORD
SEE PAGE EFHK AD 2.15 - 1

Runway 22L

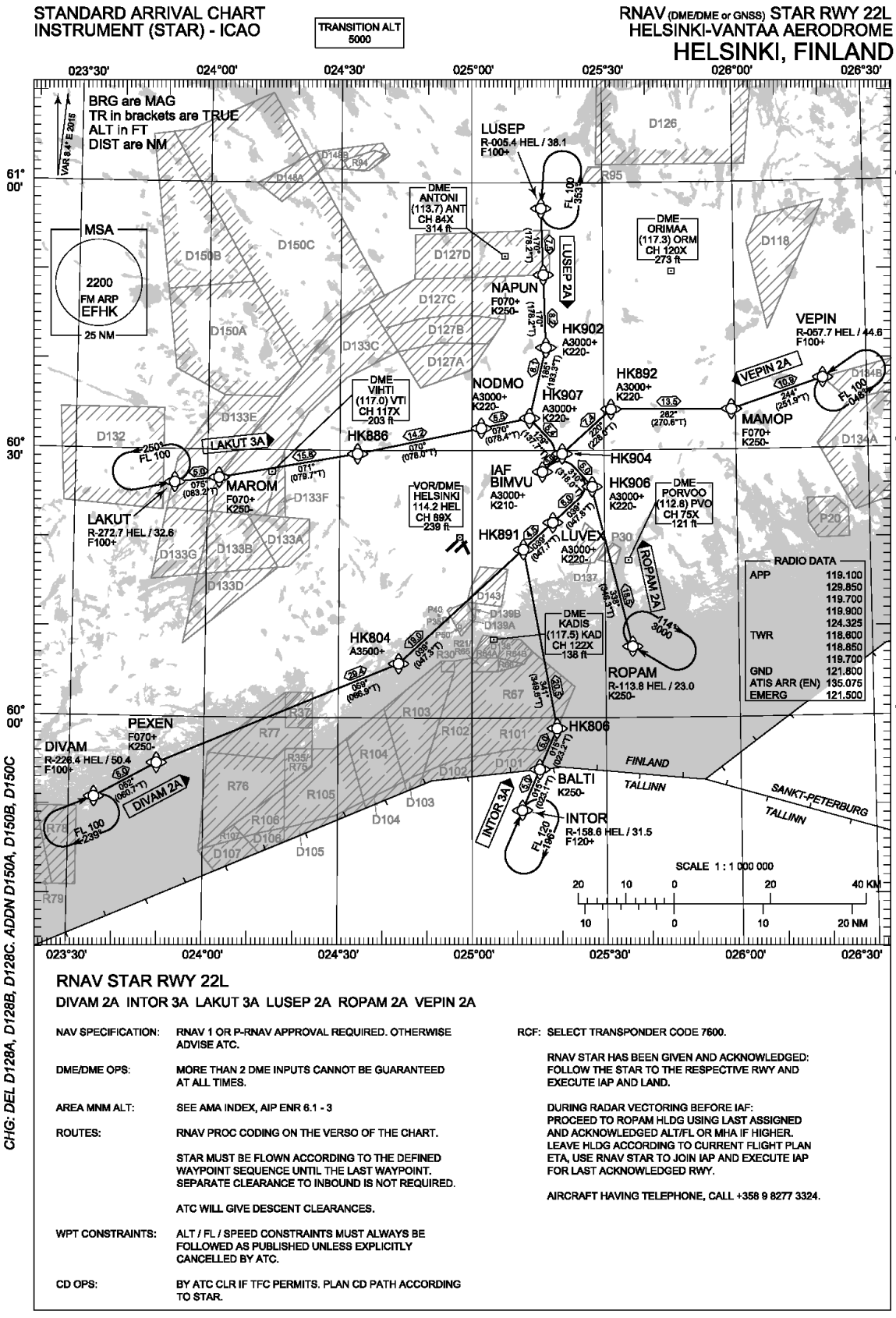

RNAV STAR RWY 22L

DIVAM 2A INTOR 3A LAKUT 3A LUSEP 2A ROPAM 2A VEPIN 2A

NAV SPECIFICATION:	RNAV 1 OR P-RNAV APPROVAL REQUIRED. OTHERWISE ADVISE ATC.
DME/DME OPS:	MORE THAN 2 DME INPUTS CANNOT BE GUARANTEED AT ALL TIMES.
AREA MNM ALT:	SEE AMA INDEX, AIP ENR 6.1 - 3
ROUTES:	RNAV PROC CODING ON THE VERSO OF THE CHART. STAR MUST BE FLOWN ACCORDING TO THE DEFINED WAYPOINT SEQUENCE UNTIL THE LAST WAYPOINT. SEPARATE CLEARANCE TO INBOUND IS NOT REQUIRED. ATC WILL GIVE DESCENT CLEARANCES.
WPT CONSTRAINTS:	ALT / FL / SPEED CONSTRAINTS MUST ALWAYS BE FOLLOWED AS PUBLISHED UNLESS EXPLICITLY CANCELLED BY ATC.
CD OPS:	BY ATC CLR IF TFC PERMITS. PLAN CD PATH ACCORDING TO STAR.
RCF:	SELECT TRANSPONDER CODE 7600. RNAV STAR HAS BEEN GIVEN AND ACKNOWLEDGED: FOLLOW THE STAR TO THE RESPECTIVE RWY AND EXECUTE IAP AND LAND. DURING RADAR VECTORING BEFORE IAF: PROCEED TO ROPAM HLDG USING LAST ASSIGNED AND ACKNOWLEDGED ALT/FL OR MHA IF HIGHER. LEAVE HLDG ACCORDING TO CURRENT FLIGHT PLAN ETA, USE RNAV STAR TO JOIN IAP AND EXECUTE IAP FOR LAST ACKNOWLEDGED RWY. AIRCRAFT HAVING TELEPHONE, CALL +358 9 8277 3324.

CHG: DEL D128A, D128B, D128C. ADDN D150A, D150B, D150C

EFHK RNAV STAR RWY 22L										
RTE NAV SPEC	SEQ NR	P/T	WPT		MAG	GEO TR	DIST NM	Turn Direction	Constraints	
			ID	Flyover					LVL	Speed
DIVAM 2A RNAV 1 or P-RNAV	010	IF	DIVAM	-	-	-	-		F100+	
	020	TF	PEXEN	-	052°	060.7°T	8.0		F070+	K250-
	030	TF	HK804	-	059°	066.9°T	29.4		A3500+	
	040	TF	HK891	-	039°	047.3°T	19.0			
	050	TF	LUVEX	-	039°	047.7°T	4.5		A3000+	K220-
	060	TF	HK906	-	039°	047.8°T	6.0	L	A3000+	K220-
	070	TF	HK904	-	310°	318.0°T	5.0	L		
	080	TF	BIMVU	-	219°	227.9°T	3.0		A3000+	K210-
INTOR 3A RNAV 1 or P-RNAV	010	IF	INTOR	-	-	-	-		F120+	
	020	TF	BALTI	-	015°	023.1°T	5.0			K250-
	030	TF	HK806	-	015°	023.2°T	5.0	L		
	040	TF	HK891	-	341°	349.6°T	20.5	R		
	050	TF	LUVEX	-	039°	047.7°T	4.5		A3000+	K220-
	060	TF	HK906	-	039°	047.8°T	6.0	L	A3000+	K220-
	070	TF	HK904	-	310°	318.0°T	5.0	L		
	080	TF	BIMVU	-	219°	227.9°T	3.0		A3000+	K210-
LAKUT 3A RNAV 1 or P-RNAV	010	IF	LAKUT	-	-	-	-		F100+	
	020	TF	MAROM	-	075°	083.2°T	5.0		F070+	K250-
	030	TF	HK886	-	071°	079.7°T	15.8			
	040	TF	NODMO	-	070°	078.0°T	14.2		A3000+	K220-
	050	TF	HK907	-	070°	078.4°T	5.5	R	A3000+	K220-
	060	TF	HK904	-	129°	137.7°T	5.4	R		
	070	TF	BIMVU	-	219°	227.9°T	3.0		A3000+	K210-
LUSEP 2A RNAV 1 or P-RNAV	010	IF	LUSEP	-	-	-	-		F100+	
	020	TF	NAPUN	-	170°	178.2°T	7.5		F070+	K250-
	030	TF	HK902	-	170°	178.2°T	8.2		A3000+	K220-
	040	TF	HK907	-	185°	193.3°T	8.1	L	A3000+	K220-
	050	TF	HK904	-	129°	137.7°T	5.4	R		
	060	TF	BIMVU	-	219°	227.9°T	3.0		A3000+	K210-
ROPAM 2A RNAV 1 or P-RNAV	010	IF	ROPAM	-	-	-	-			K250-
	020	TF	HK906	-	338°	346.3°T	18.5	L	A3000+	K220-
	030	TF	HK904	-	310°	318.0°T	5.0	L		
	040	TF	BIMVU	-	219°	227.9°T	3.0		A3000+	K210-
VEPIN 2A RNAV 1 or P-RNAV	010	IF	VEPIN	-	-	-	-		F100+	
	020	TF	MAMOP	-	244°	251.9°T	10.9		F070+	K250-
	030	TF	HK892	-	262°	270.6°T	13.5	L	A3000+	K220-
	040	TF	HK904	-	220°	228.0°T	7.4			
	050	TF	BIMVU	-	219°	227.9°T	3.0		A3000+	K210-

RNAV Holdings							
ID	INBD TR	INBD MAG	Turn Direction	MAX IAS	MNM HLDG LVL	TIME	DIST NM
DIVAM	067.4°T	059°	Right	230 KT	F100	1 MIN	-
INTOR	023.5°T	016°	Right	230 KT	F120	1 MIN	-
LAKUT	077.9°T	070°	Left	230 KT	F100	1 MIN	-
LUSEP	181.3°T	173°	Left	230 KT	F100	1 MIN	-
ROPAM	302.0°T	294°	Right	230 KT	A3000	1 MIN	-
VEPIN	236.1°T	228°	Left	230 KT	F100	1 MIN	-

WPT COORD
SEE PAGE EFHK AD 2.15 - 1

Runway 22R

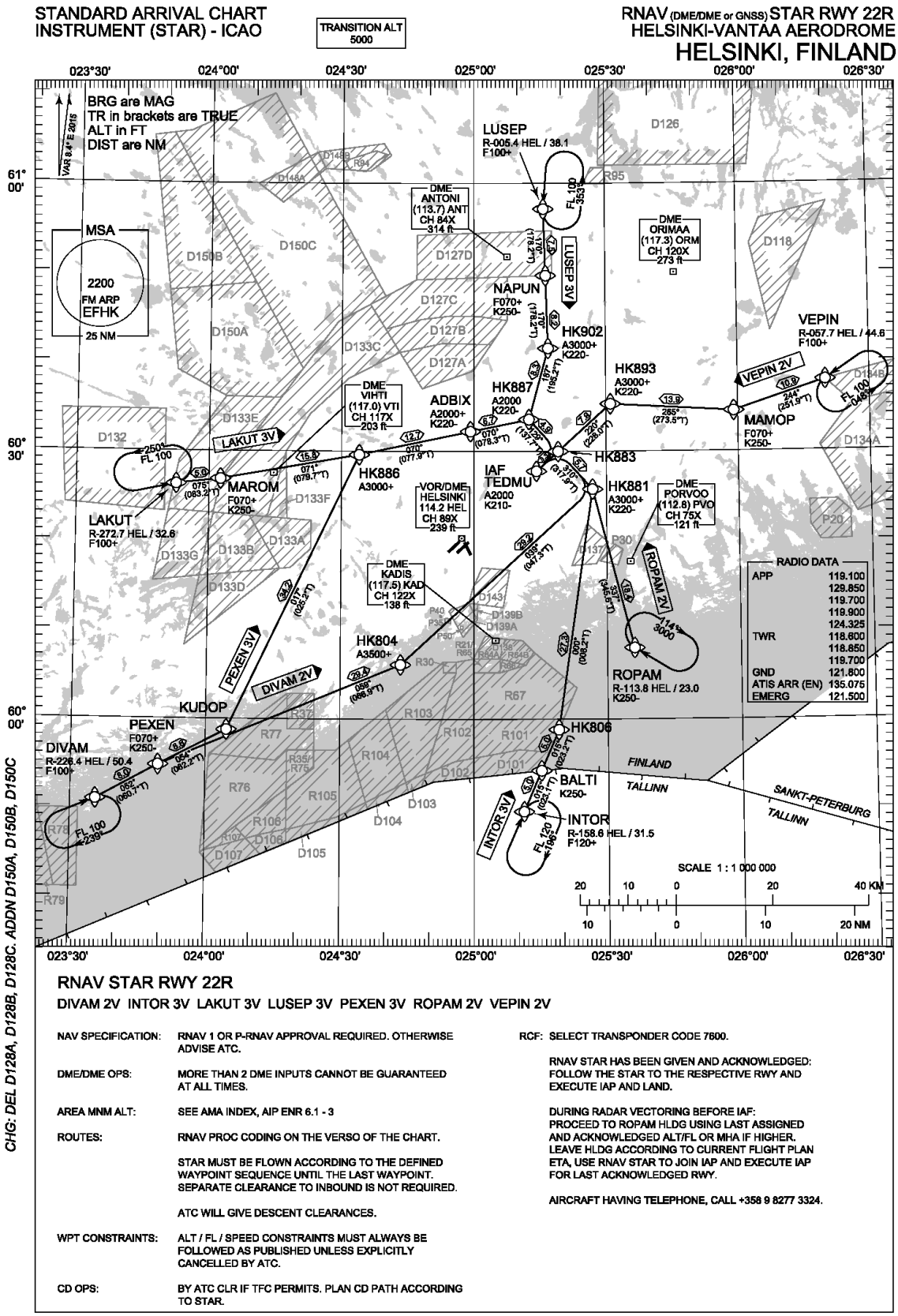

CHG: DEL D128A, D128B, D128C. ADDN D150A, D150B, D150C

RNAV STAR RWY 22R

DIVAM 2V INTOR 3V LAKUT 3V LUSEP 3V PEXEN 3V ROPAM 2V VEPIN 2V

NAV SPECIFICATION:	RNAV 1 OR P-RNAV APPROVAL REQUIRED. OTHERWISE ADVISE ATC.
DME/DME OPS:	MORE THAN 2 DME INPUTS CANNOT BE GUARANTEED AT ALL TIMES.
AREA MNM ALT:	SEE AMA INDEX, AIP ENR 6.1 - 3
ROUTES:	RNAV PROC CODING ON THE VERSO OF THE CHART. STAR MUST BE FLOWN ACCORDING TO THE DEFINED WAYPOINT SEQUENCE UNTIL THE LAST WAYPOINT. SEPARATE CLEARANCE TO INBOUND IS NOT REQUIRED. ATC WILL GIVE DESCENT CLEARANCES.
WPT CONSTRAINTS:	ALT / FL / SPEED CONSTRAINTS MUST ALWAYS BE FOLLOWED AS PUBLISHED UNLESS EXPLICITLY CANCELLED BY ATC.
CD OPS:	BY ATC CLR IF TFC PERMITS. PLAN CD PATH ACCORDING TO STAR.
RCF:	SELECT TRANSPONDER CODE 7600. RNAV STAR HAS BEEN GIVEN AND ACKNOWLEDGED: FOLLOW THE STAR TO THE RESPECTIVE RWY AND EXECUTE IAP AND LAND. DURING RADAR VECTORING BEFORE IAF: PROCEED TO ROPAM HLDG USING LAST ASSIGNED AND ACKNOWLEDGED ALT/FL OR MHA IF HIGHER. LEAVE HLDG ACCORDING TO CURRENT FLIGHT PLAN ETA, USE RNAV STAR TO JOIN IAP AND EXECUTE IAP FOR LAST ACKNOWLEDGED RWY. AIRCRAFT HAVING TELEPHONE, CALL +358 9 8277 3324.

EFHK RNAV STAR RWY 22R										
RTE NAV SPEC	SEQ NR	P/T	WPT ID	WPT Flyover	MAG	GEO TR	DIST NM	Turn Direction	Constraints LVL	Constraints Speed
DIVAM 2V RNAV 1 or P-RNAV	010	IF	DIVAM	-	-	-	-		F100+	
	020	TF	PEXEN	-	052°	060.7°T	8.0		F070+	K250-
	030	TF	HK804	-	059°	066.9°T	29.4		A3500+	
	040	TF	HK881	-	039°	047.3°T	29.2	L	A3000+	K220-
	050	TF	HK883	-	310°	317.9°T	5.7	L		
	060	TF	TEDMU	-	219°	227.8°T	3.3		A2000	K210-
INTOR 3V RNAV 1 or P-RNAV	010	IF	INTOR	-	-	-	-		F120+	
	020	TF	BALTI	-	015°	023.1°T	5.0			K250-
	030	TF	HK806	-	015°	023.2°T	5.0			
	040	TF	HK881	-	000°	008.2°T	27.3	L	A3000+	K220-
	050	TF	HK883	-	310°	317.9°T	5.7	L		
	060	TF	TEDMU	-	219°	227.8°T	3.3		A2000	K210-
LAKUT 3V RNAV 1 or P-RNAV	010	IF	LAKUT	-	-	-	-		F100+	
	020	TF	MAROM	-	075°	083.2°T	5.0		F070+	K250-
	030	TF	HK886	-	071°	079.7°T	15.8		A3000+	
	040	TF	ADBIX	-	070°	077.9°T	12.7		A2000+	K220-
	050	TF	HK887	-	070°	078.3°T	6.7	R	A2000	K220-
	060	TF	HK883	-	129°	137.7°T	4.9	R		
	070	TF	TEDMU	-	219°	227.8°T	3.3		A2000	K210-
LUSEP 3V RNAV 1 or P-RNAV	010	IF	LUSEP	-	-	-	-		F100+	
	020	TF	NAPUN	-	170°	178.2°T	7.5		F070+	K250-
	030	TF	HK902	-	170°	178.2°T	8.2		A3000+	K220-
	040	TF	HK887	-	187°	195.2°T	8.3	L	A2000	K220-
	050	TF	HK883	-	129°	137.7°T	4.9	R		
	060	TF	TEDMU	-	219°	227.8°T	3.3		A2000	K210-
PEXEN 3V RNAV 1 or P-RNAV	010	IF	DIVAM	-	-	-	-		F100+	
	020	TF	PEXEN	-	052°	060.7°T	8.0		F070+	K250-
	030	TF	KUDOP	-	054°	062.2°T	8.6	L		
	040	TF	HK886	-	017°	025.2°T	34.2	R	A3000+	
	050	TF	ADBIX	-	070°	077.9°T	12.7		A2000+	K220-
	060	TF	HK887	-	070°	078.3°T	6.7	R	A2000	K220-
	070	TF	HK883	-	129°	137.7°T	4.9	R		
	080	TF	TEDMU	-	219°	227.8°T	3.3		A2000	K210-
ROPAM 2V RNAV 1 or P-RNAV	010	IF	ROPAM	-	-	-	-			K250-
	020	TF	HK881	-	337°	345.6°T	18.4		A3000+	K220-
	030	TF	HK883	-	310°	317.9°T	5.7	L		
	040	TF	TEDMU	-	219°	227.8°T	3.3		A2000	K210-
VEPIN 2V RNAV 1 or P-RNAV	010	IF	VEPIN	-	-	-	-		F100+	
	020	TF	MAMOP	-	244°	251.9°T	10.9		F070+	K250-
	030	TF	HK893	-	265°	273.5°T	13.9	L	A3000+	K220-
	040	TF	HK883	-	220°	228.0°T	7.9			
	050	TF	TEDMU	-	219°	227.8°T	3.3		A2000	K210-

RNAV Holdings							
ID	INBD TR	INBD MAG	Turn Direction	MAX IAS	MNM HLDG LVL	TIME	DIST NM
DIVAM	067.4°T	059°	Right	230 KT	F100	1 MIN	-
INTOR	023.5°T	016°	Right	230 KT	F120	1 MIN	-
LAKUT	077.9°T	070°	Left	230 KT	F100	1 MIN	-
LUSEP	181.3°T	173°	Left	230 KT	F100	1 MIN	-
ROPAM	302.0°T	294°	Right	230 KT	A3000	1 MIN	-
VEPIN	236.1°T	228°	Left	230 KT	F100	1 MIN	-

WPT COORD
SEE PAGE EFHK AD 2.15 - 1

Runway 33

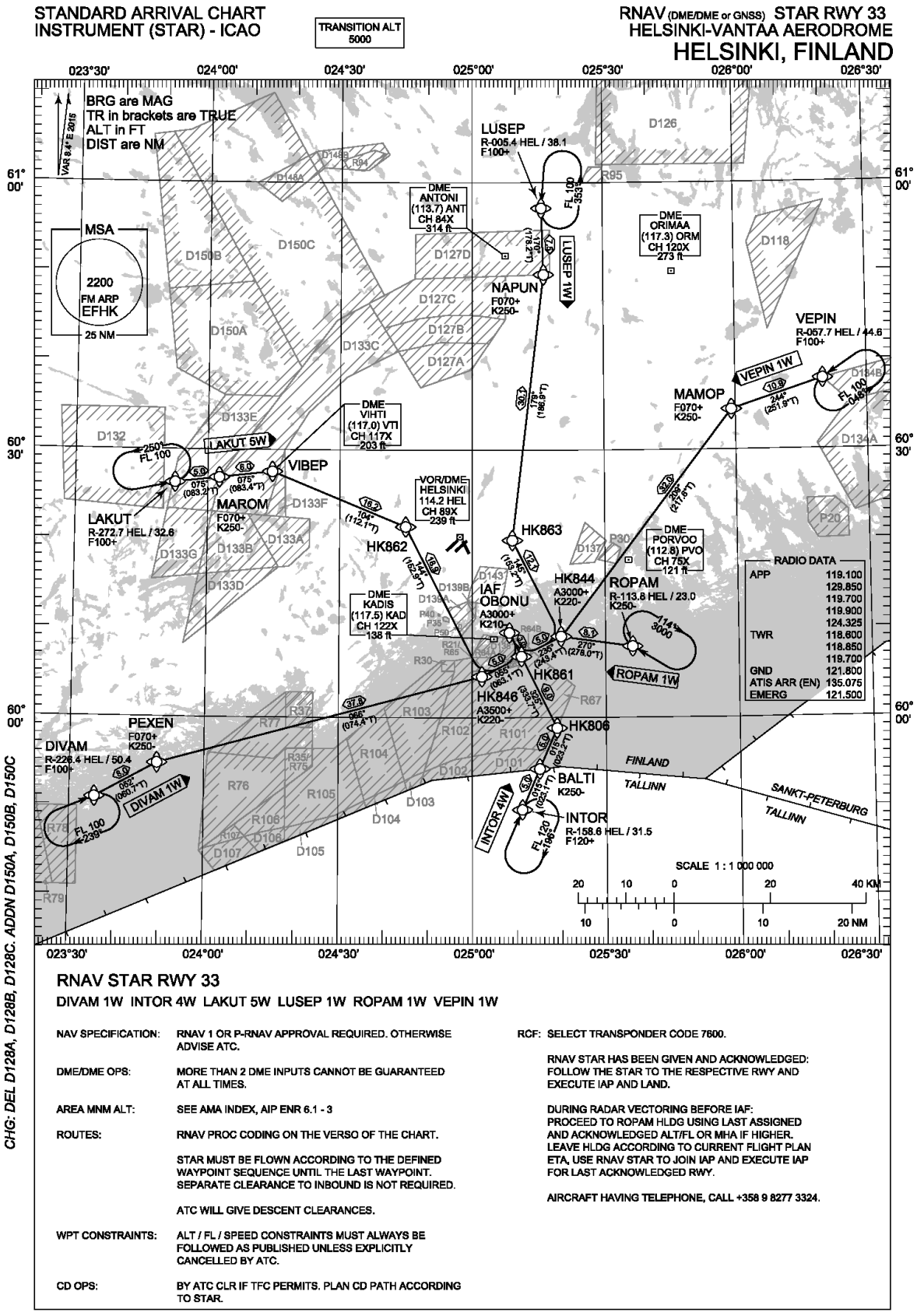

RNAV STAR RWY 33

DIVAM 1W INTOR 4W LAKUT 5W LUSEP 1W ROPAM 1W VEPIN 1W

NAV SPECIFICATION:	RNAV 1 OR P-RNAV APPROVAL REQUIRED. OTHERWISE ADVISE ATC.
DME/DME OPS:	MORE THAN 2 DME INPUTS CANNOT BE GUARANTEED AT ALL TIMES.
AREA MNM ALT:	SEE AMA INDEX, AIP ENR 6.1 - 3
ROUTES:	RNAV PROC CODING ON THE VERSO OF THE CHART. STAR MUST BE FLOWN ACCORDING TO THE DEFINED WAYPOINT SEQUENCE UNTIL THE LAST WAYPOINT. SEPARATE CLEARANCE TO INBOUND IS NOT REQUIRED. ATC WILL GIVE DESCENT CLEARANCES.
WPT CONSTRAINTS:	ALT / FL / SPEED CONSTRAINTS MUST ALWAYS BE FOLLOWED AS PUBLISHED UNLESS EXPLICITLY CANCELLED BY ATC.
CD OPS:	BY ATC CLR IF TFC PERMITS. PLAN CD PATH ACCORDING TO STAR.
RCF:	SELECT TRANSPONDER CODE 7600. RNAV STAR HAS BEEN GIVEN AND ACKNOWLEDGED: FOLLOW THE STAR TO THE RESPECTIVE RWY AND EXECUTE IAP AND LAND. DURING RADAR VECTORING BEFORE IAF: PROCEED TO ROPAM HLDG USING LAST ASSIGNED AND ACKNOWLEDGED ALT/FL OR MHA IF HIGHER. LEAVE HLDG ACCORDING TO CURRENT FLIGHT PLAN ETA, USE RNAV STAR TO JOIN IAP AND EXECUTE IAP FOR LAST ACKNOWLEDGED RWY. AIRCRAFT HAVING TELEPHONE, CALL +358 9 8277 3324.

CHG: DEL D128A, D128B, D128C. ADDN D150A, D150B, D150C

EFHK RNAV STAR RWY 33										
RTE NAV SPEC	SEQ NR	P/T	WPT ID	WPT Flyover	MAG	GEO TR	DIST NM	Turn Direction	Constraints LVL	Constraints Speed
DIVAM 1W RNAV 1 or P-RNAV	010	IF	DIVAM	-	-	-	-		F100+	
	020	TF	PEXEN	-	052°	060.7°T	8.0		F070+	K250-
	030	TF	HK846	-	066°	074.4°T	37.8		A3500+	K220-
	040	TF	HK861	-	055°	063.1°T	5.0	L		
	050	TF	OBONU	-	325°	333.2°T	3.0		A3000+	K210-
INTOR 4W RNAV 1 or P-RNAV	010	IF	INTOR	-	-	-	-		F120+	
	020	TF	BALTI	-	015°	023.1°T	5.0			K250-
	030	TF	HK806	-	015°	023.2°T	5.0	L		
	040	TF	HK861	-	325°	333.7°T	9.0			
	050	TF	OBONU	-	325°	333.2°T	3.0		A3000+	K210-
LAKUT 5W RNAV 1 or P-RNAV	010	IF	LAKUT	-	-	-	-		F100+	
	020	TF	MAROM	-	075°	083.2°T	5.0		F070+	K250-
	030	TF	VIBEP	-	075°	083.4°T	6.0	R		
	040	TF	HK862	-	104°	112.1°T	16.2	R		
	050	TF	HK846	-	144°	152.9°T	18.9	L	A3500+	K220-
	060	TF	HK861	-	055°	063.1°T	5.0	L		
	070	TF	OBONU	-	325°	333.2°T	3.0		A3000+	K210-
LUSEP 1W RNAV 1 or P-RNAV	010	IF	LUSEP	-	-	-	-		F100+	
	020	TF	NAPUN	-	170°	178.2°T	7.5		F070+	K250-
	030	TF	HK863	-	179°	186.9°T	30.1	L		
	040	TF	HK844	-	145°	153.2°T	12.1	R	A3000+	K220-
	050	TF	HK861	-	235°	243.4°T	5.0	R		
	060	TF	OBONU	-	325°	333.2°T	3.0		A3000+	K210-
ROPAM 1W RNAV 1 or P-RNAV	010	IF	ROPAM	-	-	-	-			K250-
	020	TF	HK844	-	270°	278.0°T	8.1	L	A3000+	K220-
	030	TF	HK861	-	235°	243.4°T	5.0	R		
	040	TF	OBONU	-	325°	333.2°T	3.0		A3000+	K210-
VEPIN 1W RNAV 1 or P-RNAV	010	IF	VEPIN	-	-	-	-		F100+	
	020	TF	MAMOP	-	244°	251.9°T	10.9	L	F070+	K250-
	030	TF	HK844	-	209°	217.6°T	32.0		A3000+	K220-
	040	TF	HK861	-	235°	243.4°T	5.0	R		
	050	TF	OBONU	-	325°	333.2°T	3.0		A3000+	K210-

RNAV Holdings							
ID	INBD TR	INBD MAG	Turn Direction	MAX IAS	MNM HLDG LVL	TIME	DIST NM
DIVAM	067.4°T	059°	Right	230 KT	F100	1 MIN	-
INTOR	023.5°T	016°	Right	230 KT	F120	1 MIN	-
LAKUT	077.9°T	070°	Left	230 KT	F100	1 MIN	-
LUSEP	181.3°T	173°	Left	230 KT	F100	1 MIN	-
ROPAM	302.0°T	294°	Right	230 KT	A3000	1 MIN	-
VEPIN	236.1°T	228°	Left	230 KT	F100	1 MIN	-

WPT COORD
SEE PAGE EFHK AD 2.15 - 1

Appendix 2. EFHK Waypoints and Fixes

AERONAUTICAL DATA
SIGNIFICANT POINTS FOR AERODROME

WAYPOINTS AND FIXES
HELSINKI-VANTAA AERODROME
HELSINKI, FINLAND

WAYPOINT		RNAV USAGE						
ID	COORD	ENTRY	EXIT	SID	STAR	APCH	HLDG	RMK
ABSUT	601308.61N 0244403.74E					X		
ADBIX	603213.67N 0245912.90E				X			
ADIVO	601751.00N 0235853.00E		X					
ARVEP	601458.00N 0262357.00E		X					
ASTIV	601405.00N 0242526.00E			X				
BALTI	595415.00N 0251506.00E				X			
BIMVU	602736.54N 0251558.56E				X	X		
DEVKA	600901.00N 0244601.00E			X				
DIVAM	595054.00N 0233537.00E	X			X		X	
DOBAN	594758.00N 0242709.00E		X					
ELKUN	602723.11N 0245004.30E				X	X		
ELPEN	601850.00N 0252945.00E			X				
ENUTO	602853.00N 0244632.00E			X				
ERSAV	601830.00N 0243442.00E			X				
EXEVO	601510.22N 0244829.31E					X		
GEDLO	601015.28N 0243746.68E				X	X		
GESVO	600731.08N 0244638.69E					X		
GIRLA	601127.00N 0243343.00E			X				
GOVMI	600847.00N 0252058.00E			X				
GUMVO	602338.10N 0250708.03E					X		
HK416	602352.55N 0250740.07E			X				
HK418	601154.92N 0245957.32E			X				
HK419	601947.43N 0251055.00E			X				
HK427	602144.76N 0243649.48E			X				
HK428	601605.52N 0244621.17E			X				
HK451	601816.80N 0244654.99E			X				
HK461	601905.74N 0244625.05E			X				
HK711	601619.79N 0250553.91E				X			
HK766	601553.05N 0250454.92E				X			
HK801	601019.01N 0243545.88E				X			
HK802	601359.34N 0242859.21E				X			
HK803	600514.38N 0242448.13E				X			
HK804	600606.13N 0244329.98E				X			
HK806	595849.93N 0251900.76E				X			
HK807	602504.20N 0252513.30E				X			
HK811	600813.32N 0243322.43E				X			
HK813	600508.86N 0242644.41E				X			
HK814	600432.54N 0244006.94E				X			
HK817	602118.87N 0250737.09E				X			
HK821	603002.93N 0244718.66E				X			
HK822	603218.26N 0245619.98E				X			
HK823	602900.05N 0243321.53E				X			
HK844	600905.85N 0251959.81E				X			
HK846	600436.34N 0250209.32E				X			
HK849	601822.65N 0243533.61E				X			
HK851	601240.65N 0242312.59E				X			
HK852	600817.70N 0243123.33E				X			
HK856	601455.80N 0244548.21E					X		
HK859	601708.95N 0250036.11E					X		
HK860	601439.61N 0244722.35E					X		
HK861	600651.40N 0251103.96E				X			
HK862	602123.87N 0244456.59E				X			
HK863	601952.61N 0250905.02E				X			
HK864	601749.22N 0245417.87E					X		
HK866	602114.14N 0250149.34E					X		
HK871	602602.64N 0243013.81E				X			
HK873	601504.40N 0241842.97E				X			
HK874	601228.95N 0241009.16E				X			
HK881	602544.97N 0252651.58E				X			
HK883	602959.29N 0251906.04E				X			
HK886	602936.92N 0243400.61E				X			
HK887	603334.24N 0251230.34E				X			
HK888	603518.64N 0250827.32E				X			

CONTINUES ON NEXT PAGE

WAYPOINTS AND FIXES
HELSINKI-VANTAA AERODROME
HELSINKI, FINLAND

AERONAUTICAL DATA
SIGNIFICANT POINTS FOR AERODROME

WAYPOINT		RNAV USAGE						
ID	COORD	ENTRY	EXIT	SID	STAR	APCH	HLDG	RMK
HK889	604246.80N 0251648.67E				X			
HK890	603553.50N 0251715.10E				X			
HK891	601853.92N 0251134.98E				X			
HK892	603435.11N 0253138.51E				X			
HK893	603517.34N 0253101.19E				X			
HK894	600835.87N 0244855.85E				X			
HK896	602532.74N 0245115.25E				X			
HK897	602448.12N 0245235.91E				X			
HK899	601224.52N 0242534.18E				X			
HK900	601352.08N 0250357.07E					X		
HK901	600416.70N 0250218.99E				X			
HK902	604131.66N 0251653.49E				X			
HK903	602422.06N 0245647.14E			X				
HK904	602937.07N 0252028.09E				X			
HK906	602555.07N 0252714.27E				X			
HK907	603337.33N 0251306.06E				X			
IDEPI	604239.00N 0254739.00E		X					
IDMOP	602403.00N 0250309.00E			X				
INTOR	594940.00N 0251112.00E	X			X		X	
KUDOP	595846.00N 0240436.00E				X			
KUVEM	601126.00N 0235614.00E		X					
LAKUT	602617.00N 0235235.00E	X			X		X	
LAVTU	601219.00N 0251354.00E			X				
LULAB	603021.00N 0250754.00E			X				
LUSEP	605708.00N 0251553.00E	X			X		X	
LUVEX	602154.76N 0251817.01E				X			
MAMOP	603430.00N 0255904.00E				X			
MAROM	602652.00N 0240237.00E				X			
NAPUN	604941.00N 0251622.00E				X			
NEMVI	601601.45N 0243323.97E				X			
NEPEK	604433.00N 0242908.00E		X					
NIDAG	601151.00N 0245050.00E			X				
NODMO	603231.00N 0250206.64E				X			
NUNTO	600501.00N 0235337.00E		X					
NUTRU	601724.00N 0252717.00E			X				
OBONU	600931.66N 0250821.74E				X	X		
OBUPU	602447.89N 0245244.68E					X		
PENAD	601642.00N 0252936.00E			X				
PEXEN	595447.00N 0234928.00E				X			
PODOM	601220.89N 0244010.57E				X	X		
REDBO	602538.00N 0245152.00E			X				
RENKU	595309.00N 0245348.10E		X					DEST EETN only
RILBO	601137.00N 0241643.00E			X				
RIPVI	601624.00N 0243507.00E			X				
ROLAT	601757.00N 0253120.00E			X				
ROPAM	600759.00N 0253606.00E	X*			X		X	* FM LEDUN only
RW04L	601846.61N 0245413.93E					X		
RW04R	601840.65N 0245610.94E					X		
RW15	601948.99N 0245752.19E					X		
RW22L	601950.49N 0245844.73E					X		
RW22R	601952.11N 0245638.01E					X		
RW33	601825.44N 0245917.83E					X		
SUTAX	602938.26N 0245905.08E				X			
TEDMU	602746.64N 0251409.63E				X	X		
TEVRU	604916.00N 0244929.00E		X					
UNURU	602753.00N 0244556.00E			X				
UREDA	601420.00N 0243723.00E			X				
VAGIP	601835.00N 0242520.00E			X				
VAMRA	601333.00N 0243327.00E			X				
VAVIS	601406.00N 0245039.00E			X				
VEGIK	601603.75N 0244244.46E					X		
VEPIN	603753.00N 0261959.00E	X			X		X	
VETUD	603030.00N 0244841.00E			X				

CONTINUES ON NEXT PAGE

WAYPOINT		RNAV USAGE						
ID	COORD	ENTRY	EXIT	SID	STAR	APCH	HLDG	RMK
VIBEP	602733.00N 0241439.00E				X			
XAXOL	601215.02N 0244948.05E					X		
XELBU	602336.37N 0250453.30E					X		
XOMRI	602634.00N 0251338.00E			X				
SUMMARY	**130**	**6**	**9**	**32**	**69**	**26**	**6**	

NON-RNAV FIXES		RDL AND DIST
ID	COORD	
BAMEB	600941.94N 0250831.04E	R-143.5 HEL / 12.0
DIPMO	601206.79N 0244148.99E	R-214.9 HEL / 11.2
EMPEV	601417.68N 0244425.00E	R-218.5 HEL / 8.7
LAVDI	601414.15N 0244626.73E	R-213.2 HEL / 8.1
TIXED	602544.59N 0251149.01E	R-044.3 HEL / 9.1

VFR REPORTING POINTS		COMPULSORY	RDL AND DIST
ID	COORD		
DEGER	601559N 0251233E		R-111 HEL / 8.8
HAGIS	601231N 0245400E	X	R-183 HEL / 7.9
KOLIS	602704N 0250107E	X	R-007 HEL / 7.1
LILJA	601926N 0251231E	X	R-088 HEL / 7.6
LINTU	602247N 0244104E	X	R-279 HEL / 8.4
NOKKA	601100N 0250121E		R-159 HEL / 9.5
OGELI	601351N 0245916E	X	R-163 HEL / 6.5
RASTI	601156N 0250526E		R-145 HEL / 9.3

Appendix 3. Risk Period Results

Still Air

Table A3.1. Total time in approach phase in still air.

		Total time in approach phase (still air) [min:s]					
Runway	**STAR**	**3 degree profile**		**4 degree profile**		**5 degree profile**	
		Speed profile A	**Speed profile B**	**Speed profile A**	**Speed profile B**	**Speed profile A**	**Speed profile B**
04L	DIVAM 1B	13:27	12:45	13:10	12:34	13:01	12:29
	INTOR 4B	13:10	12:29	12:53	12:18	12:44	12:12
	LAKUT 5B	12:22	11:43	12:06	11:31	11:56	11:25
	LUSEP 1B	18:14	17:31	18:02	17:27	17:56	17:25
	ROPAM 1B	13:51	13:09	13:34	12:58	13:25	12:53
	VEPIN 1B	19:20	18:37	19:09	18:34	19:04	18:32
	MAROM 4B	16:00	15:11	15:45	14:59	15:35	14:53
	NAPUN 1B	20:35	19:42	20:22	19:35	20:16	19:34
	PEXEN 4B	16:53	16:02	16:37	15:50	16:28	15:45
04R	DIVAM 1R	13:46	13:03	13:31	12:54	13:24	12:50
	INTOR 4R	14:54	14:11	14:40	14:03	14:34	14:00
	LAKUT 5R	13:35	12:52	13:20	12:42	13:12	12:38
	LUSEP 1R	19:44	19:01	19:36	18:59	19:32	18:58
	ROPAM 1R	15:04	14:20	14:50	14:12	14:43	14:09
	VEPIN 1R	20:34	19:51	20:27	19:49	20:22	19:48
15	DIVAM 1M	21:24	20:42	21:14	20:39	21:08	20:37
	INTOR 5M	16:12	15:30	15:57	15:22	15:50	15:19
	LAKUT 5M	11:14	10:38	11:01	10:26	10:49	10:19
	LUSEP 1M	12:47	12:08	12:30	11:55	12:20	11:49
	ROPAM 1M	13:17	12:36	12:59	12:25	12:50	12:19
	VEPIN 1M	15:30	14:49	15:14	14:40	15:08	14:37
22L	DIVAM 2A	21:41	20:58	21:33	20:56	21:28	20:55
	INTOR 3A	16:07	15:24	15:54	15:17	15:48	15:15
	LAKUT 3A	16:07	15:23	15:53	15:16	15:48	15:15
	LUSEP 2A	12:36	11:56	12:22	11:45	12:13	11:39
	ROPAM 2A	11:14	10:38	11:04	10:28	10:55	10:22
	VEPIN 2A	13:08	12:26	12:52	12:15	12:44	12:10
22R	DIVAM 2V	22:03	21:16	21:53	21:13	21:47	21:11
	INTOR 3V	15:48	15:02	15:31	14:51	15:22	14:46
	LAKUT 3V	16:42	15:52	16:25	15:39	16:15	15:34
	LUSEP 3V	13:03	12:22	12:57	12:16	12:50	12:09
	PEXEN 3V	23:05	22:13	22:54	22:09	22:49	22:07
	ROPAM 2V	11:39	11:01	11:30	10:53	11:21	10:45
	VEPIN 2V	13:37	12:54	13:22	12:42	13:11	12:35
33	DIVAM 1W	16:31	15:49	16:16	15:42	16:10	15:40
	INTOR 4W	09:43	09:11	09:34	09:02	09:26	08:55
	LAKUT 5W	16:35	15:54	16:21	15:47	16:15	15:45
	LUSEP 1W	17:21	16:40	17:08	16:34	17:02	16:32
	ROPAM 1W	08:15	07:47	08:09	07:41	08:04	07:36
	VEPIN 1W	15:54	15:13	15:39	15:04	15:32	15:02
Min.		08:15	07:47	08:09	07:41	08:04	07:36
Max.		23:05	22:13	22:54	22:09	22:49	22:07
Average		**15:35**	**14:52**	**15:21**	**14:44**	**15:14**	**14:40**

Table A3.2. Approach risk period in still air.

		Risk period (still air) [min:s]					
Runway	**STAR**	**3 degree profile**		**4 degree profile**		**5 degree profile**	
		Speed profile A	**Speed profile B**	**Speed profile A**	**Speed profile B**	**Speed profile A**	**Speed profile B**
04L	DIVAM 1B	13:27	12:45	13:10	12:34	05:01	04:37
	INTOR 4B	06:51	06:23	05:38	05:15	05:02	04:40
	LAKUT 5B	06:48	06:20	05:37	05:13	05:02	04:40
	LUSEP 1B	06:32	06:07	05:37	05:13	05:02	04:40
	ROPAM 1B	06:42	06:17	05:38	05:15	05:02	04:40
	VEPIN 1B	06:42	06:17	05:38	05:15	05:02	04:40
	MAROM 4B	10:42	09:57	09:20	08:47	09:06	08:34
	NAPUN 1B	09:38	09:04	09:20	08:47	09:06	08:34
	PEXEN 4B	16:53	16:02	16:37	15:50	12:32	11:50
04R	DIVAM 1R	13:46	13:03	13:31	12:54	06:45	06:15
	INTOR 4R	07:34	07:06	06:50	06:23	06:12	05:47
	LAKUT 5R	07:54	07:24	06:49	06:22	06:11	05:47
	LUSEP 1R	07:42	07:14	06:49	06:22	06:11	05:47
	ROPAM 1R	07:34	07:06	06:50	06:23	06:12	05:47
	VEPIN 1R	07:34	07:06	06:50	06:23	06:12	05:47
15	DIVAM 1M	06:12	05:48	05:13	04:51	04:37	04:17
	INTOR 5M	06:12	05:48	05:13	04:51	04:37	04:17
	LAKUT 5M	11:14	10:38	05:34	05:10	04:40	04:18
	LUSEP 1M	11:50	10:51	05:13	04:51	04:37	04:17
	ROPAM 1M	06:12	05:48	05:13	04:51	04:37	04:17
	VEPIN 1M	08:19	07:32	05:13	04:51	04:37	04:17
22L	DIVAM 2A	07:15	06:48	06:27	06:01	05:51	05:27
	INTOR 3A	07:15	06:48	06:27	06:01	05:51	05:27
	LAKUT 3A	07:23	06:55	06:27	06:01	05:51	05:28
	LUSEP 2A	12:36	11:56	06:27	06:01	05:48	05:24
	ROPAM 2A	07:24	06:56	06:27	06:01	05:51	05:27
	VEPIN 2A	13:08	12:26	10:33	09:47	06:14	05:45
22R	DIVAM 2V	08:14	07:45	07:47	07:19	07:26	06:58
	INTOR 3V	08:44	08:12	07:56	07:27	07:27	06:59
	LAKUT 3V	10:24	09:47	09:29	08:55	09:02	08:30
	LUSEP 3V	13:03	12:22	12:57	12:16	12:50	12:09
	PEXEN 3V	10:24	09:47	09:29	08:55	09:02	08:30
	ROPAM 2V	10:28	09:45	08:11	07:41	07:29	07:01
	VEPIN 2V	13:37	12:54	13:22	12:42	10:12	09:35
33	DIVAM 1W	09:07	08:41	05:20	04:59	03:30	03:09
	INTOR 4W	09:43	09:11	07:55	07:23	03:30	03:09
	LAKUT 5W	06:31	06:06	05:20	04:59	03:30	03:09
	LUSEP 1W	06:31	06:06	05:20	04:59	03:30	03:09
	ROPAM 1W	08:15	07:47	05:20	04:59	03:30	03:09
	VEPIN 1W	06:33	06:08	05:20	04:59	03:30	03:09
Min.		06:12	05:48	05:13	04:51	03:30	03:09
Max.		16:53	16:02	16:37	15:50	12:50	12:09
Average		**09:04**	**08:31**	**07:34**	**07:06**	**06:09**	**05:44**

Table A3.3. Risk period change with different profiles compared to 3 degree speed A profile in still air.

		Risk period change (still air) [%]					
Runway	**STAR**	**3 degree profile**		**4 degree profile**		**5 degree profile**	
		Speed profile A	**Speed profile B**	**Speed profile A**	**Speed profile B**	**Speed profile A**	**Speed profile B**
04L	DIVAM 1B	-	−5.2 %	−2.2 %	−6.6 %	−62.7 %	−65.6 %
	INTOR 4B	-	−6.7 %	−17.8 %	−23.4 %	−26.5 %	−31.8 %
	LAKUT 5B	-	−6.9 %	−17.4 %	−23.1 %	−25.9 %	−31.2 %
	LUSEP 1B	-	−6.3 %	−14.1 %	−20.1 %	−23.0 %	−28.5 %
	ROPAM 1B	-	−6.3 %	−15.9 %	−21.7 %	−24.8 %	−30.2 %
	VEPIN 1B	-	−6.3 %	−15.9 %	−21.7 %	−24.8 %	−30.2 %
	MAROM 4B	-	−7.0 %	−12.8 %	−17.9 %	−14.9 %	−19.9 %
	NAPUN 1B	-	−5.8 %	−3.1 %	−8.7 %	−5.4 %	−11.0 %
	PEXEN 4B	-	−5.1 %	−1.6 %	−6.3 %	−25.7 %	−30.0 %
04R	DIVAM 1R	-	−5.2 %	−1.8 %	−6.3 %	−50.9 %	−54.6 %
	INTOR 4R	-	−6.2 %	−9.8 %	−15.8 %	−18.0 %	−23.6 %
	LAKUT 5R	-	−6.3 %	−13.7 %	−19.4 %	−21.6 %	−26.7 %
	LUSEP 1R	-	−6.2 %	−11.5 %	−17.4 %	−19.6 %	−24.9 %
	ROPAM 1R	-	−6.2 %	−9.8 %	−15.8 %	−18.0 %	−23.6 %
	VEPIN 1R	-	−6.2 %	−9.8 %	−15.8 %	−18.0 %	−23.6 %
15	DIVAM 1M	-	−6.4 %	−15.8 %	−21.8 %	−25.5 %	−30.7 %
	INTOR 5M	-	−6.4 %	−15.8 %	−21.8 %	−25.5 %	−30.7 %
	LAKUT 5M	-	−5.3 %	−50.4 %	−53.9 %	−58.4 %	−61.6 %
	LUSEP 1M	-	−8.3 %	−56.0 %	−59.1 %	−61.0 %	−63.8 %
	ROPAM 1M	-	−6.4 %	−15.8 %	−21.8 %	−25.5 %	−30.7 %
	VEPIN 1M	-	−9.6 %	−37.4 %	−41.8 %	−44.6 %	−48.5 %
22L	DIVAM 2A	-	−6.3 %	−11.0 %	−17.0 %	−19.2 %	−24.8 %
	INTOR 3A	-	−6.3 %	−11.0 %	−17.0 %	−19.2 %	−24.8 %
	LAKUT 3A	-	−6.2 %	−12.5 %	−18.4 %	−20.7 %	−25.9 %
	LUSEP 2A	-	−5.3 %	−48.8 %	−52.2 %	−54.0 %	−57.2 %
	ROPAM 2A	-	−6.4 %	−12.8 %	−18.8 %	−20.9 %	−26.4 %
	VEPIN 2A	-	−5.3 %	−19.7 %	−25.5 %	−52.5 %	−56.2 %
22R	DIVAM 2V	-	−6.0 %	−5.6 %	−11.3 %	−9.9 %	−15.4 %
	INTOR 3V	-	−6.0 %	−9.2 %	−14.7 %	−14.8 %	−20.0 %
	LAKUT 3V	-	−5.9 %	−8.8 %	−14.2 %	−13.1 %	−18.2 %
	LUSEP 3V	-	−5.3 %	−0.9 %	−6.1 %	−1.7 %	−6.9 %
	PEXEN 3V	-	−5.9 %	−8.8 %	−14.2 %	−13.1 %	−18.2 %
	ROPAM 2V	-	−6.9 %	−21.8 %	−26.6 %	−28.6 %	−33.0 %
	VEPIN 2V	-	−5.2 %	−1.8 %	−6.8 %	−25.1 %	−29.6 %
33	DIVAM 1W	-	−4.7 %	−41.5 %	−45.4 %	−61.7 %	−65.4 %
	INTOR 4W	-	−5.5 %	−18.5 %	−24.1 %	−64.1 %	−67.6 %
	LAKUT 5W	-	−6.5 %	−18.1 %	−23.6 %	−46.4 %	−51.7 %
	LUSEP 1W	-	−6.5 %	−18.1 %	−23.6 %	−46.4 %	−51.7 %
	ROPAM 1W	-	−5.7 %	−35.3 %	−39.6 %	−57.6 %	−61.8 %
	VEPIN 1W	-	−6.5 %	−18.6 %	−24.0 %	−46.7 %	−51.9 %
Min.		-	−9.6 %	−56.0 %	−59.1 %	−64.1 %	−67.6 %
Max.		-	−4.7 %	−0.9 %	−6.1 %	−1.7 %	−6.9 %
Average		-	**−6.2 %**	**−16.8 %**	**−22.1 %**	**−30.9 %**	**−35.7 %**

Table A3.4. Risk period in percentage of the total time in approach in still air.

		Risk period [%] of total time in approach (still air)					
Runway	**STAR**	**3 degree profile**		**4 degree profile**		**5 degree profile**	
		Speed profile A	**Speed profile B**	**Speed profile A**	**Speed profile B**	**Speed profile A**	**Speed profile B**
04L	DIVAM 1B	100.0 %	100.0 %	100.0 %	100.0 %	38.6 %	37.0 %
	INTOR 4B	52.0 %	51.2 %	43.7 %	42.6 %	39.5 %	38.3 %
	LAKUT 5B	54.9 %	54.0 %	46.4 %	45.4 %	42.2 %	40.9 %
	LUSEP 1B	35.9 %	34.9 %	31.1 %	30.0 %	28.1 %	26.8 %
	ROPAM 1B	48.4 %	47.7 %	41.5 %	40.4 %	37.5 %	36.2 %
	VEPIN 1B	34.7 %	33.7 %	29.4 %	28.2 %	26.4 %	25.2 %
	MAROM 4B	66.9 %	65.6 %	59.2 %	58.7 %	58.4 %	57.6 %
	NAPUN 1B	46.7 %	46.0 %	45.8 %	44.9 %	44.9 %	43.8 %
	PEXEN 4B	100.0 %	100.0 %	100.0 %	100.0 %	76.2 %	75.1 %
04R	DIVAM 1R	100.0 %	100.0 %	100.0 %	100.0 %	50.4 %	48.7 %
	INTOR 4R	50.8 %	50.1 %	46.6 %	45.4 %	42.6 %	41.3 %
	LAKUT 5R	58.1 %	57.5 %	51.1 %	50.1 %	46.9 %	45.8 %
	LUSEP 1R	39.0 %	38.0 %	34.8 %	33.5 %	31.7 %	30.5 %
	ROPAM 1R	50.3 %	49.5 %	46.1 %	44.9 %	42.2 %	40.9 %
	VEPIN 1R	36.8 %	35.8 %	33.4 %	32.2 %	30.5 %	29.2 %
15	DIVAM 1M	28.9 %	28.0 %	24.5 %	23.5 %	21.8 %	20.8 %
	INTOR 5M	38.2 %	37.4 %	32.7 %	31.5 %	29.1 %	28.0 %
	LAKUT 5M	100.0 %	100.0 %	50.6 %	49.6 %	43.1 %	41.8 %
	LUSEP 1M	92.6 %	89.5 %	41.7 %	40.6 %	37.4 %	36.3 %
	ROPAM 1M	46.6 %	46.0 %	40.1 %	39.0 %	35.9 %	34.8 %
	VEPIN 1M	53.7 %	50.8 %	34.2 %	33.0 %	30.5 %	29.4 %
22L	DIVAM 2A	33.4 %	32.4 %	29.9 %	28.7 %	27.3 %	26.1 %
	INTOR 3A	45.0 %	44.1 %	40.6 %	39.4 %	37.1 %	35.7 %
	LAKUT 3A	45.8 %	45.0 %	40.6 %	39.4 %	37.0 %	35.9 %
	LUSEP 2A	100.0 %	100.0 %	52.2 %	51.3 %	47.5 %	46.3 %
	ROPAM 2A	65.9 %	65.2 %	58.3 %	57.4 %	53.7 %	52.6 %
	VEPIN 2A	100.0 %	100.0 %	81.9 %	79.8 %	48.9 %	47.3 %
22R	DIVAM 2V	37.4 %	36.4 %	35.6 %	34.5 %	34.1 %	32.9 %
	INTOR 3V	55.3 %	54.6 %	51.1 %	50.2 %	48.4 %	47.3 %
	LAKUT 3V	62.2 %	61.6 %	57.7 %	56.9 %	55.6 %	54.7 %
	LUSEP 3V	100.0 %	100.0 %	100.0 %	100.0 %	100.0 %	100.0 %
	PEXEN 3V	45.0 %	44.0 %	41.4 %	40.3 %	39.6 %	38.5 %
	ROPAM 2V	89.9 %	88.5 %	71.2 %	70.6 %	65.9 %	65.3 %
	VEPIN 2V	100.0 %	100.0 %	100.0 %	100.0 %	77.4 %	76.1 %
33	DIVAM 1W	55.2 %	54.9 %	32.8 %	31.7 %	21.6 %	20.1 %
	INTOR 4W	100.0 %	100.0 %	82.8 %	81.6 %	37.1 %	35.4 %
	LAKUT 5W	39.3 %	38.3 %	32.6 %	31.6 %	21.5 %	20.0 %
	LUSEP 1W	37.6 %	36.6 %	31.1 %	30.1 %	20.5 %	19.1 %
	ROPAM 1W	100.0 %	100.0 %	65.4 %	64.8 %	43.3 %	41.4 %
	VEPIN 1W	41.2 %	40.3 %	34.1 %	33.1 %	22.5 %	21.0 %
Min.		28.9 %	28.0 %	24.5 %	23.5 %	20.5 %	19.1 %
Max.		100.0 %	100.0 %	100.0 %	100.0 %	100.0 %	100.0 %
Average		**62.2 %**	**61.4 %**	**51.8 %**	**50.9 %**	**41.8 %**	**40.6 %**

Table A3.5. Total time in approach phase in 20 knot headwind.

		Total time in approach phase (20 kt headwind) [min:s]					
Runway	**STAR**	**3 degree profile**		**4 degree profile**		**5 degree profile**	
		Speed profile A	**Speed profile B**	**Speed profile A**	**Speed profile B**	**Speed profile A**	**Speed profile B**
04L	DIVAM 1B	15:00	14:07	14:39	13:53	14:29	13:47
	INTOR 4B	14:41	13:49	14:21	13:36	14:10	13:29
	LAKUT 5B	13:49	13:00	13:31	12:45	13:19	12:38
	LUSEP 1B	20:08	19:14	19:54	19:09	19:47	19:07
	ROPAM 1B	15:25	14:32	15:05	14:19	14:55	14:14
	VEPIN 1B	21:19	20:25	21:07	20:21	21:00	20:19
	MAROM 4B	17:49	16:48	17:33	16:34	17:21	16:27
	NAPUN 1B	22:46	21:40	22:30	21:31	22:24	21:29
	PEXEN 4B	18:48	17:43	18:29	17:29	18:18	17:23
04R	DIVAM 1R	15:22	14:28	15:04	14:17	14:55	14:12
	INTOR 4R	16:36	15:40	16:19	15:31	16:11	15:27
	LAKUT 5R	15:09	14:15	14:52	14:04	14:43	13:59
	LUSEP 1R	21:47	20:52	21:38	20:50	21:32	20:49
	ROPAM 1R	16:46	15:50	16:29	15:41	16:21	15:38
	VEPIN 1R	22:42	21:46	22:32	21:44	22:27	21:43
15	DIVAM 1M	23:32	22:40	23:21	22:36	23:14	22:34
	INTOR 5M	17:56	17:03	17:38	16:53	17:30	16:51
	LAKUT 5M	12:35	11:49	12:19	11:35	12:06	11:26
	LUSEP 1M	14:16	13:25	13:55	13:11	13:44	13:04
	ROPAM 1M	14:48	13:56	14:27	13:42	14:16	13:36
	VEPIN 1M	17:11	16:19	16:52	16:08	16:44	16:05
22L	DIVAM 2A	23:53	22:58	23:43	22:56	23:38	22:55
	INTOR 3A	17:53	16:58	17:37	16:50	17:31	16:48
	LAKUT 3A	17:53	16:58	17:37	16:49	17:30	16:47
	LUSEP 2A	14:07	13:15	13:50	13:02	13:39	12:56
	ROPAM 2A	12:38	11:50	12:25	11:39	12:14	11:32
	VEPIN 2A	14:40	13:47	14:22	13:35	14:12	13:29
22R	DIVAM 2V	24:17	23:18	24:05	23:14	23:58	23:12
	INTOR 3V	17:34	16:35	17:13	16:22	17:03	16:17
	LAKUT 3V	18:35	17:31	18:15	17:17	18:03	17:10
	LUSEP 3V	14:38	13:46	14:30	13:38	14:22	13:30
	PEXEN 3V	25:27	24:21	25:15	24:17	25:08	24:15
	ROPAM 2V	13:04	12:16	12:54	12:06	12:43	11:57
	VEPIN 2V	15:13	14:19	14:55	14:04	14:42	13:56
33	DIVAM 1W	18:16	17:24	17:59	17:15	17:52	17:13
	INTOR 4W	10:57	10:16	10:47	10:06	10:36	09:56
	LAKUT 5W	18:21	17:29	18:04	17:20	17:57	17:18
	LUSEP 1W	19:10	18:18	18:55	18:11	18:48	18:08
	ROPAM 1W	09:21	08:44	09:14	08:38	09:08	08:31
	VEPIN 1W	17:36	16:44	17:18	16:34	17:11	16:32
Min.		09:21	08:44	09:14	08:38	09:08	08:31
Max.		25:27	24:21	25:15	24:17	25:08	24:15
Average		**17:18**	**16:24**	**17:02**	**16:15**	**16:54**	**16:10**

Table A3.6. Approach risk period in 20 knot headwind.

		Risk period (20 kt headwind) [min:s]					
Runway	**STAR**	**3 degree profile**		**4 degree profile**		**5 degree profile**	
		Speed profile A	**Speed profile B**	**Speed profile A**	**Speed profile B**	**Speed profile A**	**Speed profile B**
04L	DIVAM 1B	15:00	14:07	14:39	13:53	14:29	13:47
	INTOR 4B	14:41	13:49	07:39	07:04	06:37	06:05
	LAKUT 5B	13:49	13:00	07:33	06:59	06:36	06:04
	LUSEP 1B	07:53	07:19	07:23	06:51	06:36	06:04
	ROPAM 1B	08:04	07:29	07:33	07:00	06:37	06:05
	VEPIN 1B	08:55	08:20	07:33	07:00	06:37	06:05
	MAROM 4B	17:49	16:48	10:50	10:08	10:36	09:54
	NAPUN 1B	13:11	12:26	10:52	10:09	10:36	09:54
	PEXEN 4B	18:48	17:43	18:29	17:29	18:18	17:23
04R	DIVAM 1R	15:22	14:28	15:04	14:17	14:55	14:12
	INTOR 4R	09:06	08:29	08:37	08:00	08:11	07:35
	LAKUT 5R	15:05	14:04	08:57	08:18	08:04	07:28
	LUSEP 1R	09:15	08:36	08:44	08:08	08:05	07:28
	ROPAM 1R	09:06	08:29	08:37	08:00	08:11	07:35
	VEPIN 1R	09:06	08:29	08:37	08:00	08:11	07:35
15	DIVAM 1M	07:29	06:57	06:58	06:27	06:05	05:37
	INTOR 5M	07:29	06:57	06:58	06:27	06:05	05:37
	LAKUT 5M	12:35	11:49	12:19	11:35	06:32	06:01
	LUSEP 1M	14:16	13:25	10:47	09:57	06:05	05:37
	ROPAM 1M	07:29	06:57	06:58	06:27	06:05	05:37
	VEPIN 1M	17:11	16:19	07:15	06:40	06:05	05:37
22L	DIVAM 2A	08:44	08:07	08:14	07:38	07:45	07:08
	INTOR 3A	08:44	08:07	08:14	07:38	07:45	07:08
	LAKUT 3A	09:04	08:26	08:21	07:45	07:38	07:04
	LUSEP 2A	14:07	13:15	13:50	13:02	07:38	07:04
	ROPAM 2A	10:03	09:17	08:23	07:47	07:37	07:03
	VEPIN 2A	14:40	13:47	14:22	13:35	12:24	11:41
22R	DIVAM 2V	11:00	10:20	09:14	08:36	08:50	08:13
	INTOR 3V	12:13	11:19	09:40	08:59	08:59	08:22
	LAKUT 3V	18:35	17:31	11:27	10:42	10:44	10:01
	LUSEP 3V	14:38	13:46	14:30	13:38	14:22	13:30
	PEXEN 3V	17:14	16:22	11:27	10:42	10:44	10:01
	ROPAM 2V	13:04	12:16	10:41	09:56	09:17	08:38
	VEPIN 2V	15:13	14:19	14:55	14:04	14:42	13:56
33	DIVAM 1W	18:16	17:24	07:19	06:46	06:13	05:44
	INTOR 4W	10:57	10:16	10:47	10:06	08:56	08:16
	LAKUT 5W	07:51	07:17	07:17	06:45	06:13	05:44
	LUSEP 1W	07:51	07:17	07:17	06:45	06:13	05:44
	ROPAM 1W	09:21	08:44	08:21	07:25	06:13	05:44
	VEPIN 1W	14:45	13:47	07:18	06:46	06:13	05:44
Min.		07:29	06:57	06:58	06:27	06:05	05:37
Max.		18:48	17:43	18:29	17:29	18:18	17:23
Average		**12:12**	**11:26**	**09:51**	**09:11**	**08:42**	**08:06**

Table A3.7. Risk period change with different profiles compared to 3 degree speed A profile in 20 knot headwind.

		Risk period change (20 kt headwind) [%]					
Runway	**STAR**	**3 degree profile**		**4 degree profile**		**5 degree profile**	
		Speed profile A	**Speed profile B**	**Speed profile A**	**Speed profile B**	**Speed profile A**	**Speed profile B**
04L	DIVAM 1B	-	−5.9 %	−2.3 %	−7.4 %	−3.5 %	−8.0 %
	INTOR 4B	-	−5.9 %	−47.9 %	−51.8 %	−55.0 %	−58.5 %
	LAKUT 5B	-	−6.0 %	−45.3 %	−49.4 %	−52.2 %	−56.1 %
	LUSEP 1B	-	−7.2 %	−6.5 %	−13.1 %	−16.4 %	−23.1 %
	ROPAM 1B	-	−7.1 %	−6.3 %	−13.2 %	−18.0 %	−24.5 %
	VEPIN 1B	-	−6.5 %	−15.2 %	−21.4 %	−25.8 %	−31.7 %
	MAROM 4B	-	−5.8 %	−39.2 %	−43.1 %	−40.5 %	−44.5 %
	NAPUN 1B	-	−5.6 %	−17.5 %	−22.9 %	−19.5 %	−24.9 %
	PEXEN 4B	-	−5.7 %	−1.7 %	−7.0 %	−2.7 %	−7.5 %
04R	DIVAM 1R	-	−5.9 %	−1.9 %	−7.1 %	−2.9 %	−7.6 %
	INTOR 4R	-	−6.9 %	−5.3 %	−12.1 %	−10.2 %	−16.7 %
	LAKUT 5R	-	−6.7 %	−40.6 %	−44.9 %	−46.5 %	−50.4 %
	LUSEP 1R	-	−7.0 %	−5.6 %	−12.2 %	−12.6 %	−19.2 %
	ROPAM 1R	-	−6.9 %	−5.3 %	−12.1 %	−10.2 %	−16.7 %
	VEPIN 1R	-	−6.9 %	−5.3 %	−12.1 %	−10.2 %	−16.7 %
15	DIVAM 1M	-	−7.3 %	−6.9 %	−13.8 %	−18.7 %	−25.1 %
	INTOR 5M	-	−7.3 %	−6.9 %	−13.8 %	−18.7 %	−25.1 %
	LAKUT 5M	-	−6.1 %	−2.1 %	−8.0 %	−48.1 %	−52.2 %
	LUSEP 1M	-	−5.9 %	−24.4 %	−30.2 %	−57.3 %	−60.7 %
	ROPAM 1M	-	−7.3 %	−6.9 %	−13.8 %	−18.7 %	−25.1 %
	VEPIN 1M	-	−5.1 %	−57.8 %	−61.3 %	−64.6 %	−67.3 %
22L	DIVAM 2A	-	−7.1 %	−5.8 %	−12.6 %	−11.3 %	−18.4 %
	INTOR 3A	-	−7.1 %	−5.8 %	−12.6 %	−11.3 %	−18.4 %
	LAKUT 3A	-	−7.0 %	−7.9 %	−14.5 %	−15.9 %	−22.1 %
	LUSEP 2A	-	−6.1 %	−2.0 %	−7.6 %	−46.0 %	−50.0 %
	ROPAM 2A	-	−7.6 %	−16.6 %	−22.6 %	−24.2 %	−29.8 %
	VEPIN 2A	-	−6.0 %	−2.0 %	−7.4 %	−15.4 %	−20.3 %
22R	DIVAM 2V	-	−6.0 %	−16.0 %	−21.7 %	−19.7 %	−25.3 %
	INTOR 3V	-	−7.4 %	−20.9 %	−26.4 %	−26.4 %	−31.5 %
	LAKUT 3V	-	−5.7 %	−38.4 %	−42.5 %	−42.2 %	−46.1 %
	LUSEP 3V	-	−6.0 %	−0.9 %	−6.9 %	−1.8 %	−7.7 %
	PEXEN 3V	-	−5.1 %	−33.6 %	−38.0 %	−37.7 %	−41.8 %
	ROPAM 2V	-	−6.1 %	−18.2 %	−23.9 %	−29.0 %	−34.0 %
	VEPIN 2V	-	−5.9 %	−1.9 %	−7.6 %	−3.3 %	−8.4 %
33	DIVAM 1W	-	−4.8 %	−59.9 %	−62.9 %	−66.0 %	−68.6 %
	INTOR 4W	-	−6.4 %	−1.6 %	−7.9 %	−18.5 %	−24.5 %
	LAKUT 5W	-	−7.2 %	−7.1 %	−13.9 %	−20.8 %	−26.9 %
	LUSEP 1W	-	−7.2 %	−7.1 %	−13.9 %	−20.8 %	−26.9 %
	ROPAM 1W	-	−6.6 %	−10.7 %	−20.7 %	−33.5 %	−38.7 %
	VEPIN 1W	-	−6.5 %	−50.5 %	−54.1 %	−57.9 %	−61.1 %
Min.		-	−7.6 %	−59.9 %	−62.9 %	−66.0 %	−68.6 %
Max.		-	−4.8 %	−0.9 %	−6.9 %	−1.8 %	−7.5 %
Average		-	**−6.4 %**	**−16.4 %**	**−22.2 %**	**−26.4 %**	**−31.6 %**

Table A3.8. Risk period in percentage of the total time in approach in 20 knot headwind.

		Risk period [%] of total time in approach (20 kt headwind)					
Runway	**STAR**	**3 degree profile**		**4 degree profile**		**5 degree profile**	
		Speed profile A	**Speed profile B**	**Speed profile A**	**Speed profile B**	**Speed profile A**	**Speed profile B**
04L	DIVAM 1B	100.0 %	100.0 %	100.0 %	100.0 %	100.0 %	100.0 %
	INTOR 4B	100.0 %	100.0 %	53.3 %	52.0 %	46.7 %	45.1 %
	LAKUT 5B	100.0 %	100.0 %	55.9 %	54.8 %	49.6 %	48.0 %
	LUSEP 1B	39.2 %	38.1 %	37.1 %	35.8 %	33.3 %	31.8 %
	ROPAM 1B	52.3 %	51.5 %	50.1 %	48.9 %	44.3 %	42.8 %
	VEPIN 1B	41.8 %	40.8 %	35.8 %	34.4 %	31.5 %	30.0 %
	MAROM 4B	100.0 %	100.0 %	61.8 %	61.2 %	61.1 %	60.2 %
	NAPUN 1B	57.9 %	57.4 %	48.3 %	47.2 %	47.4 %	46.1 %
	PEXEN 4B	100.0 %	100.0 %	100.0 %	100.0 %	100.0 %	100.0 %
04R	DIVAM 1R	100.0 %	100.0 %	100.0 %	100.0 %	100.0 %	100.0 %
	INTOR 4R	54.8 %	54.1 %	52.8 %	51.6 %	50.5 %	49.1 %
	LAKUT 5R	99.5 %	98.7 %	60.3 %	59.1 %	54.8 %	53.4 %
	LUSEP 1R	42.5 %	41.2 %	40.4 %	39.0 %	37.5 %	35.9 %
	ROPAM 1R	54.3 %	53.5 %	52.3 %	51.0 %	50.0 %	48.5 %
	VEPIN 1R	40.1 %	38.9 %	38.2 %	36.8 %	36.4 %	34.9 %
15	DIVAM 1M	31.8 %	30.6 %	29.9 %	28.6 %	26.2 %	24.9 %
	INTOR 5M	41.8 %	40.7 %	39.6 %	38.2 %	34.8 %	33.3 %
	LAKUT 5M	100.0 %	100.0 %	100.0 %	100.0 %	54.0 %	52.6 %
	LUSEP 1M	100.0 %	100.0 %	77.5 %	75.5 %	44.3 %	43.0 %
	ROPAM 1M	50.6 %	49.8 %	48.3 %	47.1 %	42.6 %	41.3 %
	VEPIN 1M	100.0 %	100.0 %	43.0 %	41.3 %	36.3 %	34.9 %
22L	DIVAM 2A	36.6 %	35.3 %	34.7 %	33.3 %	32.8 %	31.1 %
	INTOR 3A	48.8 %	47.8 %	46.7 %	45.4 %	44.3 %	42.4 %
	LAKUT 3A	50.7 %	49.7 %	47.4 %	46.1 %	43.6 %	42.1 %
	LUSEP 2A	100.0 %	100.0 %	100.0 %	100.0 %	55.9 %	54.6 %
	ROPAM 2A	79.6 %	78.5 %	67.5 %	66.8 %	62.2 %	61.2 %
	VEPIN 2A	100.0 %	100.0 %	100.0 %	100.0 %	87.4 %	86.7 %
22R	DIVAM 2V	45.3 %	44.3 %	38.4 %	37.0 %	36.8 %	35.4 %
	INTOR 3V	69.5 %	68.2 %	56.1 %	54.9 %	52.7 %	51.4 %
	LAKUT 3V	100.0 %	100.0 %	62.8 %	61.9 %	59.4 %	58.4 %
	LUSEP 3V	100.0 %	100.0 %	100.0 %	100.0 %	100.0 %	100.0 %
	PEXEN 3V	67.7 %	67.2 %	45.4 %	44.0 %	42.7 %	41.4 %
	ROPAM 2V	100.0 %	100.0 %	82.9 %	82.1 %	73.0 %	72.2 %
	VEPIN 2V	100.0 %	100.0 %	100.0 %	100.0 %	100.0 %	100.0 %
33	DIVAM 1W	100.0 %	100.0 %	40.7 %	39.2 %	34.8 %	33.3 %
	INTOR 4W	100.0 %	100.0 %	100.0 %	100.0 %	84.2 %	83.2 %
	LAKUT 5W	42.7 %	41.7 %	40.3 %	38.9 %	34.6 %	33.1 %
	LUSEP 1W	40.9 %	39.8 %	38.5 %	37.1 %	33.1 %	31.6 %
	ROPAM 1W	100.0 %	100.0 %	90.3 %	86.0 %	68.1 %	67.3 %
	VEPIN 1W	83.8 %	82.4 %	42.2 %	40.8 %	36.2 %	34.7 %
Min.		31.8 %	30.6 %	29.9 %	28.6 %	26.2 %	24.9 %
Max.		100.0 %	100.0 %	100.0 %	100.0 %	100.0 %	100.0 %
Average		**74.3 %**	**73.8 %**	**61.5 %**	**60.4 %**	**54.1 %**	**52.9 %**

Appendix 4. Result Visualisations – Risk Areas

Runway 04L

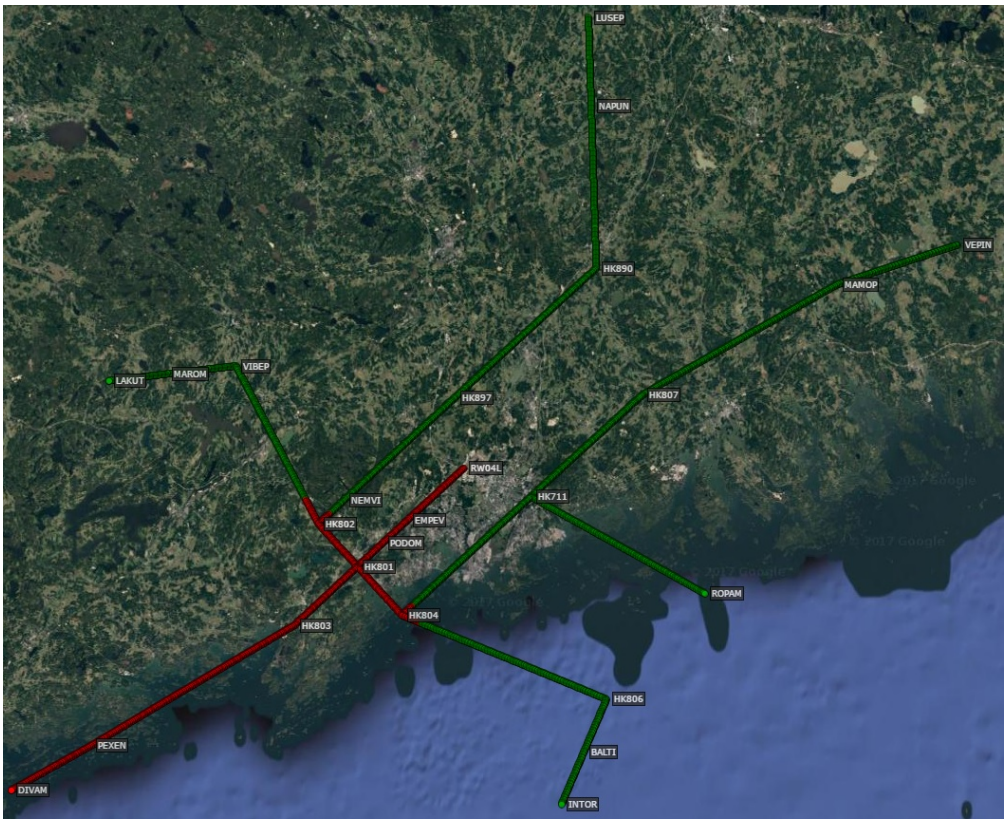

Figure A4.1. Runway 04L risk areas, 3 degree descent profile, speed profile A, still air, 1/2.

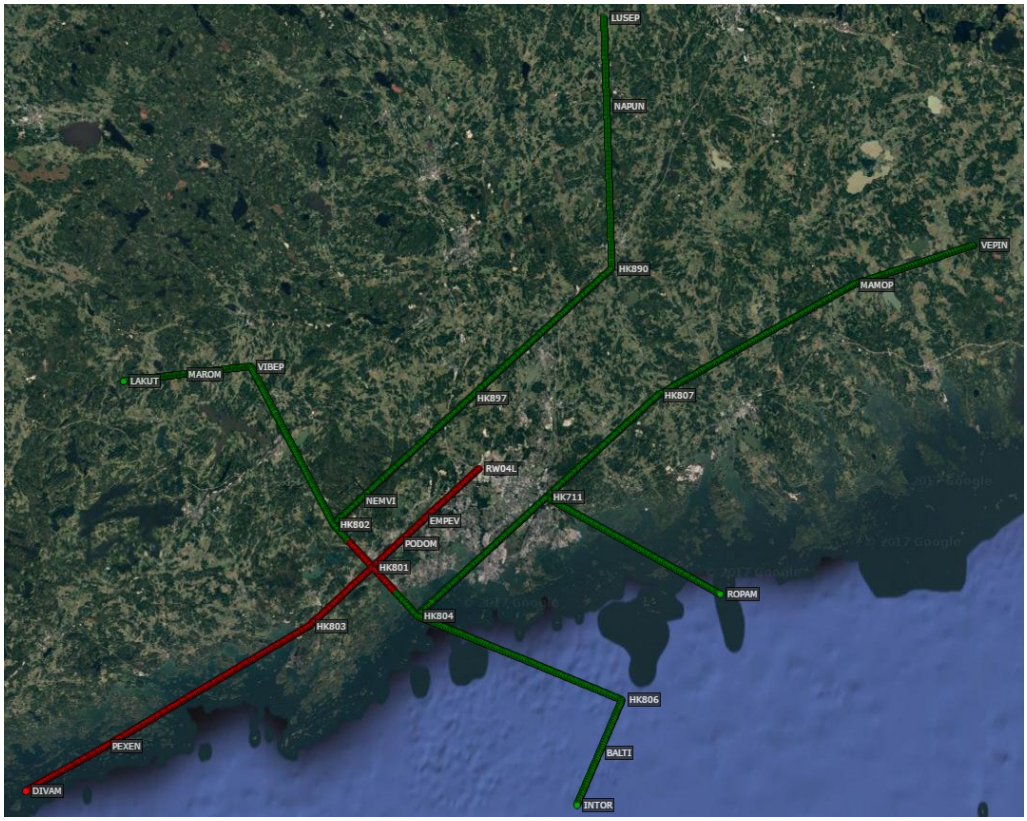

Figure A4.2. Runway 04L risk areas, 4 degree descent profile, speed profile A, still air, 1/2.

Figure A4.3. Runway 04L risk areas, 5 degree descent profile, speed profile A, still air, 1/2.

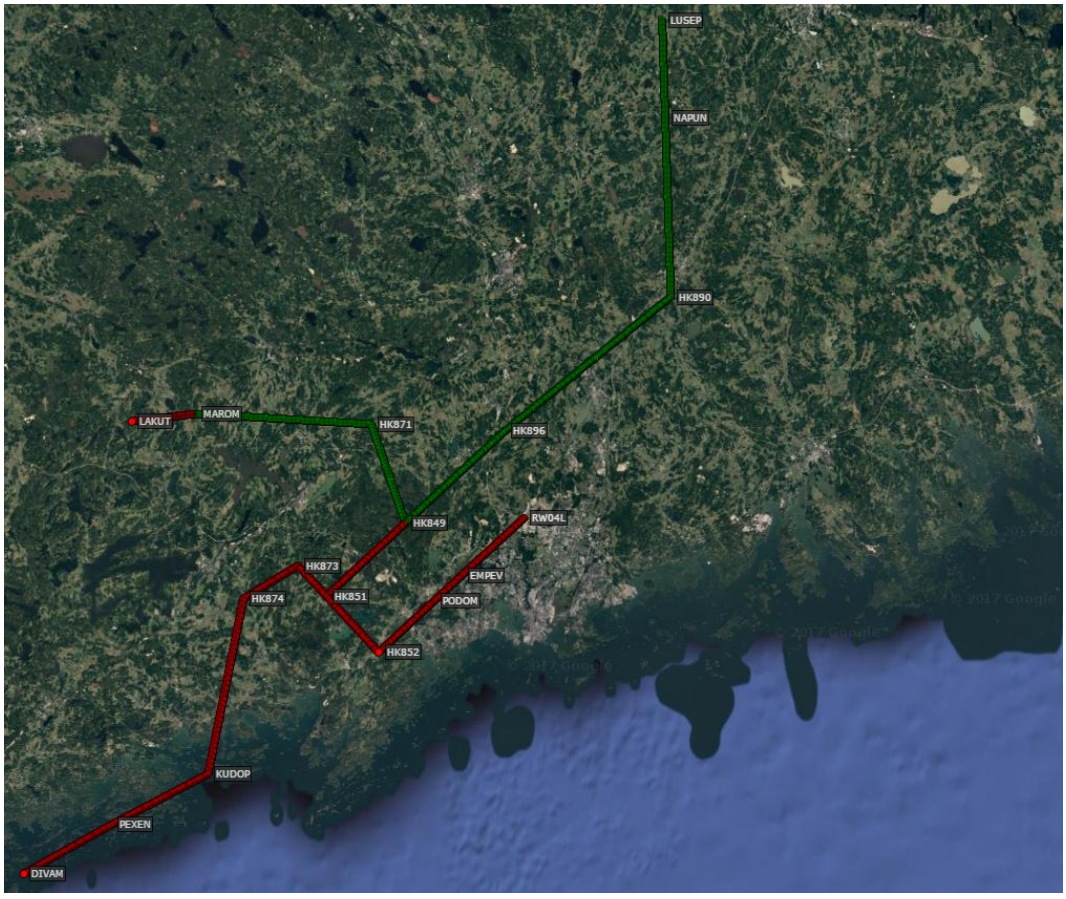

Figure A4.4. Runway 04L risk areas, 3 degree descent profile, speed profile A, still air, 2/2.

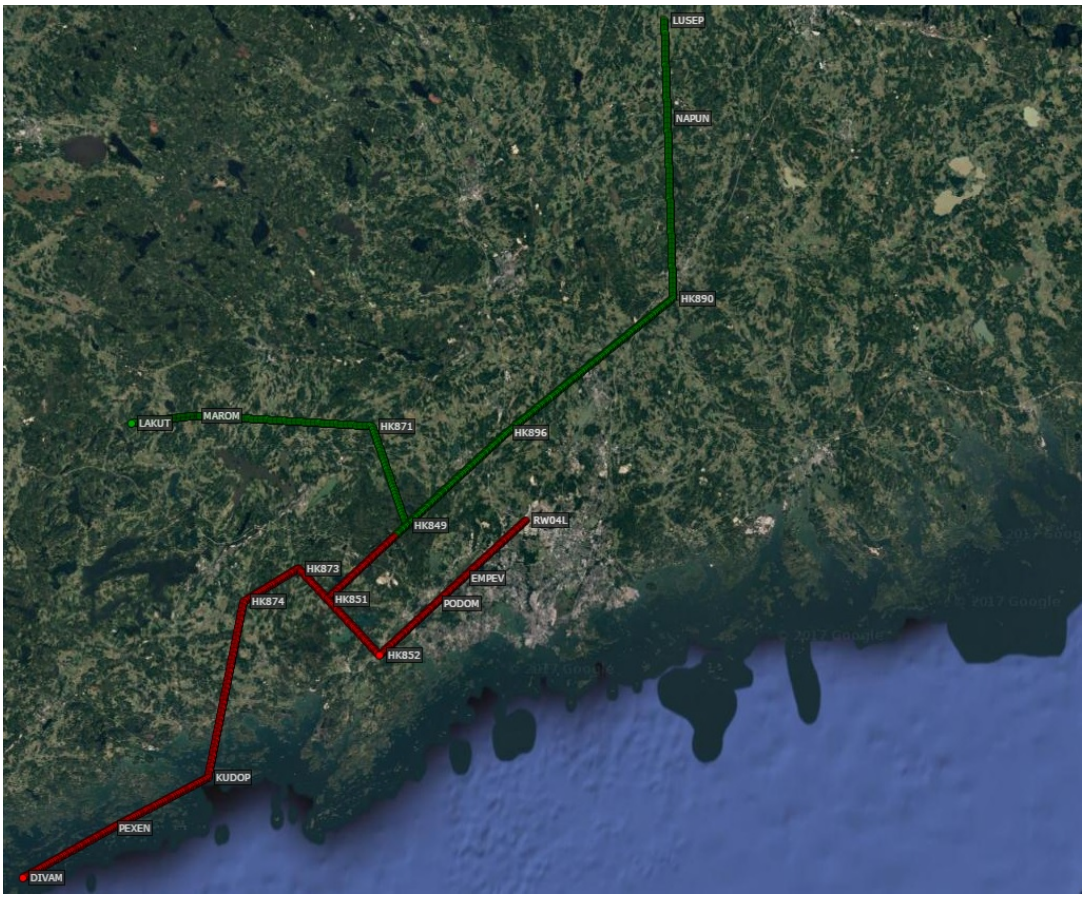

Figure A4.5. Runway 04L risk areas, 4 degree descent profile, speed profile A, still air, 2/2.

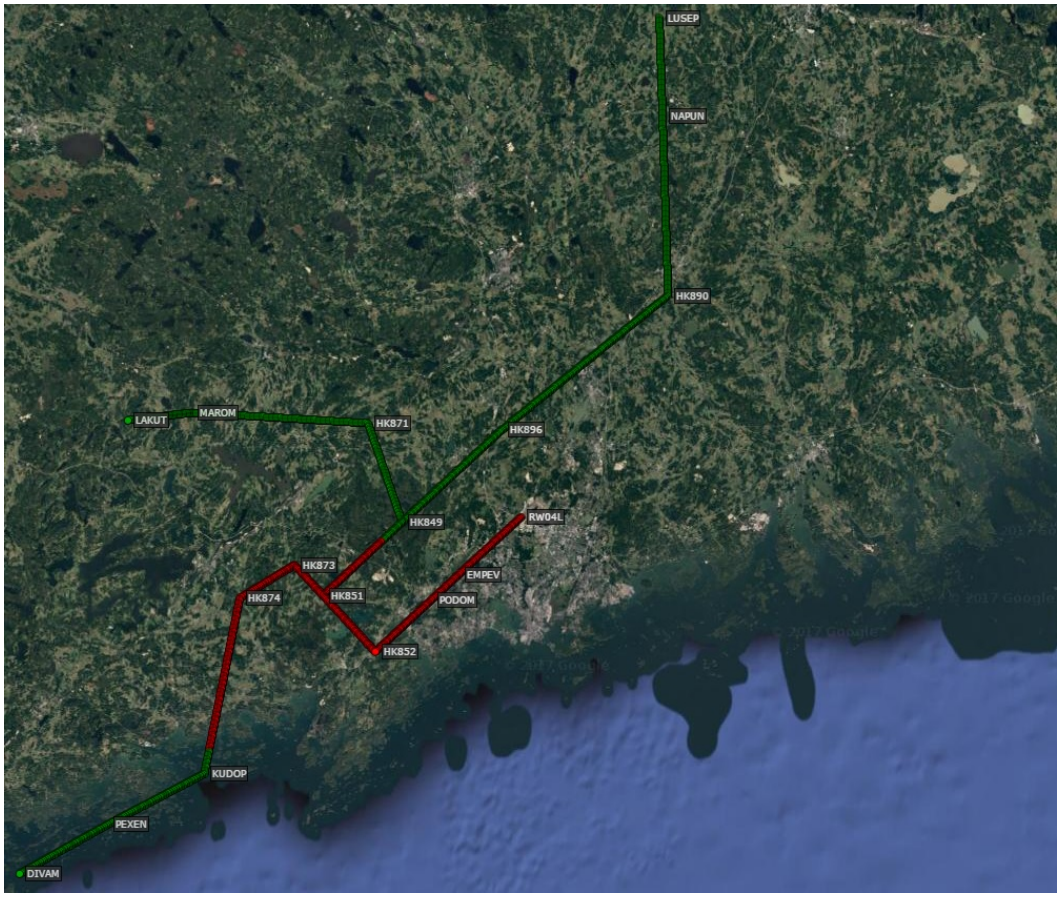

Figure A4.6. Runway 04L risk areas, 5 degree descent profile, speed profile A, still air, 2/2.

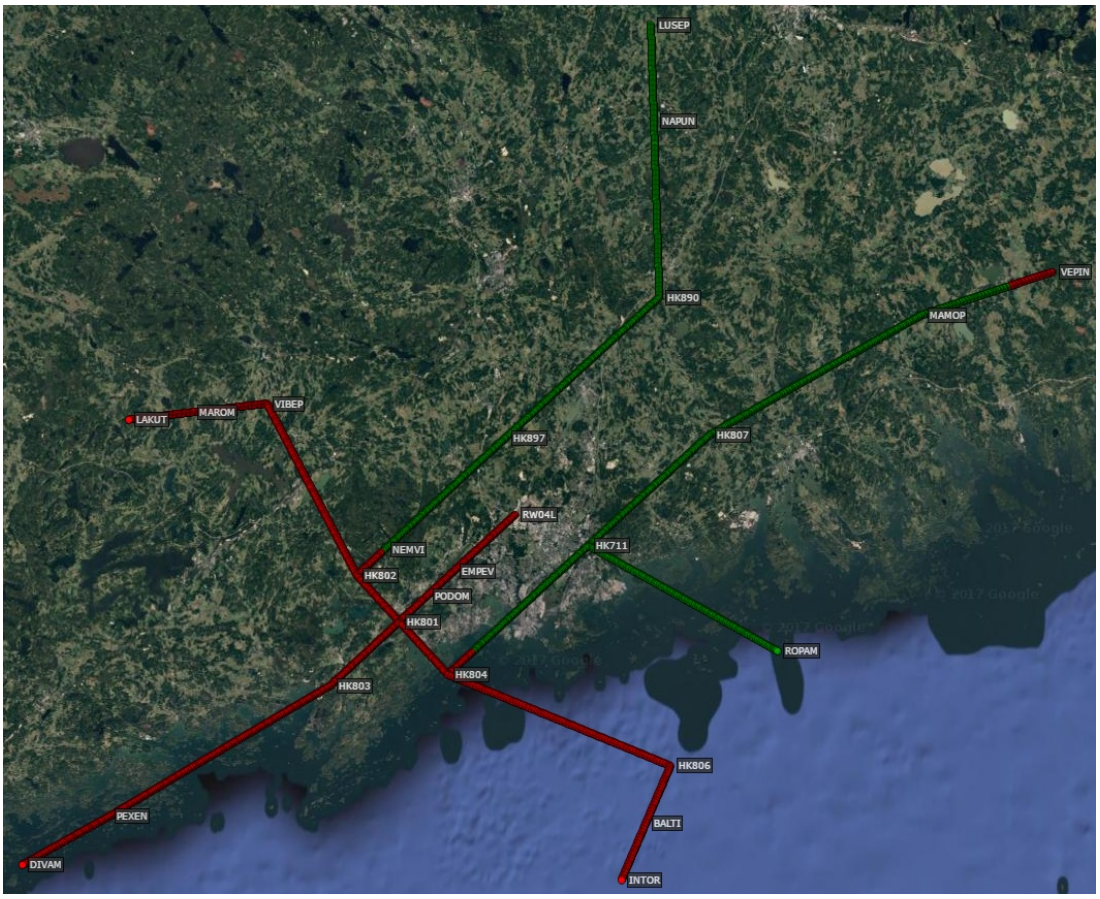

Figure A4.7. Runway 04L risk areas, 3 degree descent profile, speed profile A, 20 kt headwind, 1/2.

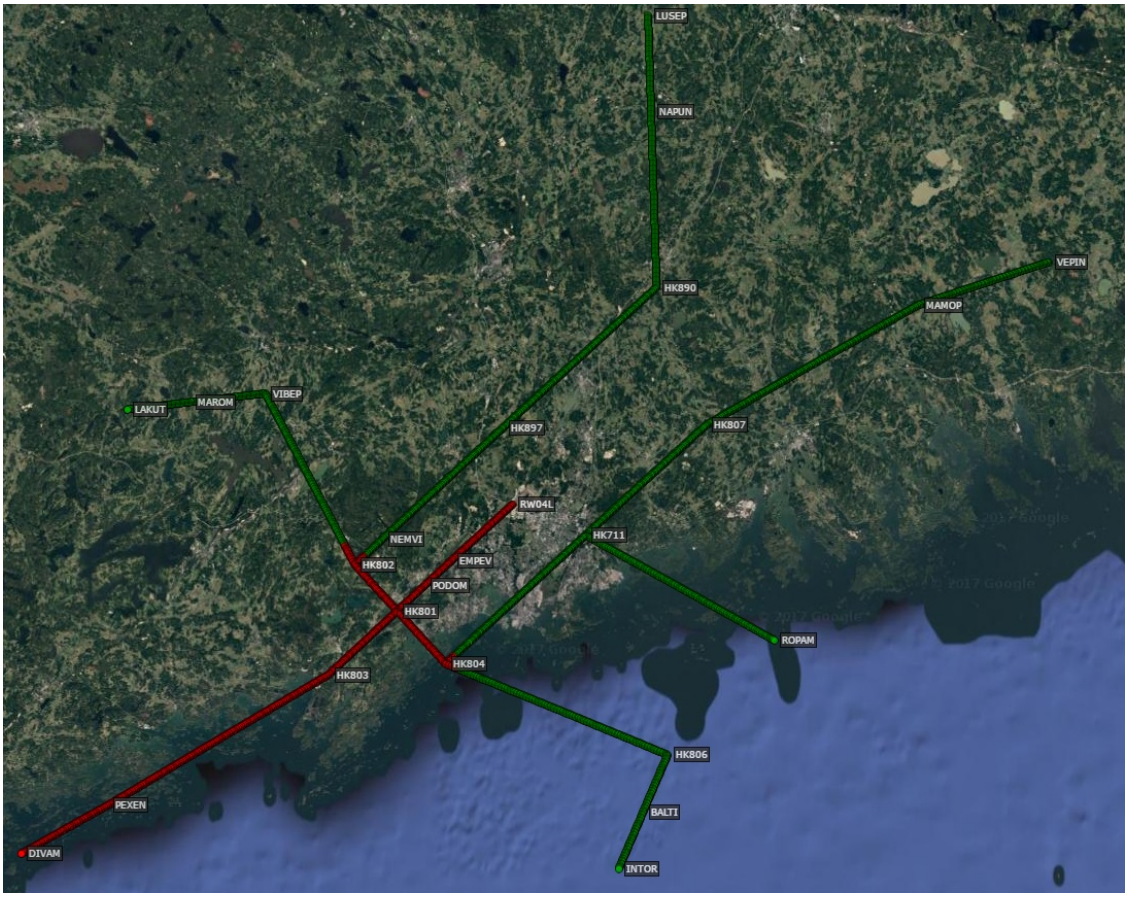

Figure A4.8. Runway 04L risk areas, 4 degree descent profile, speed profile A, 20 kt headwind, 1/2.

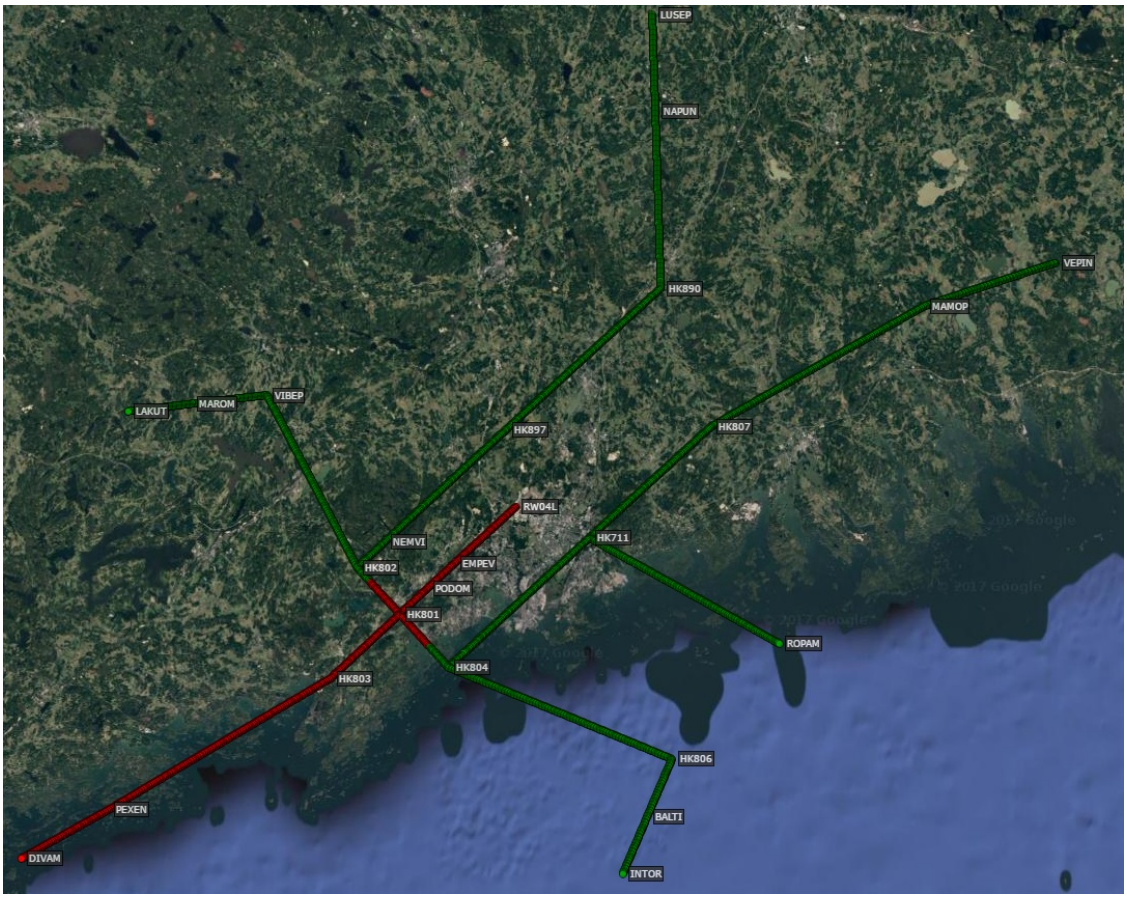

Figure A4.9. Runway 04L risk areas, 5 degree descent profile, speed profile A, 20 kt headwind, 1/2.

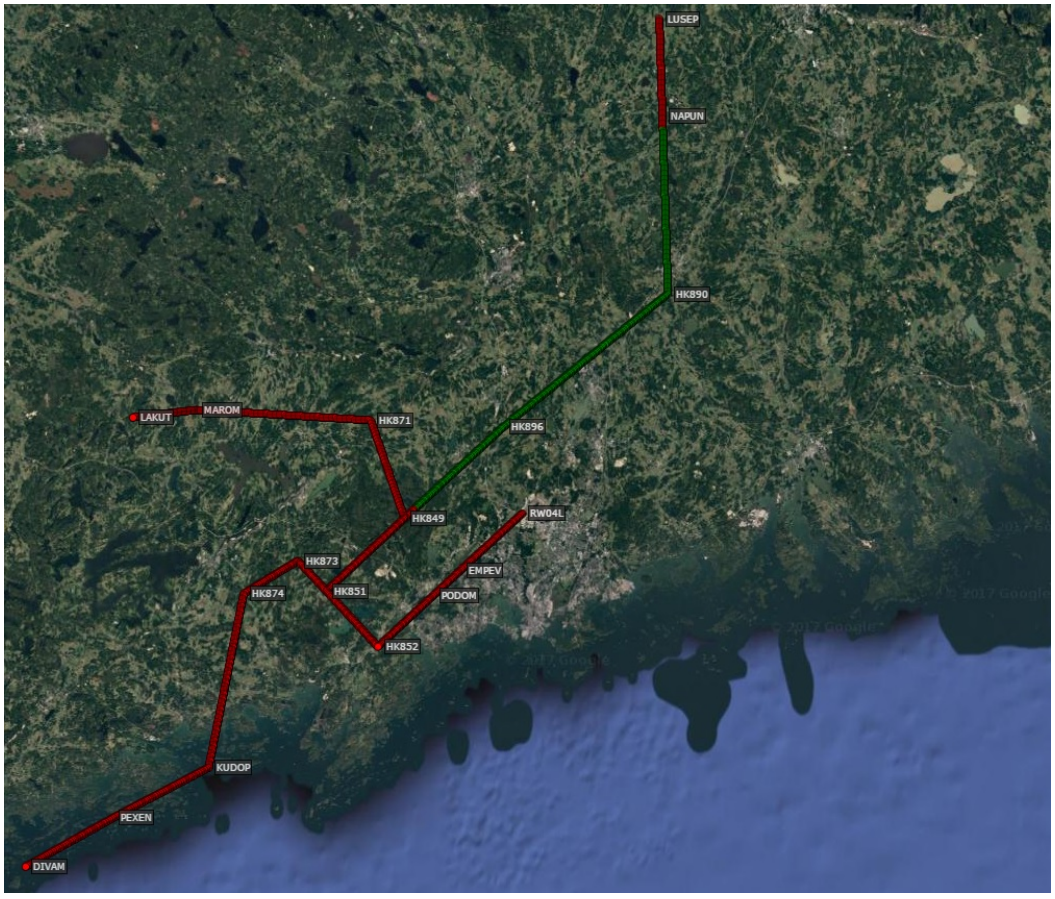

Figure A4.10. Runway 04L risk areas, 3 degree descent profile, speed profile A, 20 kt headwind, 2/2.

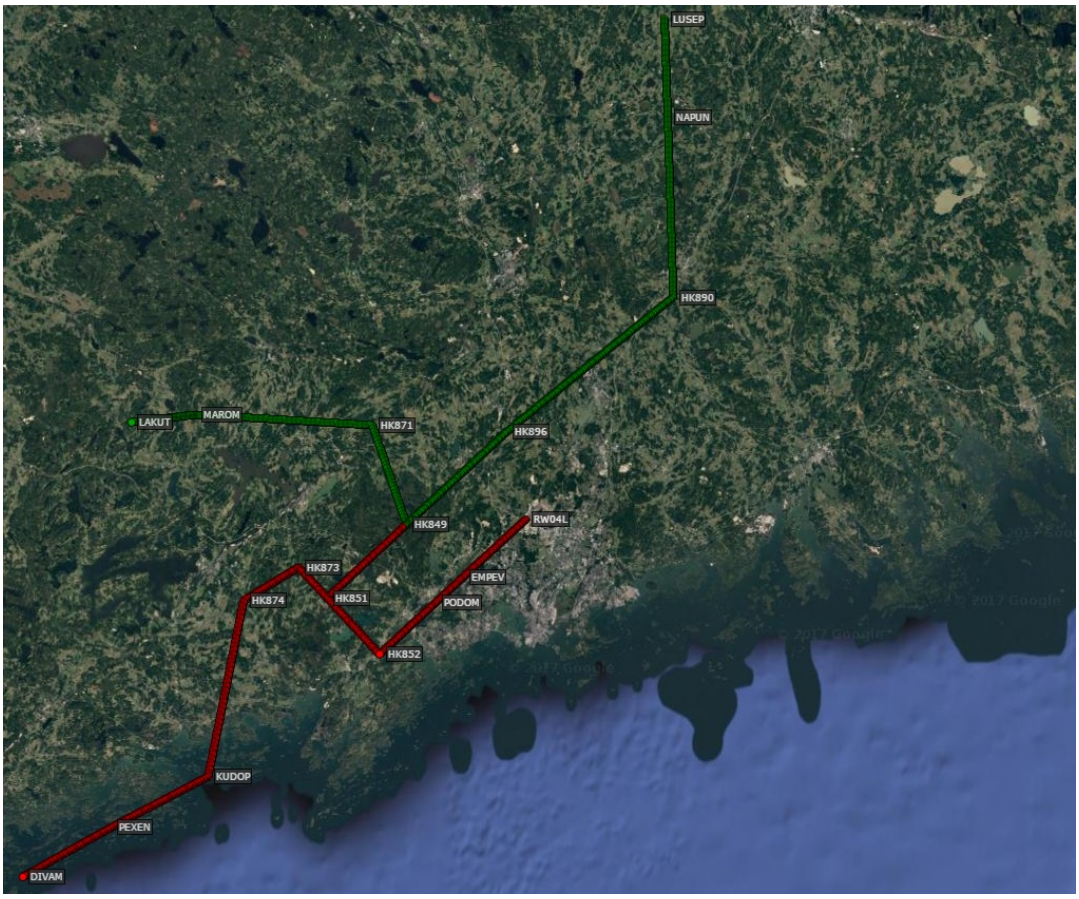

Figure A4.11. Runway 04L risk areas, 4 degree descent profile, speed profile A, 20 kt headwind, 2/2.

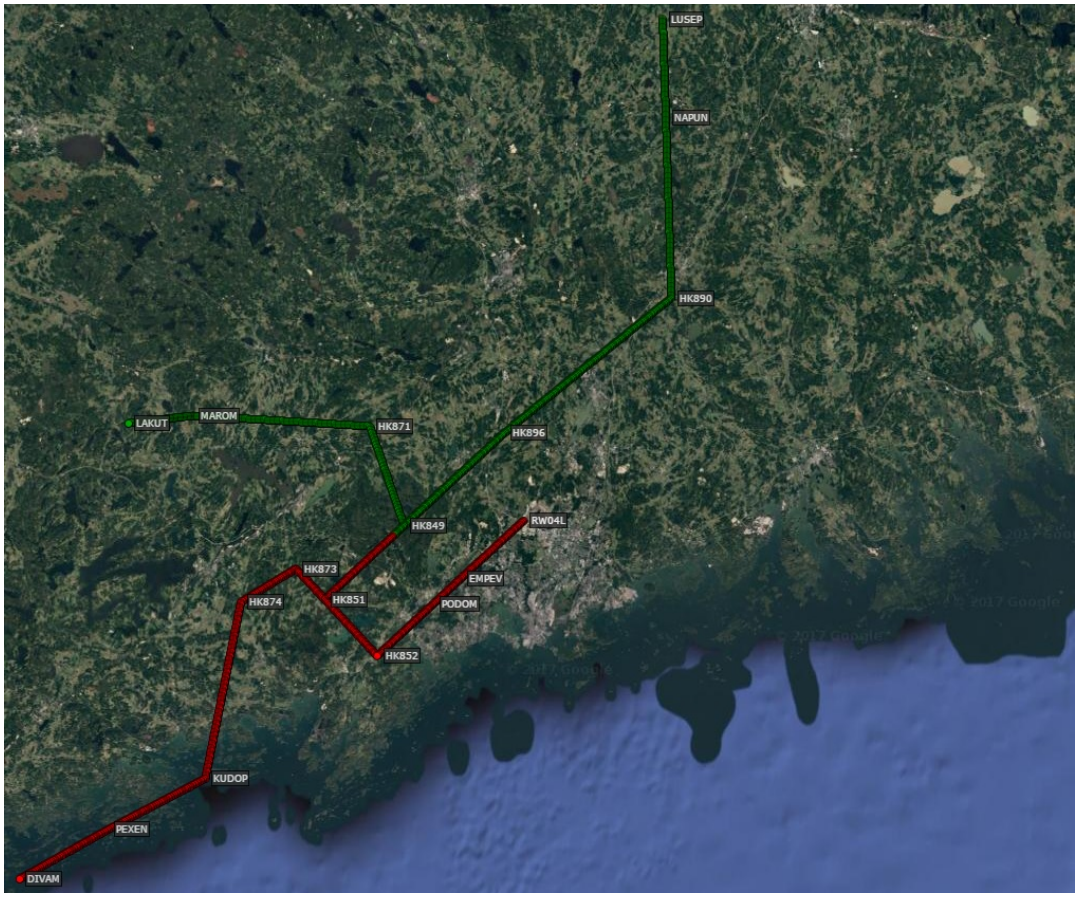

Figure A4.12. Runway 04L risk areas, 5 degree descent profile, speed profile A, 20 kt headwind, 2/2.

Runway 04R

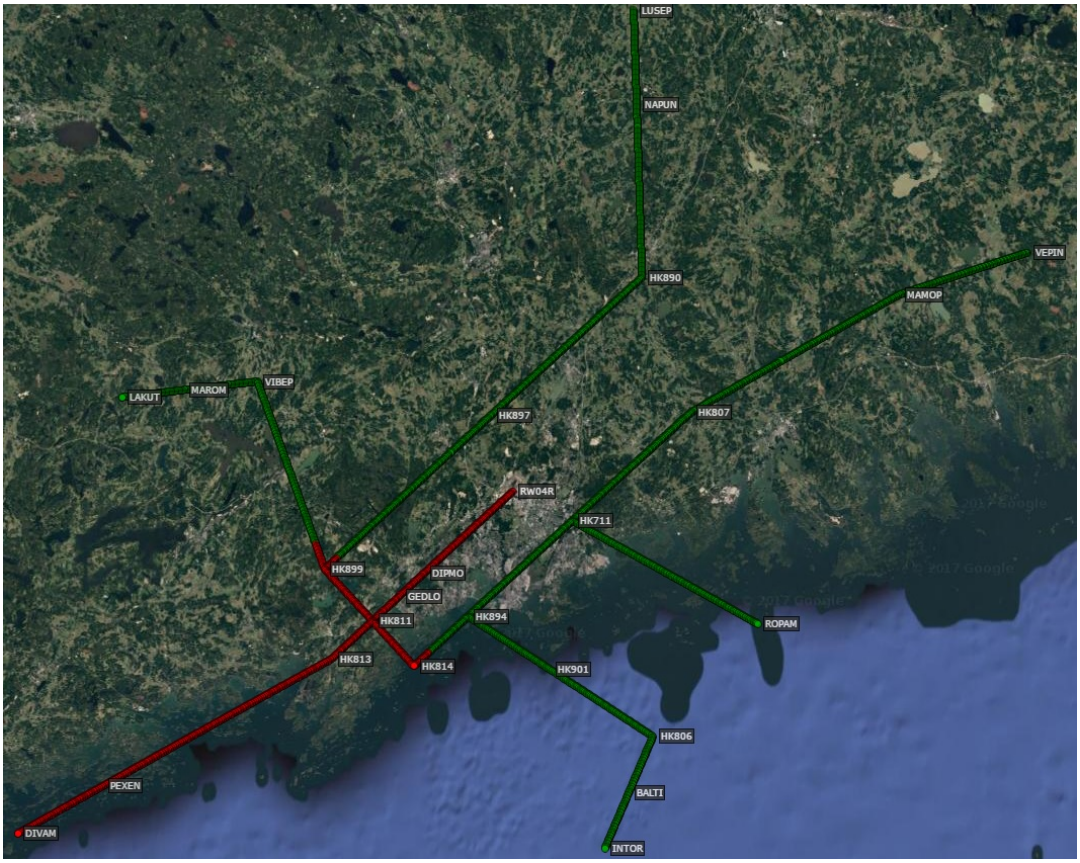

Figure A4.13. Runway 04R risk areas, 3 degree descent profile, speed profile A, still air.

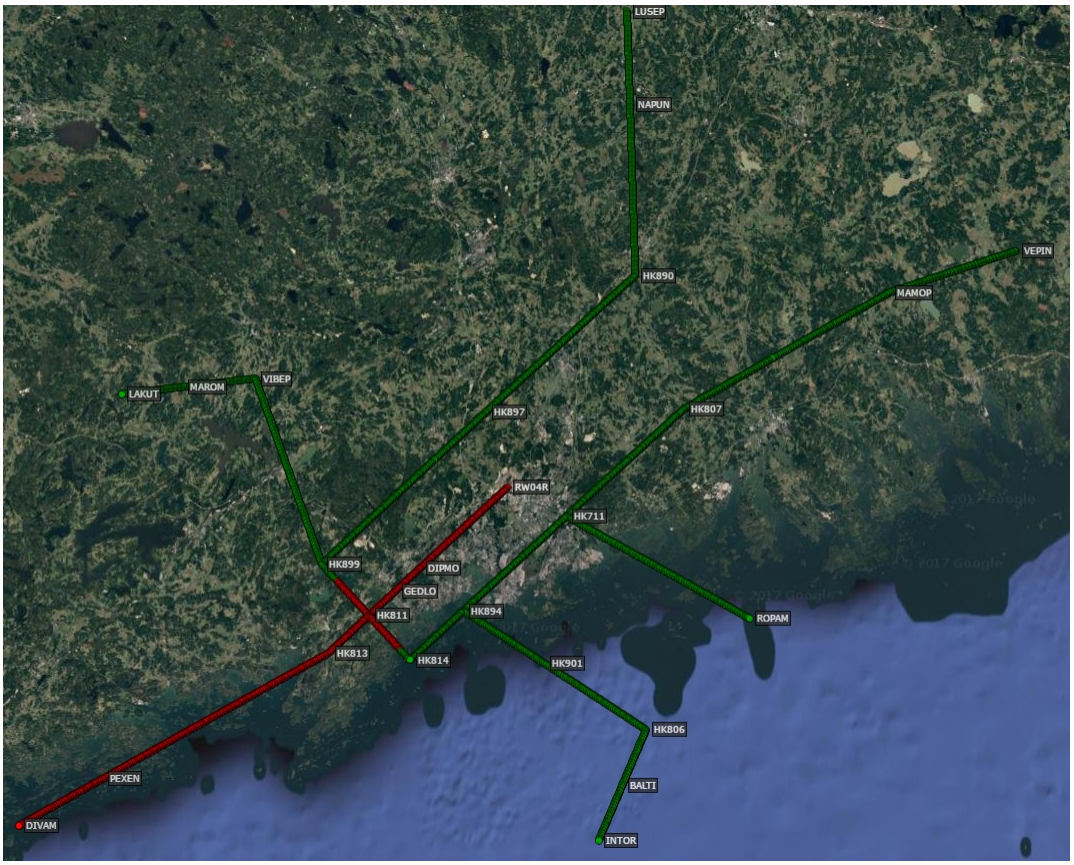

Figure A4.14. Runway 04R risk areas, 4 degree descent profile, speed profile A, still air.

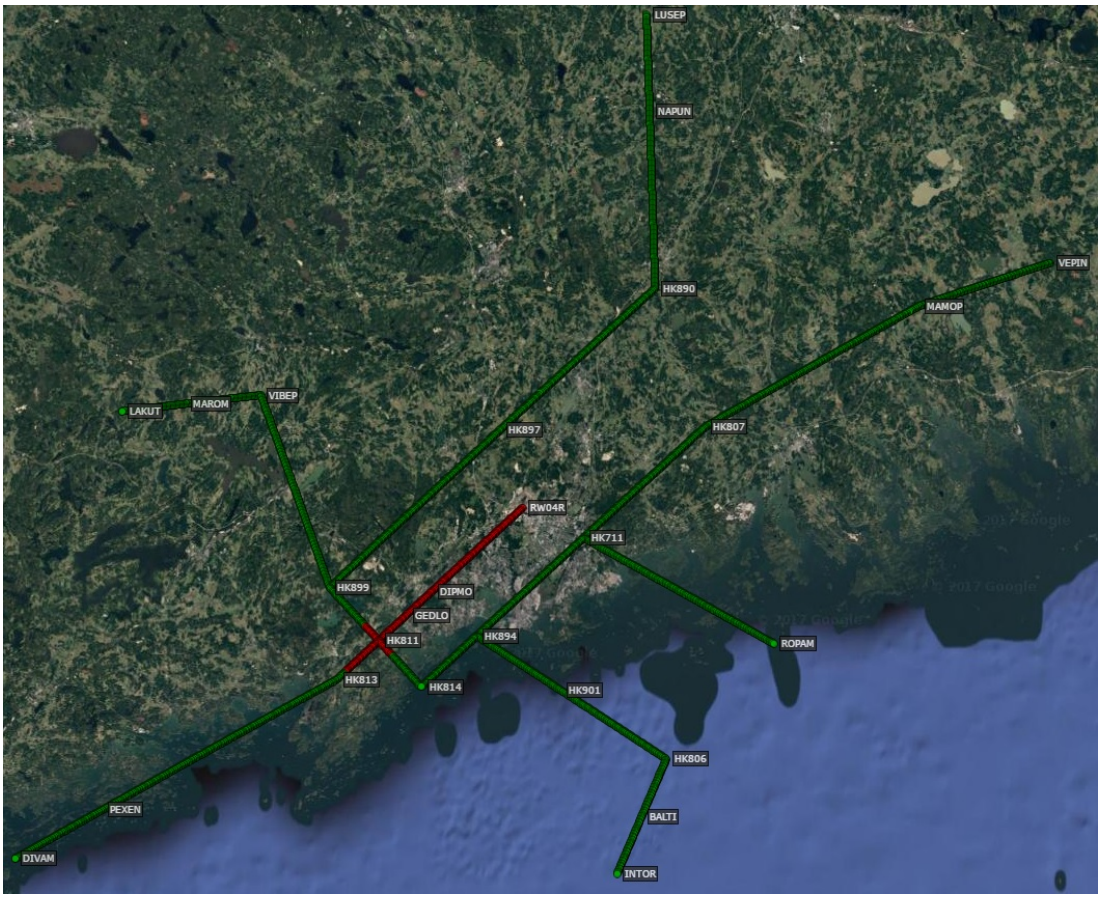

Figure A4.15. Runway 04R risk areas, 5 degree descent profile, speed profile A, still air.

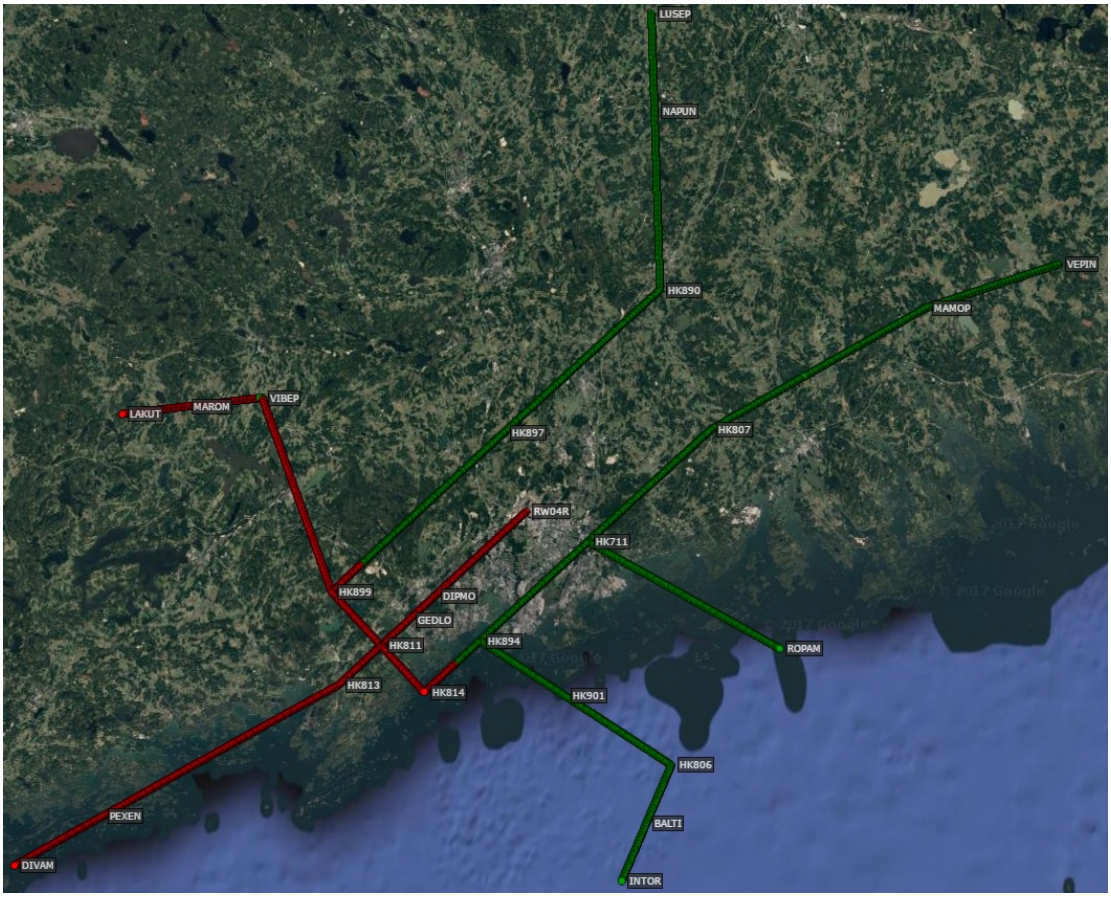

Figure A4.16. Runway 04R risk areas, 3 degree descent profile, speed profile A, 20 kt headwind.

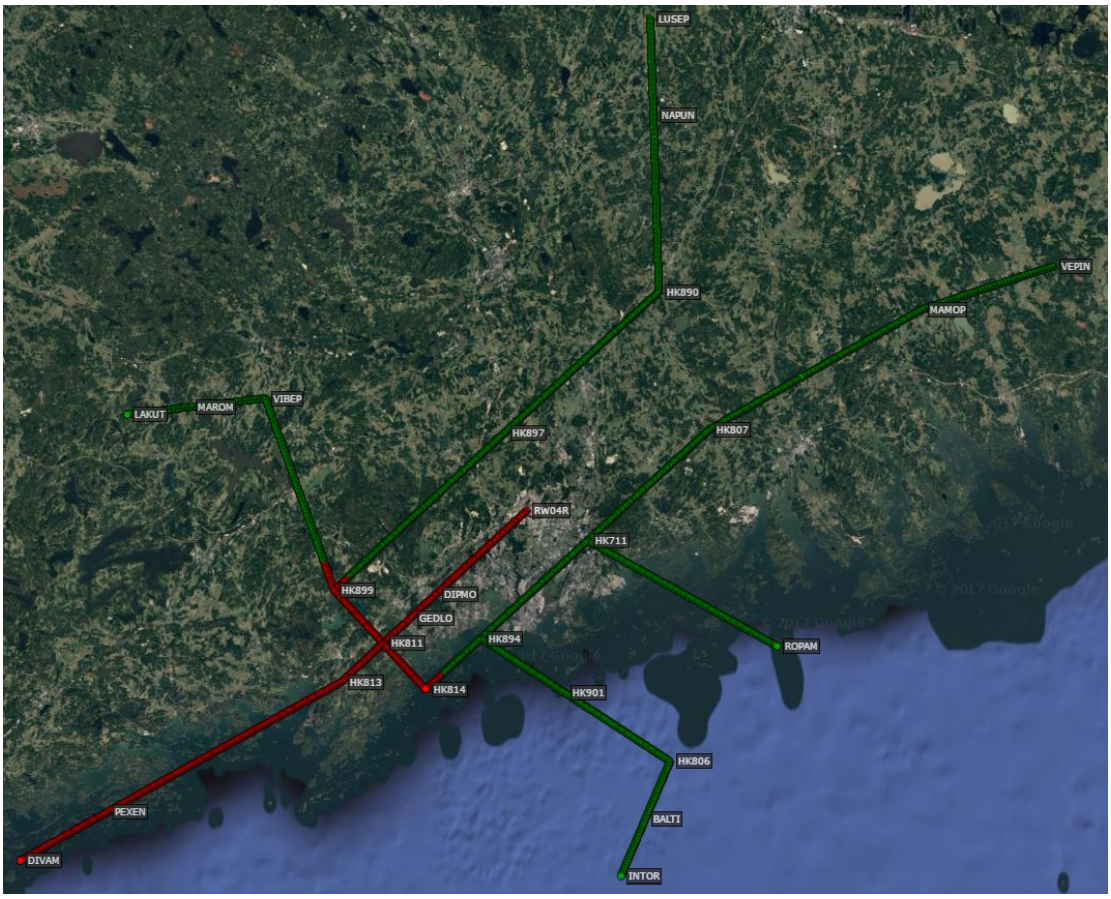

Figure A4.17. Runway 04R risk areas, 4 degree descent profile, speed profile A, 20 kt headwind.

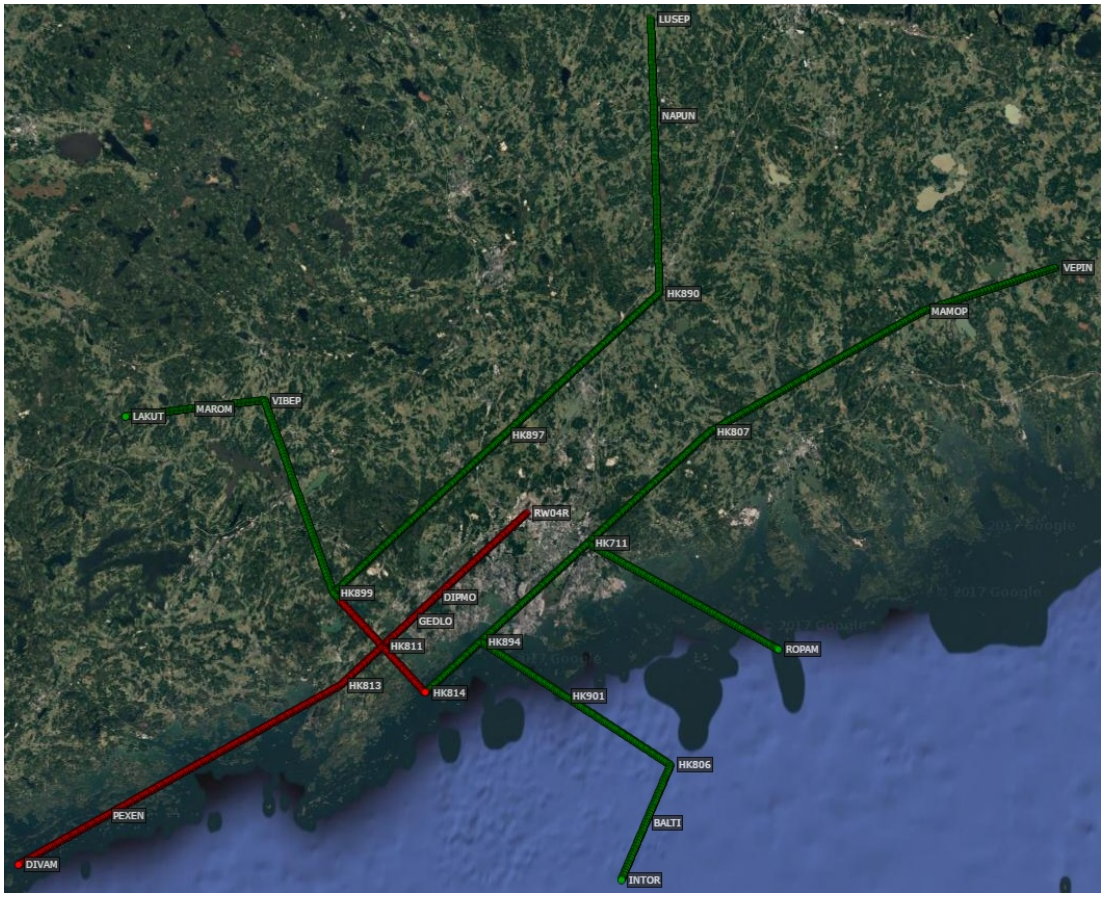

Figure A4.18. Runway 04R risk areas, 5 degree descent profile, speed profile A, 20 kt headwind.

Runway 15

Figure A4.19. Runway 15 risk areas, 3 degree descent profile, speed profile A, still air.

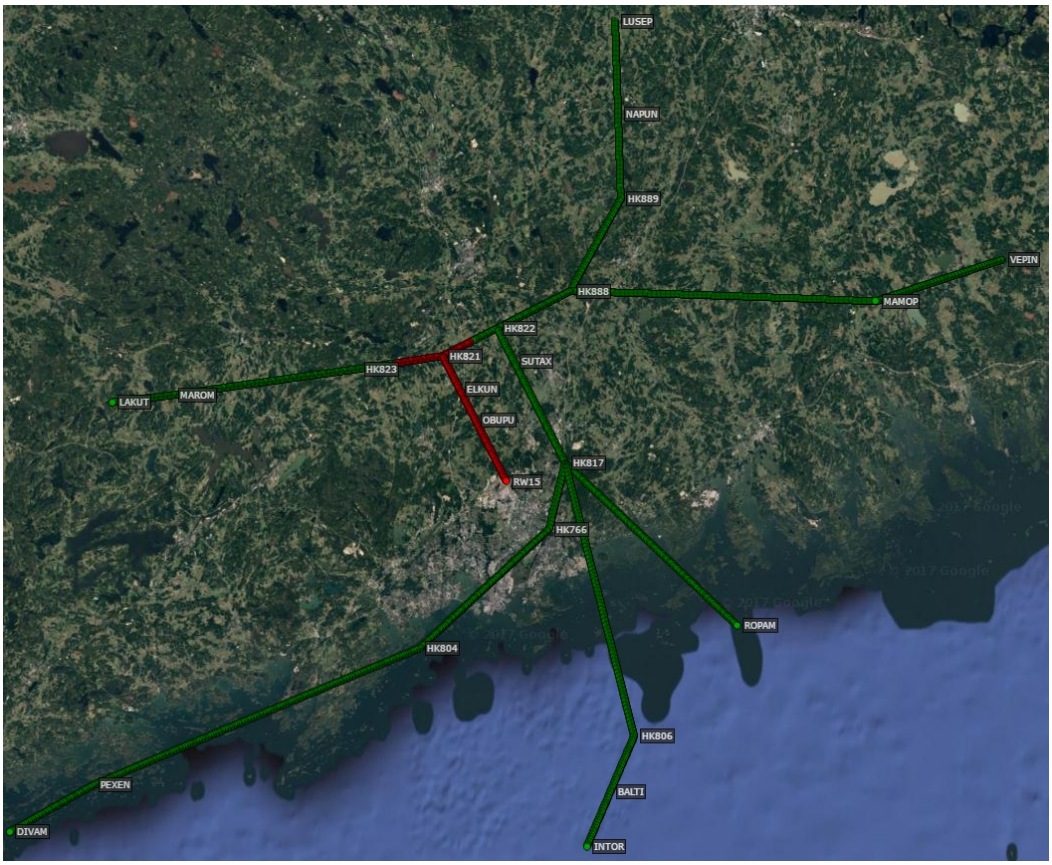

Figure A4.20. Runway 15 risk areas, 4 degree descent profile, speed profile A, still air.

Figure A4.21. Runway 15 risk areas, 5 degree descent profile, speed profile A, still air.

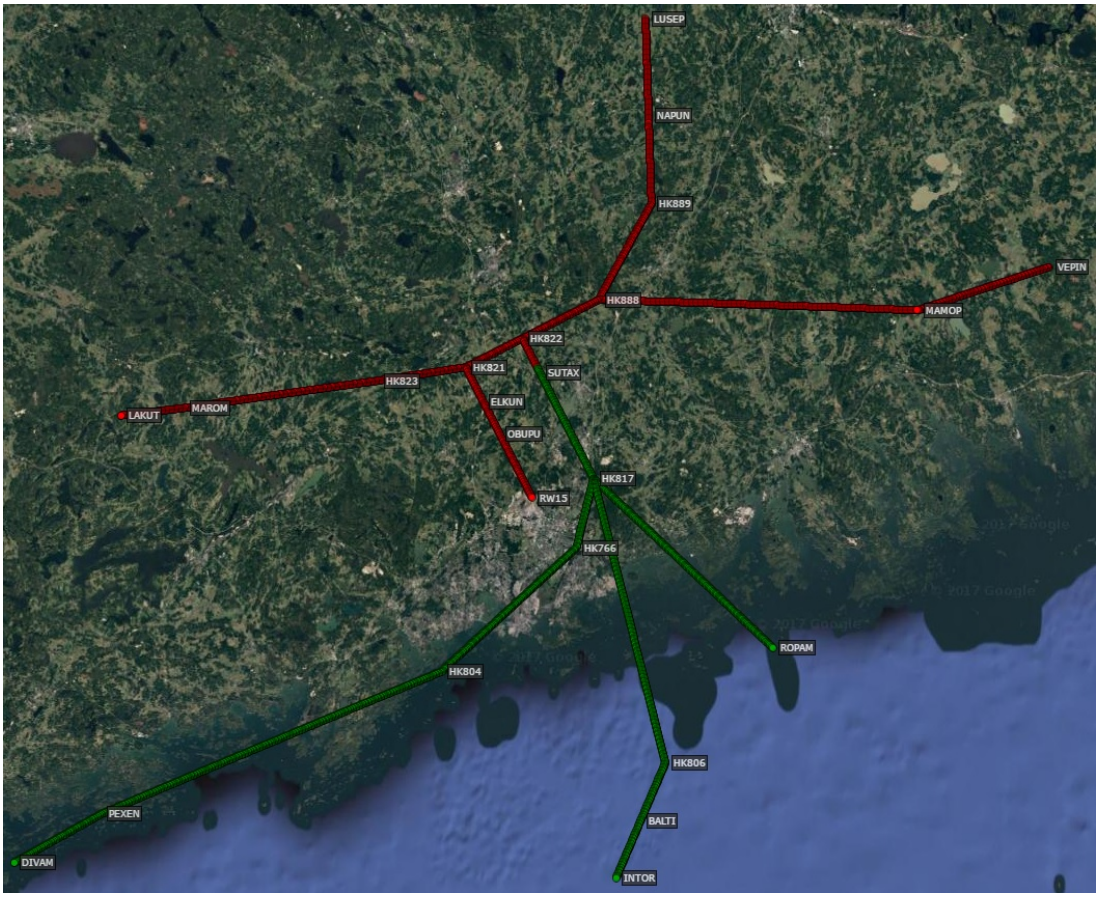

Figure A4.22. Runway 15 risk areas, 3 degree descent profile, speed profile A, 20 kt headwind.

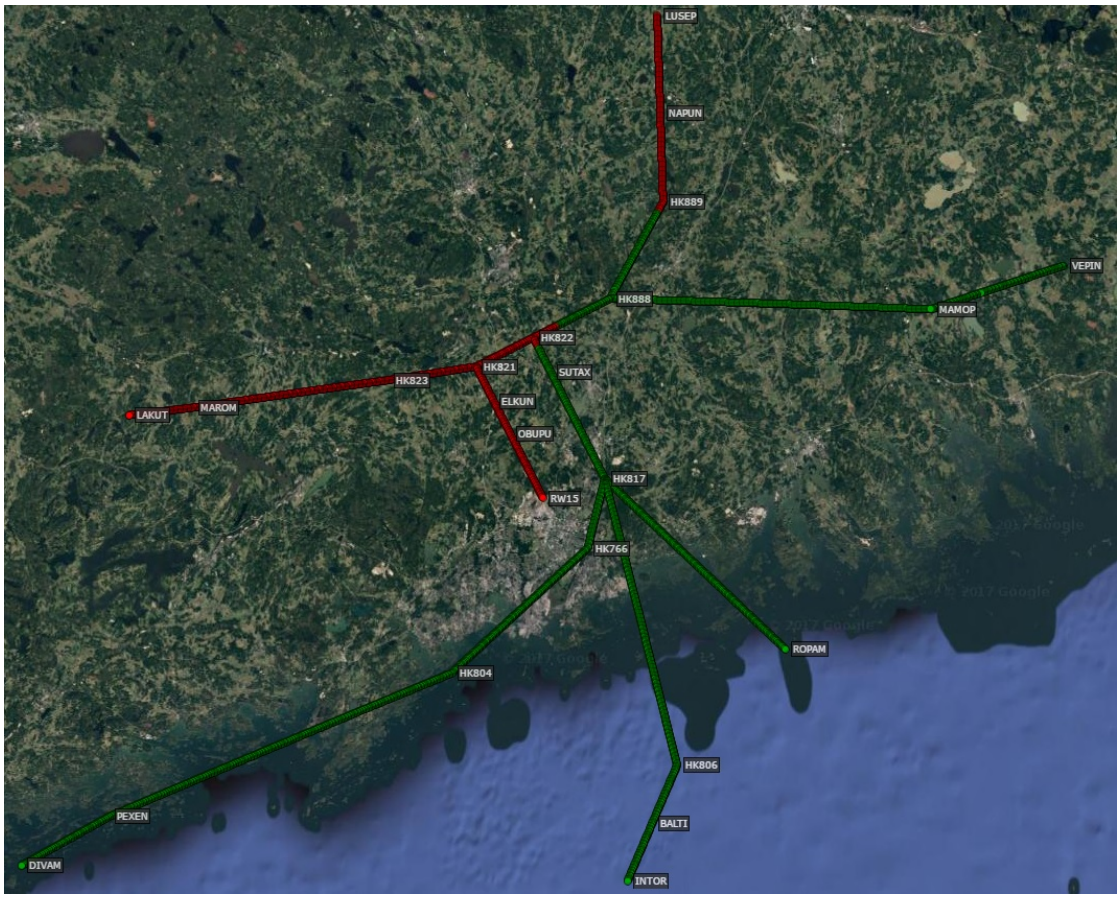

Figure A4.23. Runway 15 risk areas, 4 degree descent profile, speed profile A, 20 kt headwind.

Figure A4.24. Runway 15 risk areas, 5 degree descent profile, speed profile A, 20 kt headwind.

Runway 22L

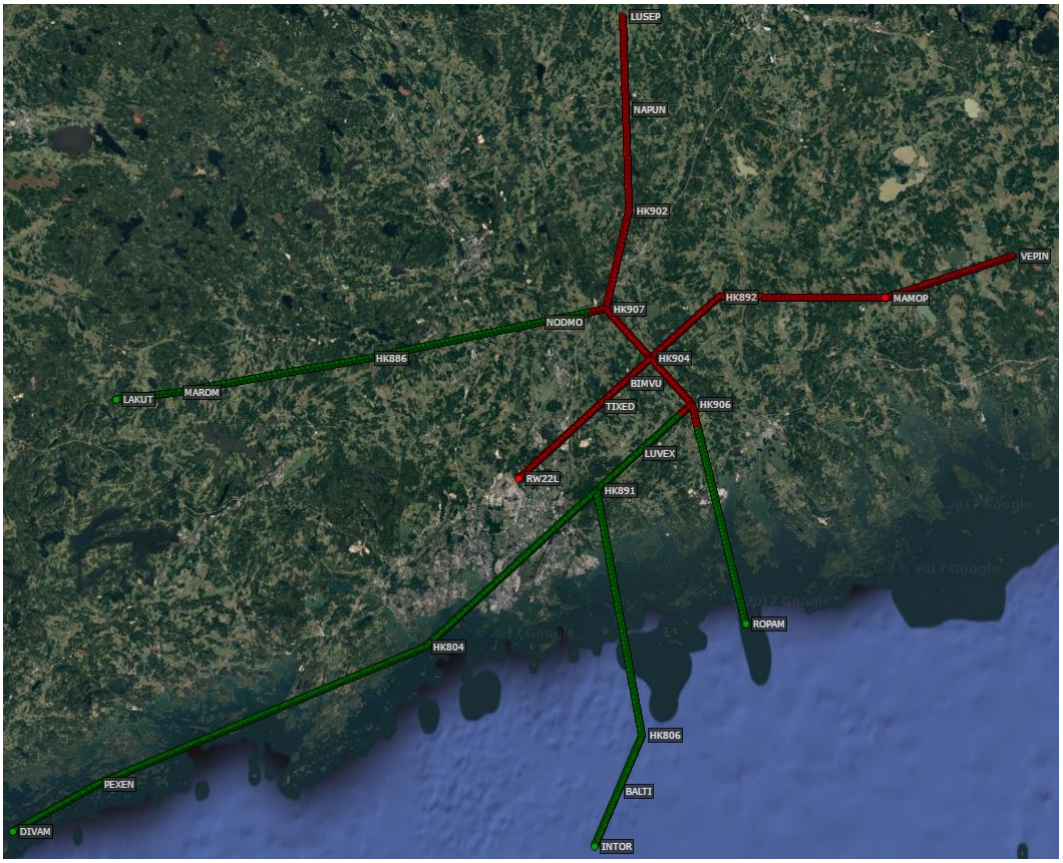

Figure A4.25. Runway 22L risk areas, 3 degree descent profile, speed profile A, still air.

Figure A4.26. Runway 22L risk areas, 4 degree descent profile, speed profile A, still air.

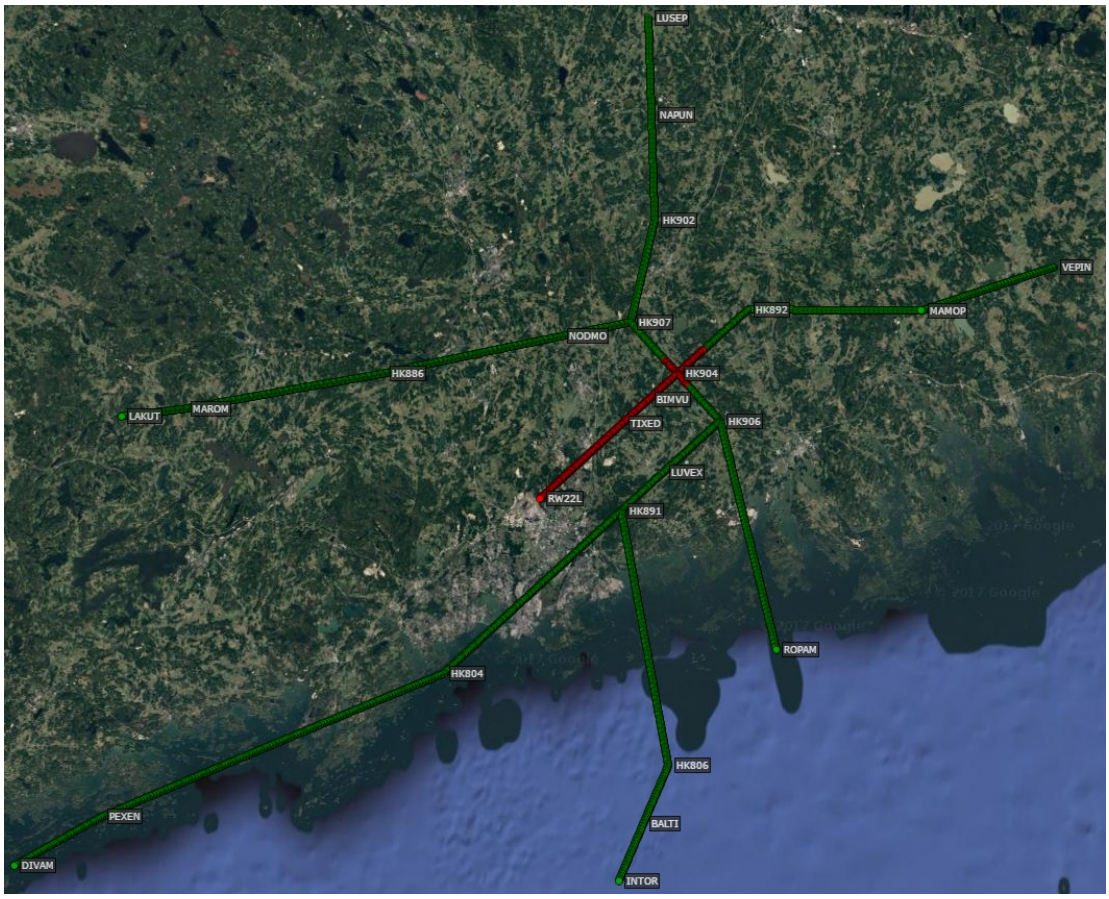

Figure A4.27. Runway 22L risk areas, 5 degree descent profile, speed profile A, still air.

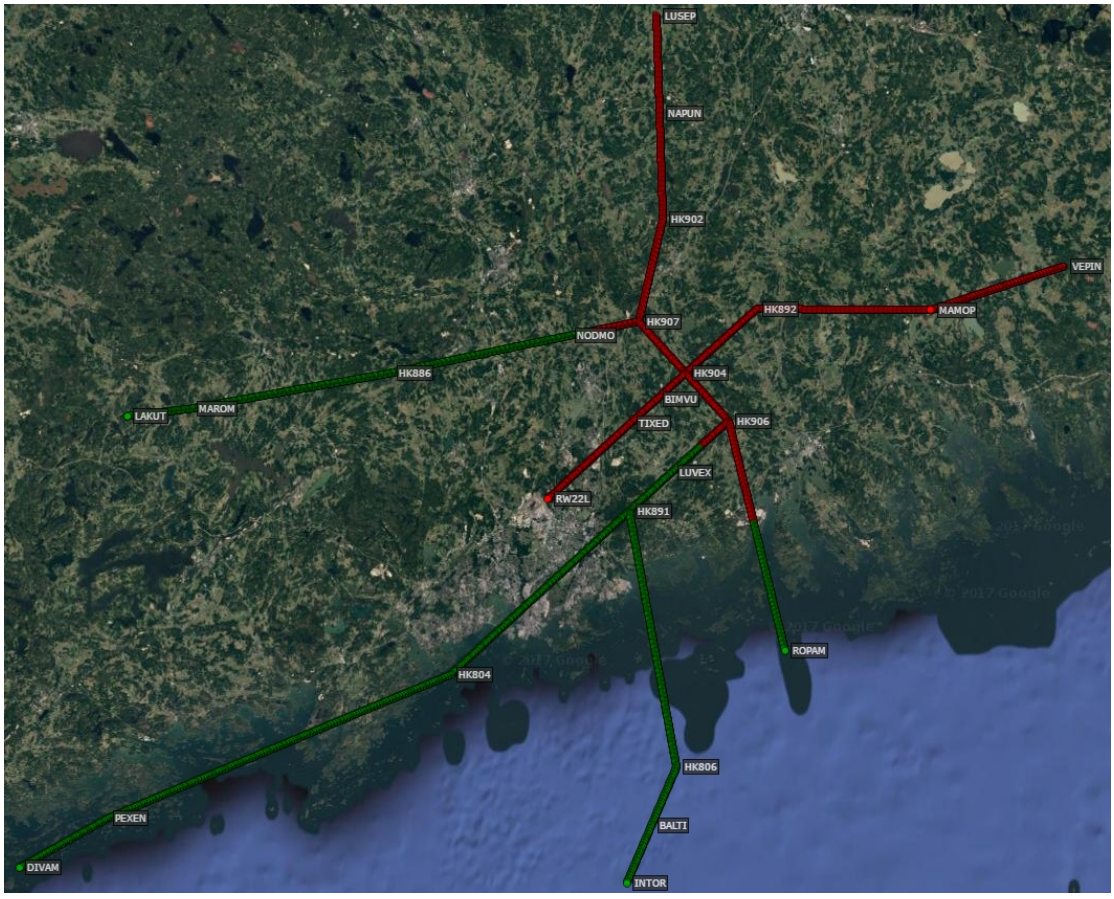

Figure A4.28. Runway 22L risk areas, 3 degree descent profile, speed profile A, 20 kt headwind.

Figure A4.29. Runway 22L risk areas, 4 degree descent profile, speed profile A, 20 kt headwind.

Figure A4.30. Runway 22L risk areas, 5 degree descent profile, speed profile A, 20 kt headwind.

Runway 22R

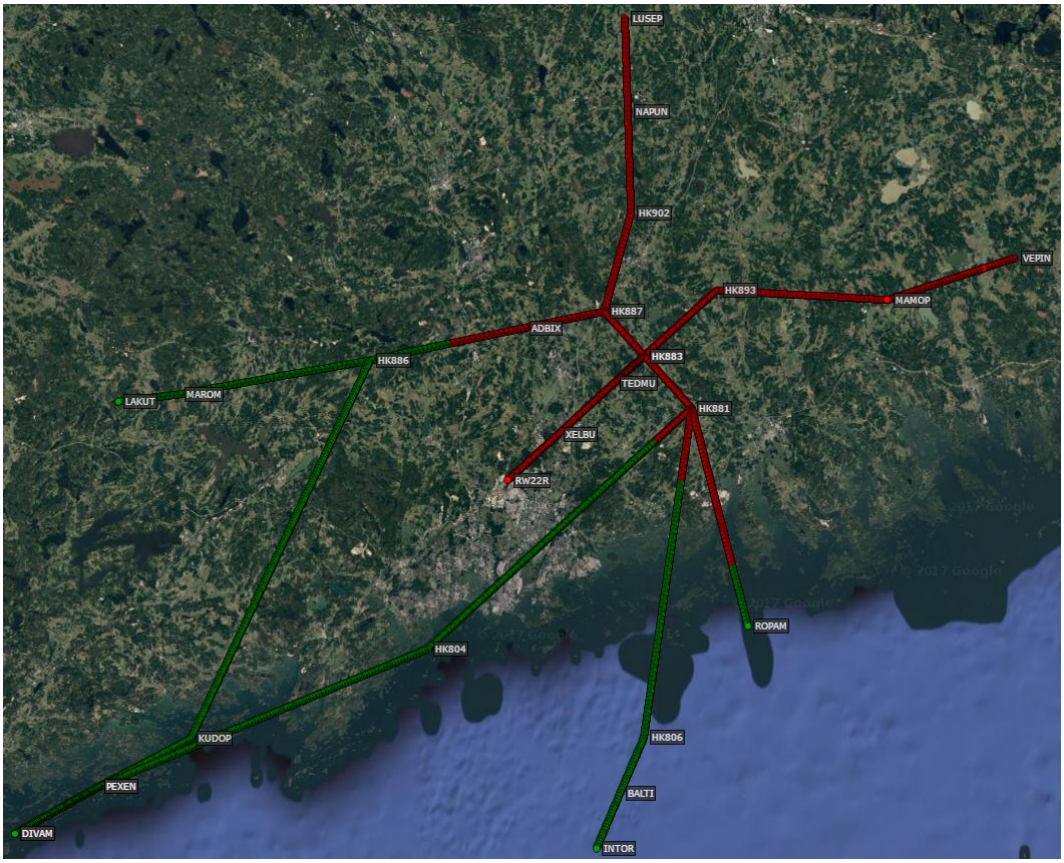

Figure A4.31. Runway 22R risk areas, 3 degree descent profile, speed profile A, still air.

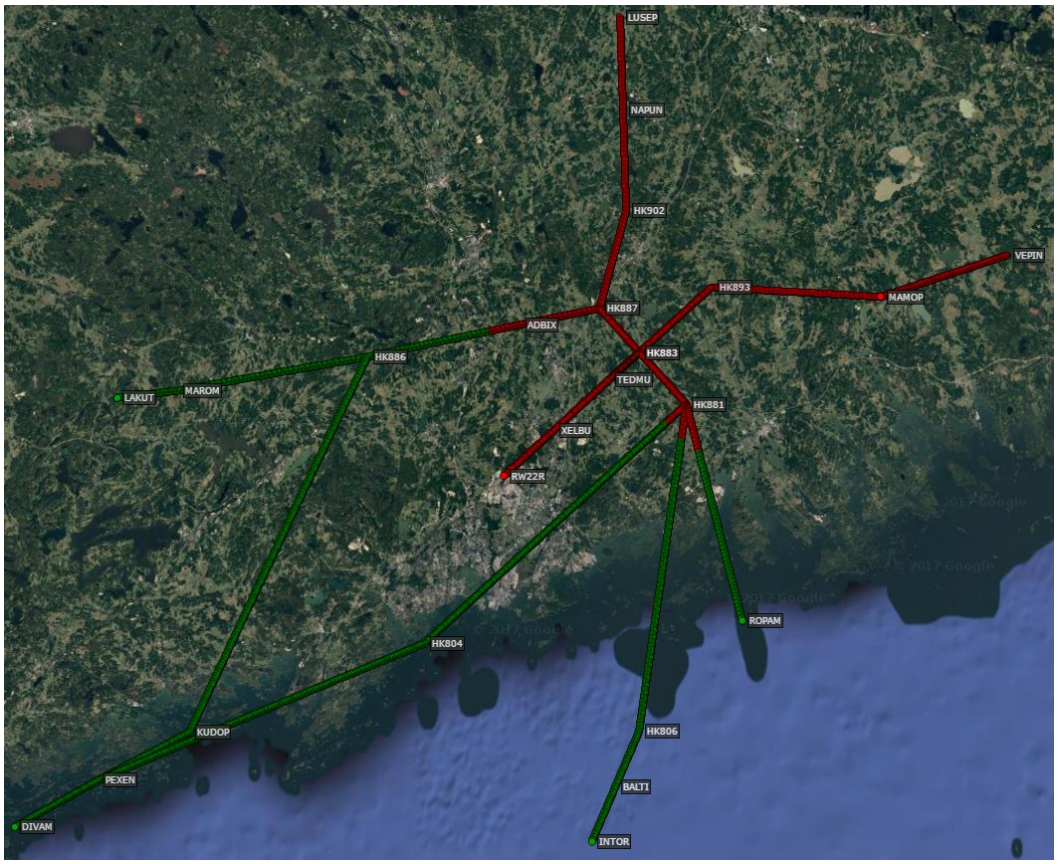

Figure A4.32. Runway 22R risk areas, 4 degree descent profile, speed profile A, still air.

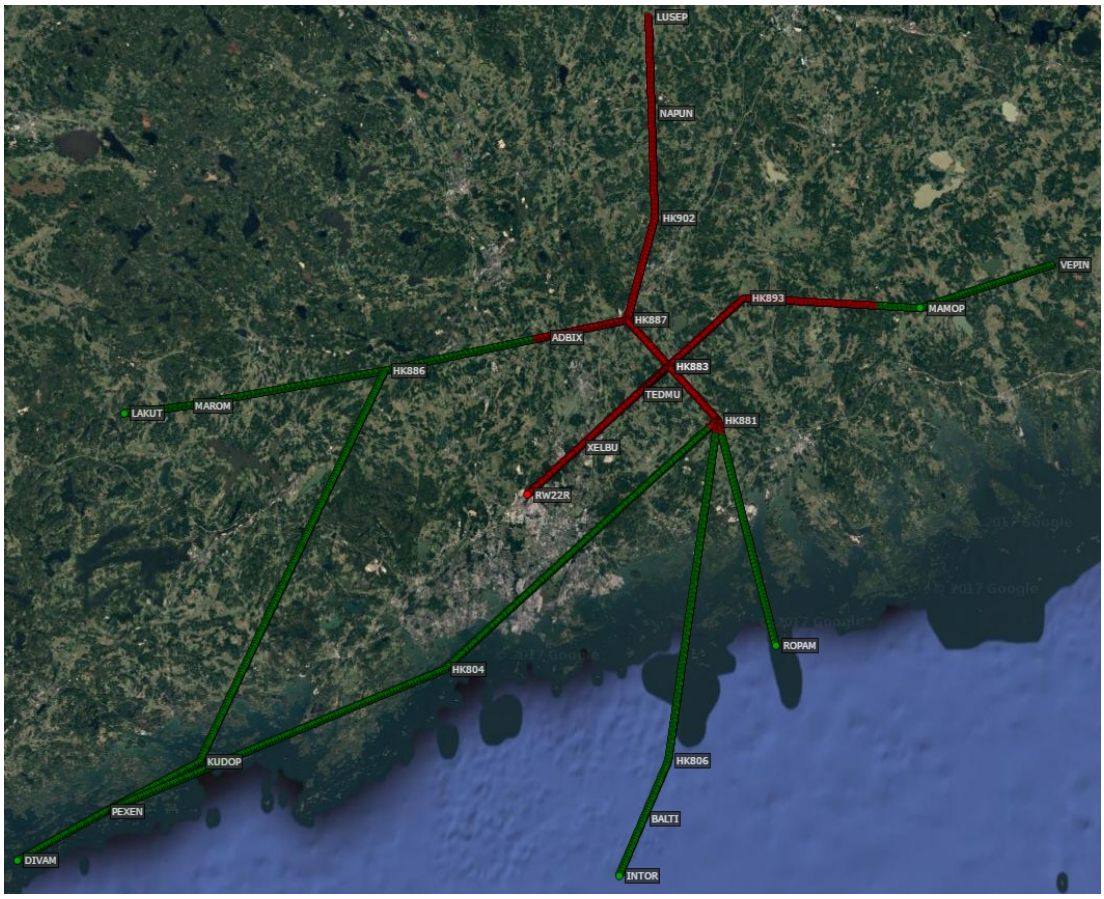

Figure A4.33. Runway 22R risk areas, 5 degree descent profile, speed profile A, still air.

Figure A4.34. Runway 22R risk areas, 3 degree descent profile, speed profile A, 20 kt headwind.

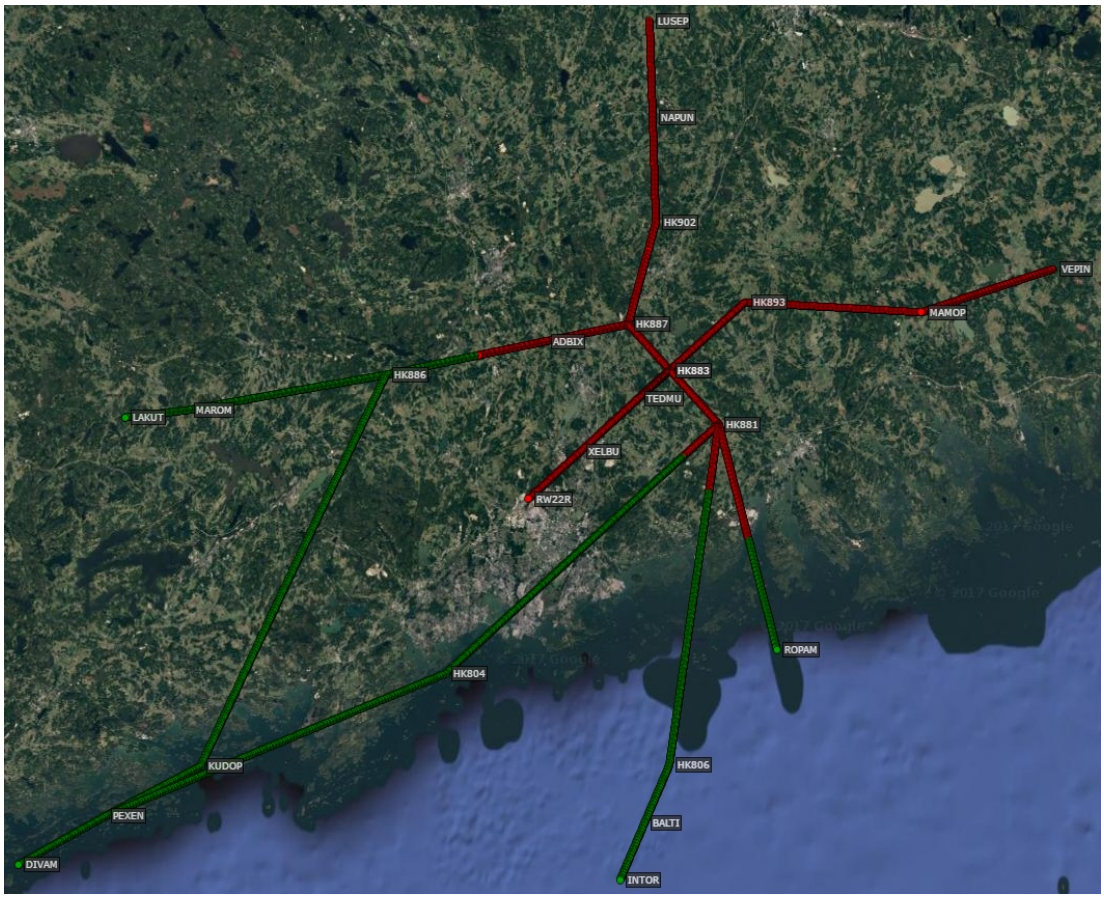

Figure A4.35. Runway 22R risk areas, 4 degree descent profile, speed profile A, 20 kt headwind.

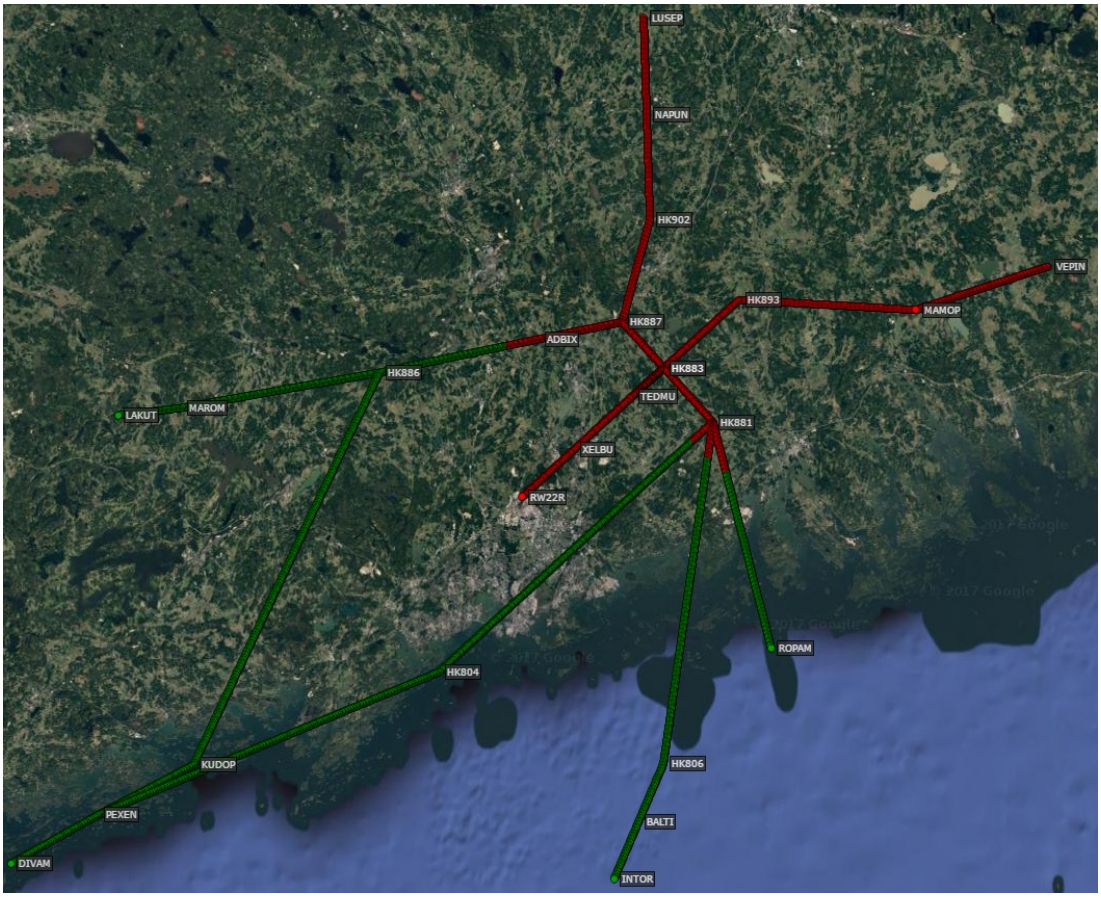

Figure A4.36. Runway 22R risk areas, 5 degree descent profile, speed profile A, 20 kt headwind.

Runway 33

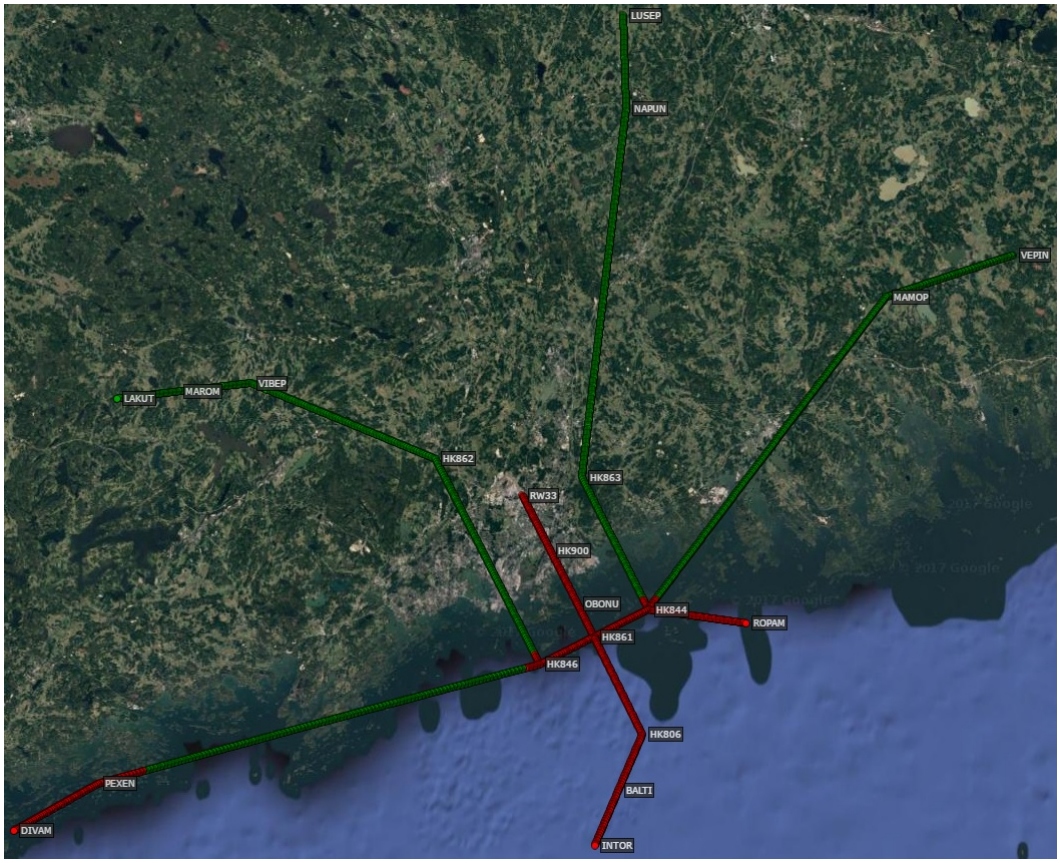

Figure A4.37. Runway 33 risk areas, 3 degree descent profile, speed profile A, still air.

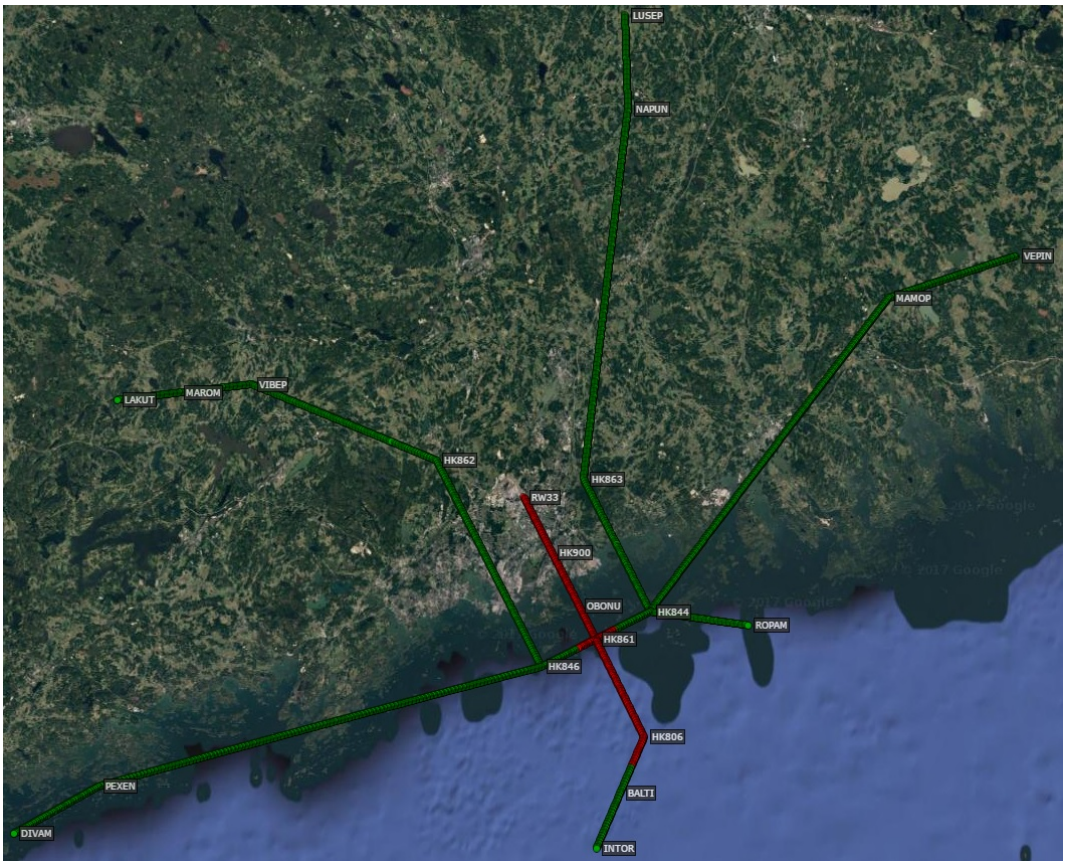

Figure A4.38. Runway 33 risk areas, 4 degree descent profile, speed profile A, still air.

Figure A4.39. Runway 33 risk areas, 5 degree descent profile, speed profile A, still air.

Figure A4.40. Runway 33 risk areas, 3 degree descent profile, speed profile A, 20 kt headwind.

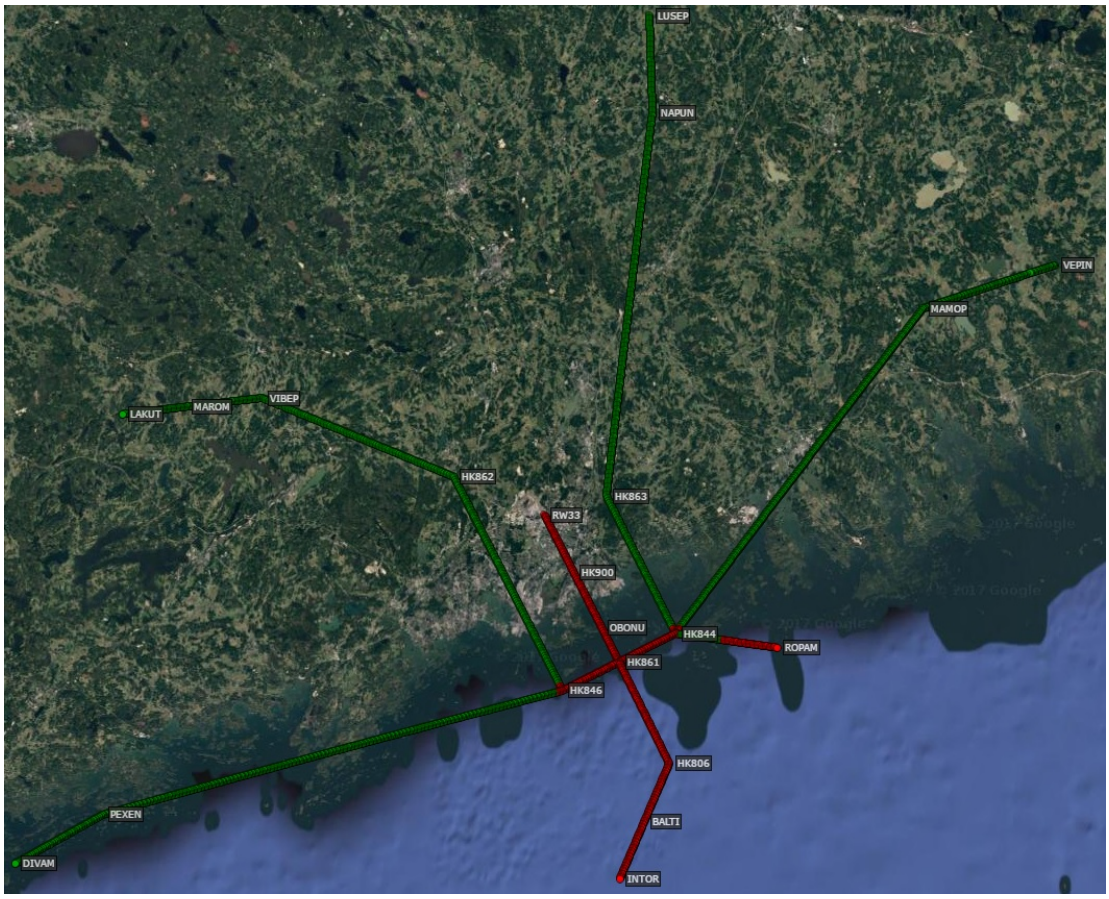

Figure A4.41. Runway 33 risk areas, 4 degree descent profile, speed profile A, 20 kt headwind.

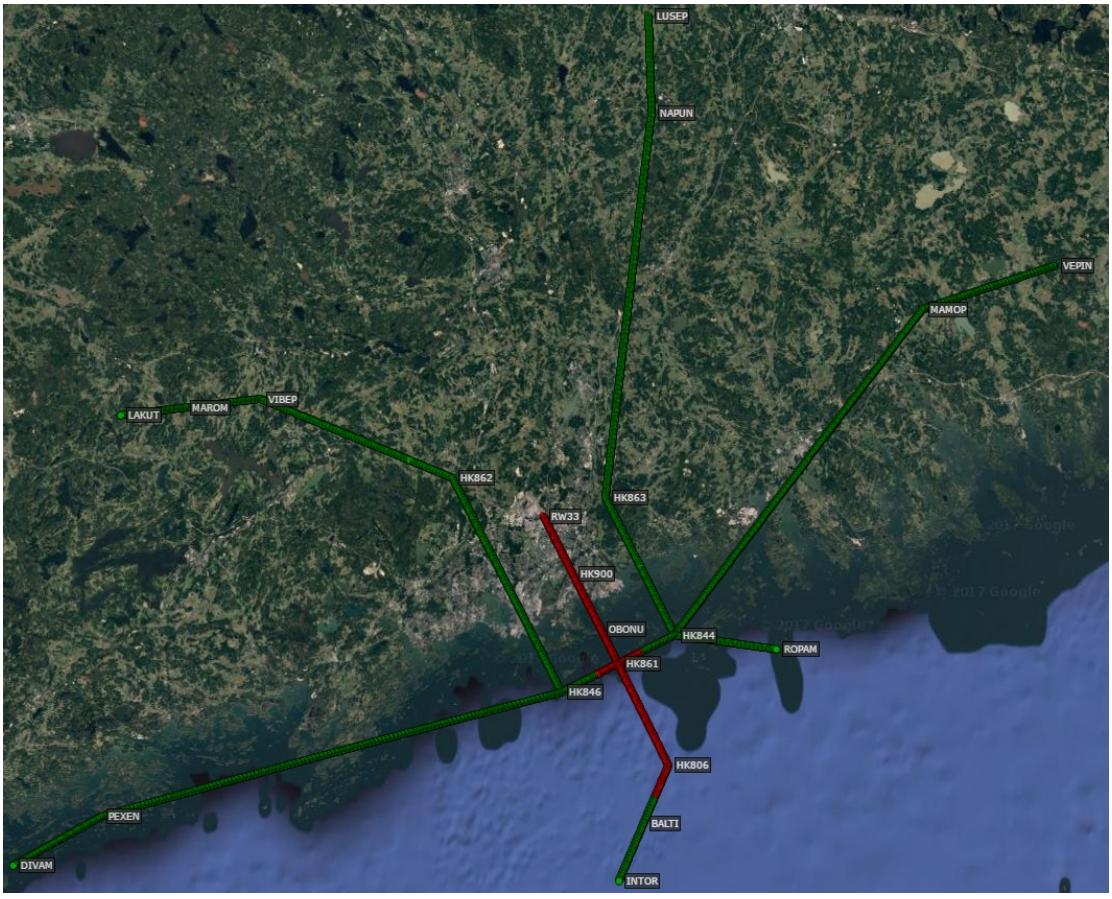

Figure A4.42. Runway 33 risk areas, 5 degree descent profile, speed profile A, 20 kt headwind.